JULIANA CRISTINA DA SILVA

BIOREFINERY OF LIGNOCELLULOSIC MATERIALS: NOVEL PRODUCTS, METHODS AND APPLICATIONS OF FOREST AND AGRICULTURAL FEEDSTOCKS

Tese apresentada à Universidade Federal de Viçosa, como parte das exigências do Programa de Pós-Graduação em Ciência Florestal, para obtenção do título de *Doctor Scientiae*.

VIÇOSA
MINAS GERAIS – BRASIL
2015

JULIANA CRISTINA DA SILVA

BIOREFINERY OF LIGNOCELLULOSIC MATERIALS: NOVEL PRODUCTS, METHODS AND APPLICATIONS OF FOREST AND AGRICULTURAL FEEDSTOCKS

Tese apresentada à Universidade Federal de Viçosa, como parte das exigências do Programa de Pós-Graduação em Ciência Florestal, para obtenção do título de *Doctor Scientiae*.

APROVADA:

Prof. PhD. Dalton Longue Júnior	Prof. Dra. Andréia S. Magaton
Dr. Fernando José Borges Gomes	Dr. Diego Pierre de Almeida

Prof. Rubens Chaves de Oliveira

(Orientador)

I dedicate this thesis to my parents and my brother.

“The clouds always change position, but are always clouds in the sky. So we should be every day, mutants, but loyal to what we think and dream; remember, everything melts into air, less thoughts ".

Paulo Beleki

ACKNOWLEDGEMENTS

This thesis is the result of my studies at the Pulp and Paper Laboratory, Universidade Federal de Viçosa. The realization of this work was allowed by the collaboration of several people whom I want to express my sincere acknowledgements:

My parents and brother, to whom I will be eternally grateful for all the love, affection, encouragement, and for believing in my potential.

My advisor Rubens Chaves de Oliveira, to whom I would like to express my gratitude for accepting me as his PhD student and for all that I have learned from him about science, research and life.

Professors, colleagues and officials of the Pulp and Paper Laboratory (specially Carla, Luciano and Carlinhos), who greatly contributed to my technical improvement and the conduction of this work.

I am grateful to Bianca Barbosa, João Vítor Assis, Daniela Leocardio and Tiago Daniel for all time dedicated to help me in several analyses and for all enlightening discussions on various topics covered in this study.

My uncle Né, Leonel, and Gilson for their willingness and readiness to help me whenever I needed.

Universidade Federal de Viçosa and Department of Forest Engineering, for the opportunity offered.

CNPq and CAPES for the financial support, which greatly helped me during my stay in Viçosa and in the realization of my sandwich PhD.

Finally, I would like to thank the Forest Biomaterials Department of North Carolina State University (NCSU), students and colleagues at the CIG. I would like to highlight the assistance from Dr. Rojas, for the wonderful experience of realization of part of my studies abroad and for the exchange of knowledge during my stay there. In fact, it was one of the most important experiences in my life.

Summary

LIST OF ABBREVIATIONS

°C: degree Celsius
°SR: Schopper riegler degree
AG: acetyl groups
Ara: arabinose
AX: Arabinoxylan
AXac: acetylated Arabinoxylan
BET: Brunauer–Emmet–Teller
BOD: biological chemical demand
Cd: cadmium
Cl: crystallinity index
cm^3: cubic centimeter
CMT: Corrugated Medium Test
CNC: cellulose nanocrystal
COD: chemical oxygen demand
DS: substitution degree
DSL : Dynamic Light Scattering
FTIR-ATR: Fourier transform infrared spectroscopy - Attenuated total reflection
g: gram
gal: galactose
glc: glucose
h: height of the cylinder
H_2SO_4: sulfuric acid
HNO_3: nitric acid
HPAEC-PAD: High Performance Anion Exchange Chromatography with Pulse Amperometric Detection
HPLC: High-performance liquid chromatography
Hz: Hertz
Kg: kilogram
KV: Kilovolt
L: liter
man: mannose
MFC: microfibrillated cellulose
mL: mililiter
mm: Millimetre
MOE: Modulus of Elasticity
MPa: megapascal
mV: milivolt
N: newton
N: normal
N2: nitrogen gas
NaOH: Sodium hydroxide
NFC: nanofibrilada cellulose
nm: nanometer
NMR: Nuclear magnetic resonance
Pa: Pascal
PAE: polyamine-epichlorohydrin

Pb: lead
pH: potential of hydrogen
qe: Capacity adsorption
qe’: Capacity adsorption/ aerogel surface area
r^2: radius squared
RCT: Ring Crush Test
rpm: Revolutions per minute
SEM: Scanning electron microscopy images
TAPPI: Technical Association of the Pulp and Paper Industry
TGA: Thermogravimetric analysis
TOC: total organic carbon
Ton: tonne
UV: Ultraviolet
V: volt
W: Watts
WRV: water retention value
wt%: percentage by weight
xyl: xylose
Zn: Zinc
π : Pi, approximately 3.142

RESUMO

SILVA, Juliana Cristina da, D.Sc., Universidade Federal de Viçosa, dezembro de 2015. **Biorefinery of lignocellulosic materials: novel products, methods and applications of forest and agricultural feedstocks**. Orientador: Rubens Chaves de Oliveira.

A diversificação no portfólio de produtos e a otimização de técnicas e processos vem sendo objetivado por várias indústrias atualmente e cada vez mais se vem buscando matérias primas de fontes renováveis e biodegradáveis. Neste contexto, biorrefinarias de produtos florestais e agrícolas se enquadram como modelos que permitem obter um maior valor agregado aos produtos oriundos da biomassa. Assim, na presente tese objetivou-se, dentro dos conceitos de biorrefinaria, explorar a biomassa lignocelulósica, de origem florestal e agrícola, para melhoria de qualidade e tecnologia de produtos amplamente utilizados, como papéis. Também se buscou a produção de materiais que podem substituir produtos de base petrolífera, como os plásticos, com a produção de biofilmes. Além disso, a produção e caracterização de aerogéis foi realizada e dentro da grande gama de aplicações, foi avaliada seu potencial para tratamento de água com a remoção de metais pesados. As nanoceluloses, celulose microfibrilada (CMF), celulose nanofibrilada (CNF) e celulose nanocristalina (CNC), juntamente com as hemiceluloses ricas em xilanas foram detalhadamente estudadas e empregadas para atingir os objetivos deste estudo, apresentado em forma de capítulos. No primeiro capítulo, hemiceluloses ricas em xilana foram extraídas de sabugo de milho e adicionadas em polpas celulósicas. À medida que se aumentaram a concentração das hemiceluloses, foi observado aumento na resistência à drenagem e também nas propriedades dos papéis diretamente influenciadas pelas ligações interfibras. O volume específico aparente dos papéis foi inversamente proporcional à adição de hemiceluloses. No segundo capítulo, hemiceluloses extraídas da mesma forma do que no capítulo 1 foram usadas para produção de biofilmes, submetidas ou não à processos de acetilação. Nestes biofilmes foram adicionados agentes de reforço como celulose nanofibrilada (CNF), resina poliamina-epiclorohidrina (PAE) e alguns plastificantes. Os resultados obtidos mostraram que é possível produzir filmes a partir das hemiceluloses e que quando estes carboidratos são acetilados resultam em filmes mais resistentes à tração e maior deformação. Outra característica importante foi o aumento da hidrofobicidade dos filmes a partir da acetilação. Todos os filmes apresentaram alta resistência à passagem de ar. No terceiro capítulo, as nanoceluloses (CNF, CMF e CNC)

foram adicionadas à polpas não branqueadas de pinus, refinadas em diferentes intensidades. Os resultados mostraram que as propriedades dos papéis relacionadas à ligações interfibras aumentaram com a incorporação das nanoceluloses, sendo que a incorporação das CMF foram as que apresentaram maiores incrementos se comparados com a polpa referência. No capítulo 4, foram caracterizados aerogéis formados a partir de CNF, reforçados com hemiceluloses ricas em xilanas. Os resultados mostraram que a relação CNF: xilana influencia na forma, resistência, área superficial, capacidade de absorção de água. Por fim, os aerogéis descritos no capítulo 4 foram avaliados quanto à capacidade de remoção de metais pesados de soluções aquosas. Os resultados mostraram que os aerogéis formados apresentam alta capacidade de adsorção de íons metálicos Zn^{2+}, Pb^{2+} e Cd^{2+}. Aspectos como formulação, pH, concentração inicial, tempo de contato influenciaram na capacidade de adsorção dos aerogéis.

ABSTRACT

SILVA, Juliana Cristina da, D.Sc., Universidade Federal de Viçosa, dezembro de 2015. **Biorefinery of lignocellulosic materials: novel products, methods and applications of forest and agricultural feedstocks.** Adviser: Rubens Chaves de Oliveira.

Currently, the diversification in product portfolio and optimization of techniques and processes have become a concern formany industries that are seeking raw materials from renewable and biodegradable sources. Biorefineries of forest and agricultural products stand out as templates that allow obtaining greater value for products from lignocellulosic biomass. Thus, within the concepts of biorefinery, this thesis aimed toexplore the lignocellulosic biomass from forest and agriculture to improve quality and technology of widely used products, such as paper. In addition, it sought to produce materials that can replace oil-based products such as plastics, with the production of biofilms. Furthermore, the production and characterization of aerogels was performed, and into the wide range of their applications, their potential was evaluated for water treatment to remove heavy metals. Nanocelluloses, microfibrillated cellulose (MFC), nanofibrilada cellulose (NFC) and cellulose nanocrystal (CNC), along with the xylan- rich in hemicelluloses have been exploited and employed to achieve the objectives of this study, presented in the form of chapters. In the first chapter, xylan -rich hemicelluloses were extracted from corn cobs and added in cellulosic pulps. The increased concentration of hemicellulose led to an increase in drain resistance and in paper properties directly affected by the inter-fiber bonds. The paper bulk was inversely proportional to the addition of hemicelluloses. In the second chapter, hemicelluloses extracted in the same way as in Chapter 1 were used for the production of biofilms. The hemicelluloses were subjected or not to acetylation processes. The biofilms were reinforced with agents as nanofibrillated cellulose (NFC), polyamine-epichlorohydrin resin (PAE) and some plasticizers. The results showed that it is possible to produce films from hemicelluloses and that when these carbohydrates were acetylated, the films showed higher tensile index and greater strain. Another important feature was the hydrophobicity of the films after acetylation. All films showed high air resistance. In the third chapter, the nanocelluloses were added to unbleached pulp from Pinus, refined at different intensities. The results showed that the handsheet properties related to increased inter-fiber bonds increased with the incorporation of nanoceluloses, and the incorporation of the MFC demonstrated greater increases compared to the reference pulp. In Chapter 4,

aerogels formed from NFC reinforced with xylan -rich hemicelluloses were characterized. The results showed that NFC:xylan ratio affects the shape, strength, surface area and water absorption capacity of aerogels. Finally, the aerogels described in Chapter 4 were assessed for the ability to remove heavy metals from aqueous solutions. The results showed that the aerogels exhibit high adsorption capacity for metal ions Zn^{2+}, Pb^{2+} and Cd^{2+}. Aspects such as formulation, pH, initial concentration and contact time influenced the adsorption capacity of the aerogels.

GENERAL INTRODUCTION

The term Biorefinery refers to a complex integration of processes, technology and equipment dedicated to the production of energy, fuels and chemicals from biomass. Therefore, biomass conversion technologies and their residues employed in a biorefinery emerge as alternatives for the use these solid residues. The processes involved in the improvement of these renewable feedstocks should integrate the principles of green chemistry and green engineering, and low environmental impact technologies for the sustainable production of high value chemicals.

Forest based biorefinery uses nonfood woody biomass feedstocks composed of lignocelluloses (BRIGHT T. KUSEMAA, 2012). Lignocellulosic material consists of three primary fractions; cellulose, hemicellulose and lignin, which are the most available and renewable resources and a low cost raw material. Producing multiple products and maximizing the value derived from the biomass feedstock are economically and sustainably advantageous (SILVA, 2011).

In order to expand the range of natural bioresources, the rapidly evolving tools of biotechnology can lower the conversion costs and enhance the target yield of the product of interest. Green biotechnology has become a promising approach to convert most of the solid forest and agricultural wastes into novel materials with higher aggregated value, particularly lignocellulosic materials..

This thesis contributes to the development of new materials derived from biomass that can be used as chemical additives, binders, coating and packaging materials and biosorbents, thus providing ecologically correct, socially fair and economically viable products to the market. The thesis is comprised of five chapters. The research presented in chapters 4 and 5 were carried out in the Department of Forest Biomaterials, at North Carolina State University, USA.

On the chapter 1, Xylan-rich hemicelluloses were isolated from corn cob and added in the eucalyptus pulp to produce paper. Then, the physical and mechanical properties were assessed. In addition, the chemical characterization of the raw material was carried out and assessed.

The second chapter approached the biofilm production from the same hemicelluloses used in the chapter 1. These biofilms was reinforced with NFC and

plasticizers together with hemicelluloses were also used in order to obtain continuous and self-supporting hemicellulose based films with improved mechanical properties.

Chapter 3 addresses the addition of nanocellulose structures in paper production,which tends to increase paper properties. This study aimed to evaluate how the addition of NFC, MFC and CNC in the handsheetaffects its physical and mechanical properties.

Chapter 4 focuseson the creation of a new product, using NFC and hemicelluloses, the aerogels, as main raw materials. Some characteristics, such as low density and high surface area, give aerogels the possibility of multiple uses, such as gas or liquid permeation and adsorption, thermal and acoustic insulation, optical applications, carriers for catalysis or drug release, among others.

Chapter 5 approached ion adsorption by aerogels. In this chapter, it was evaluated the adsorption capacity of cations Pb^{2+}, Zn^{2+} and Cd^{2+} by NFC reinforced with xylan-rich hemicelluloses-based aerogel.

Chapter 1

Published as original paper (Procedia Materials Science, Volume 8C, 2015, Pages 793-801)

Extraction, addition and characterization of hemicelluloses from corn cobs to development of properties of papers

Abstract

Corn cob is a product found in significant amounts in the residues of agriculture, whose potential for use underexploited. This paper presents a study on the chemical characterization of corn cobs, the extraction and application of hemicelluloses present in these wastes. Two fractions of hemicelluloses were obtained. The first was obtained after neutralization and precipitation of the alkaline solution; the second, after the addition of ethanol in the supernatant of the same solution. Handsheets were made by using bleached kraft eucalyptus pulp, and adding hemicelluloses. Then, their physical and mechanical properties were evaluated, according to the TAPPI Standard. Increased resistance was observed in drainage and in the properties directly affected by the inter-fiber bonds as hemicellulose content increased; and handsheets with lower bulk were obtained as the levels of these carbohydrates increased.

Keywords: Hemicelluloses; corn cob; properties of papers.

INTRODUCTION

Hemicelluloses are polysaccharides that differ from cellulose for containing several types of sugar units in their composition (D- xylose, D- mannose, D- glucose, L-arabinose, etc). They are branched polymers (amorphous) with shorter chains (degree of polymerization of up to 200 sugar units) compared with cellulose [1, 2].

The monosaccharides that form the structures of hemicelluloses are composed of hexose sugars (glucose, mannose and galactose) and pentose (arabinose and xylose), and can provide varying amounts of uronic acids and deoxy- hexose in some types of vegetables.

In the specific case of corn cobs, the xylans usually present a chemical structure formed by 4-O- methyl- D -glucuronic acid, L- arabinose and D- xylose in the ratio 2:07:19 [3]. In recent years, evidence has emerged that the arabinoxylans (xylans which have a large number of residues in the side chains of arabinose) contained in cereal grains are interconnected in the cell wall by cross-linking occurring by esterification with the diferulic acid, and/or by formation of complexes with proteins. These structures would be

responsible for the difficulty for the extraction and purification of xylans and time of digestion of cereal grains [3].

Several studies have addresses the hemicellulose isolation processes [4-16] and the relationship between cellulose and hemicellulose levels in paper properties [9, 11, 13-15, 17-21].

Studies evaluating the effects of different levels of hemicelluloses on pulp properties are performed through drastic variations in pulping and/or bleaching processes. More recently, research works were carried out adding hemicellulose in the pulp, which requires the removal of hemicelluloses from a certain source and their introduction into the pulp. The main drawback of this approach is the difficulty of obtaining hemicelluloses in an economically viable way [21]. The amount of hemicellulose added and the consistency of the fibrous suspension can affect the results. The lower the dose of hemicelluloses, the faster the maximum adsorption [13]. However, at higher doses, most hemicelluloses tend to be kept in the pulp [16, 21].

The hemicellulose content is extremely important in papermaking processes. No other wood chemical component has more influence on the properties of paper, since cellulose chains are not very damaged or degraded [22].

Pulps having reduced levels of hemicelluloses, such as recycled pulps, are more difficult to be refined and have smaller and weaker bonds between the fibers when compared with pulps with higher levels of hemicelluloses [16].

Hemicelluloses are responsible for most of the bonds among fibers and affect the properties that depend of these bonds directly. [9, 14, 23-27]. A certain study found that the adsorption of xylans leads to increased negative ionic charge of the pulp, which is directly related to the tensile strength of the paper produced. This is explained by the fact that negative charges promote increased swelling, which increases the flexibility of the fiber. Fibers that contain higher levels of hemicelluloses are able to produce papers with higher strengths, better bonds between fibers, better surface smoothness, but lower porosity and bulk [28].The use of corn cobs as a source of hemicelluloses gives greater added value for this product whose potential use has not been explored and that can be found in significant amounts in agricultural waste.

For each 100 kg of corn ear, about 18 kg of corn cob are produced. World production of corn cob was about 144 million ton in 2008. Despite the large amount generated, its potential for use has not been exploited [29].

Thus, this study aimed to perform the chemical characterization of corn cob, the isolation of hemicelluloses present in this material and application in bleached eucalyptus kraft pulp for the improvement of paper properties.

METHODOLOGY

Hemicelluloses were obtained following the methodology described in literature [3], with adaptations. The procedure was repeated several times until the desired amounts of hemicelluloses were obtained.

Hemicellulose isolation

Initially, dried corn cobs were crushed in a mill and classified through a series of sieves. The fraction retained between 40 mesh and 60 mesh screens were subjected to various treatments, as described below.

Aqueous extraction

The crushed material was subjected to aqueous extraction at a ratio of 30 g of powdered corn cobs to 1,000 ml of distilled water with constant stirring for 12 hours, at room temperature. Then, the mixture was centrifuged and the solid phase was dried in a climatized room at 23 °C and 50 % humidity for 24 hours.

Lipid removal

Following the aqueous extraction, the material was treated with acetone in a Soxhlet -type apparatus, with 6 cycles per hour for 3 h for lipid extraction. Next, it was dried under a fume hood for 3 hours to evaporate the acetone, and then remained in a desiccator for 24 hours.

Delignification

After drying, the material was treated in an organosolv pulping process, taking into account the efficiency of lignin removal, as described in the literature [3]. 10 g of sample was dispersed in 1,000 ml of a mixture composed by 97% of 1,4-dioxane and 3% of hydrochloric acid . The system was kept under stirring at room temperature for 3 hours. At the end of the delignification, the suspension was filtered and the residue containing hemicelluloses was washed several times with 1,4-dioxane and then with distilled water

with pH around 1. The residue was dispersed in distilled water and then neutralized with aqueous sodium hydroxide 4 % to reach pH = 7.0. The solution was centrifuged and the residue was dried under vacuum.

Alkaline extraction

Solubilization of hemicelluloses was performed by alkaline treatment of corn cob powder with 4% NaOH at room temperature. A ratio of 10 g of powder per 200 ml solution was used. The system remained in low agitation for 5 hours. After vacuum filtration, the solution was neutralized by adding glacial acetic acid to reach pH=7.0. At this stage, it observed the appearance of a precipitate in the medium, which was recognized as Hemicelluloses A. After centrifugation, the fraction of hemicelluloses suffered several washings with ethanol and were dried under vacuum. The filtrate containing Hemicelluloses B was precipitated by the addition of ethyl alcohol at the proportion of three volumes of ethanol for each volume of the solution. The obtained product was centrifuged and washed several times with ethanol.

Quantitative chemical characterization

The carbohydrate composition of raw materials was evaluated by High Performance Anion Exchange Chromatography with Pulse Amperometric Detection (HPAEC-PAD). It was performed after pre-treatment (30°C, 1 h) with aqueous 72% H_2SO_4 followed by hydrolysis with 3% H_2SO_4 in an autoclave (100°C, 3 h). HPAEC-PAD was carried out in a Dionex ICS-3000 system equipped with a CarboPac PA1 (250 x 4mm) analytical column. The monosaccharides were separated isocratically with 0.001 M NaOH (45 min, flowrate 1 mL/min) [30]. The solid residue after hydrolysis was considered as Klason lignin, according to T222 cm-11 standard procedure [31]. Ashes were determined by calcination according to TAPPI standard T211 om-12 [31]. Acid soluble lignin was determined by measuring the UV-absorbance of the filtrate at 205 nm [32]. Total uronic acids in raw material hydrolysates were measured by the colorimetric method, involving 3,5-dimethylphenol [33]. The content of acetyl groups was also determined [34]. All results were calculated from two replicate determinations.

Hemicellulose dosage

Hemicelluloses have been added to the fibrous suspension, at 0.2 % consistency (16 g pulp bleached eucalyptus kraft absolutely dry) and maintained under constant

agitation. The entire contents were stirred for 10 minutes for adsorption to occur on the surfaces of the fibers. Handsheets were produced according to TAPPI 205 [31]. Hemicelluloses were applied at doses of 0 %, 1%, 2.5% and 5% based on the dry weight of the pulp, and differentiated in Hemicelluloses A (formed by the hemicelluloses fraction obtained after neutralizing the pH of the solution hemicelluloses alkaline) and Hemicelluloses B (obtained after the addition of ethanol to the resulting supernatant gives extraction of hemicelluloses A). In order to verify the effect of the hemicelluloses, the same procedure was performed without the addition of these carbohydrates.

Physical and mechanical tests

The formed handsheets were placed in an environment with a relative humidity of 50 ± 2% and at the temperature of 23 ± 1 ° C (TAPPI 402 SP- 98) [31].

Experimental tests were performed according to TAPPI [31] standard procedures and methodologies, as shown in the table below.

Table 1. Analytical Procedures for analysis of pulps

Test	Methodologies
Drainage resistance	TAPPI 200 sp-01
Tensile resistance	TAPPI 494 om-96
Tear resistance	TAPPI T 414 om-98
Bulk	TAPPI 220 sp-01

RESULTS AND DISCUSSION

Quantitative Chemical characterization

The chemical composition of corn cob (percentage relative to the dry weight) is shown in Table 2. This raw material is defined by its content of glucose, xylose, arabinose, galactose, mannose, acetyl groups, lignin, ash and uronic acid. Due to the presence of sodium carbonate, the analysis of the acid insoluble lignin provided an overestimated value; however, the values obtained were corrected for ash content. [35].

The chemical composition of corn cob showed that its total sugar constitution is very different from that found in Eucalyptus. It presents a total of 82.9 %, and Eucalyptus,61 % [39], and the differences are more significant in the amounts of xylose and arabinose. Total lignin was 17.8 %, while their uronic acid and ash contents were 2.2 % and 1.2%, respectively. In relation to the glucose content (47.1 %), the experimental

result was higher than that reported by other authors [36-38], a fact that may be explained by the method used by each author for the quantification of carbohydrates. Values of 28.0 % xylose; 5.4 % arabinose; 0.2 %mannose; and 2,9% acetyl groups, for the samples determined in this study, are closely comparable to those reported by them [36 - 38] for similar samples.

Table 2. Chemical composition of corn cob and reported by other authors

Component,%	**Corn cob**			
	Results	**Van Dongen et al., 2011[36]**	**Lili et al., 2011[37]**	**Garrote et al., 2007[38]**
Glucose	47.1	34	34.6	34.3[a]
Xylose	28.0	28	27.0	31.1[a]
Arabinose	5.4	2.4	3.6	3.01[a]
Galactose	2.2	0.8	-	-
Mannose	0.2	0.1	-	-
Acetyl groups	2.9	-	0.3	3.07
Uronic acids	2.2	1.8	-	3.45
Lignin[c]	17.8	18.3	9.4[b]	18.8
Ash	1.2	-	2.5	1.3

a All sugars expressed as anhydro-units in polymers;
b Lignin values were measured as acid insoluble lignin contents;
c Lignin values were measured as acid insoluble lignin contents and acid soluble.

Physical and mechanical properties of the pulps and papers

The two hemicelluloses fractions, called Hemicelluloses A and Hemicelluloses B, were isolated from corn cobs. The first was obtained after neutralization of the pH of the alkaline solution and the second, after the addition of ethanol to the supernatant of the same solution.

Other authors obtained different values for the intrinsic viscosity of the fractions; 56 mL / g for Hemicelluloses A and 75 mL / g for Hemicelluloses B. These authors indicate that the main difference between these two fractions is the larger hydrodynamic volume of Hemicelluloses B, driven by greater number of substituents (L-arabinose). The presence of substituents tend to increase the rigidity of the polymer chain and the steric repulsions. It would be responsible for increased hydrodynamic volume and intrinsic viscosity of hemicellulose B.

Drainage Resistance

Figure 1 shows that the pulps with lower levels of hemicelluloses had lower drainage resistance than those with higher content of these carbohydrates.

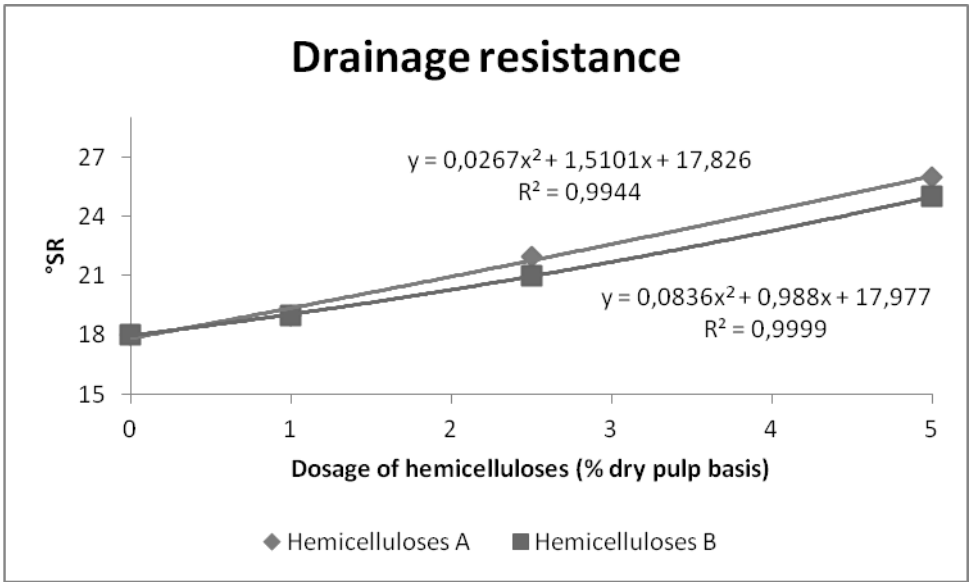

Figure 1. Drainage resistance as a function of dosage of hemicelluloses.

The Reference pulp, without the addition of hemicelluloses, showed 18 ° SR, while those that received hemicelluloses A and B showed a maximum value of 26 ° SR and 25, respectively, at a dosage of 5%.

The high content of hemicelluloses associated with a large fibrous population and low viscosity results in pulp with high water retention, which causes great difficulty to drain and dehydrate it in the paper machine [22].

Tensile resistance

Figure 2 shows the effect of the addition of the hemicelluloses in the tensile strength of the paper. As it can be seen, increased doses of such carbohydratesraise the tensile strength rate. Hemicelluloses contribute greatly to intra and inter- linked fiber, resulting in handsheets with more tensile resistance [17], which is clearly demonstrated in this study.

Recent findings show that the tensile strength rising due to the addition of xylan can be completely explained by the higher content of xylan in the fiber surface, since the xylan located in the inner fiber does not affect tensile strength and tear resistance [9].

In this study, the highest tensile index was achieved with a dose of 5 % based on dry pulp in all situations. An increase of 62.3% was observed in this property in the papers to which 5% Hemicelluloses A were added. The pulp to which the same dose of Hemicelluloses B was added showed an increase of 53.4%.

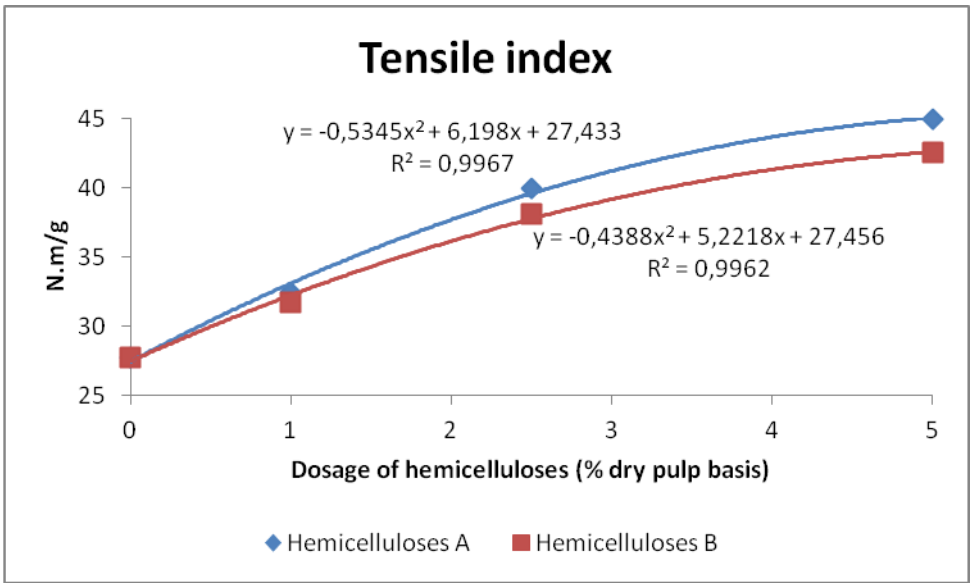

Figure 2. Tensile resistance as a function of dosage of hemicelluloses.

Tear resistance

Figure 3 shows values for tear index for the papers produced in accordance with variations in the dosage of hemicelluloses. The values of tear strength were higher for the papers receiving higher doses of hemicelluloses.

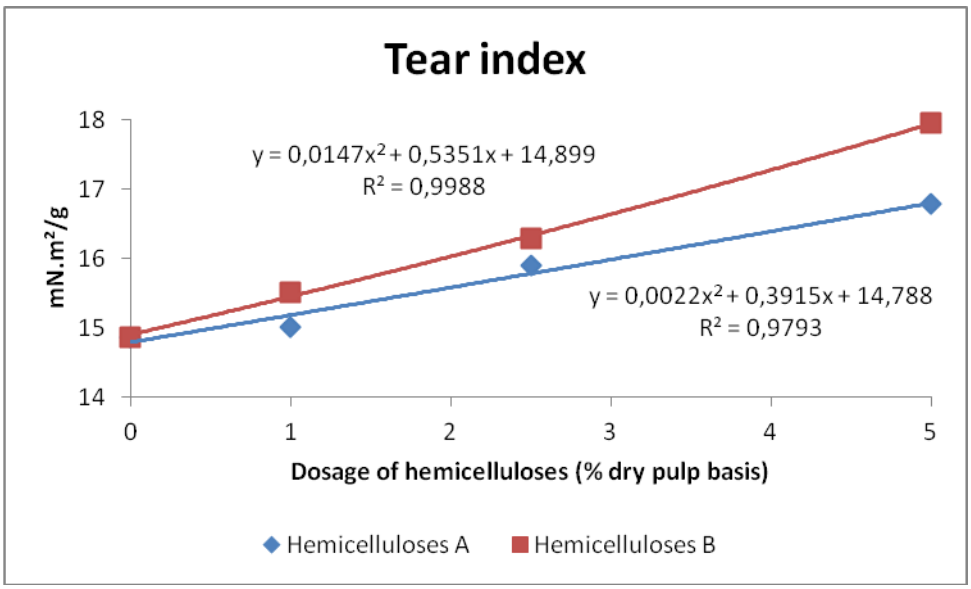

Figure 3. Tear resistance as a function of dosage of hemicelluloses.

It was observed that, for the same dosages, pulps which have received the Hemicelluloses B showed a greater tear resistance than those receiving Hemicelluloses A. The highest value was achieved at a maximum dose of 5 %, with an increase of 12.8% for pulps with addition of Hemicelluloses A, and 20.7% for those receiving Hemicelluloses B.

Researchers noted the same trend in the Pinus and Eucalyptus refined pulps and said that hemicelluloses improved the refining process, but at the same time reduced the tensile index with respect to the tear index, due to the decreased proportion of cellulose [40]. Other researchers found no change in fiber resistance with different percentages of hemicelluloses. They found no increase in tear index, although the tensile index of pulp has increased [18].

Bulk

Figure 4 shows the results of bulk for the papers produced by varying the dosage of hemicelluloses added. The highest values of bulk in papers were observed in papers with lower content of hemicelluloses, consequently generating denser papers insofar as the dose is increased.

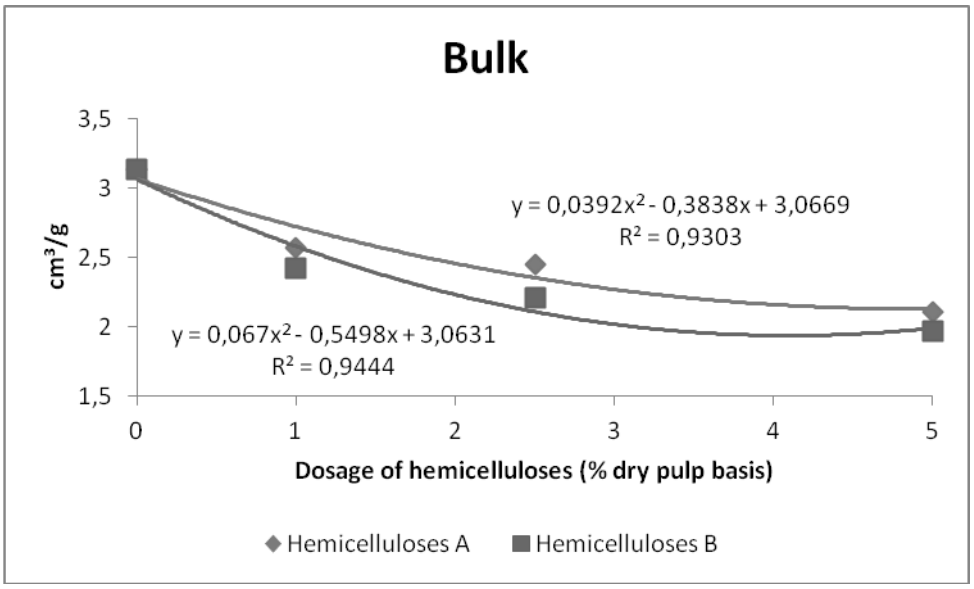

Figure 4. Bulk as a function of dosage of hemicelluloses.

In this study, the higher bulk was achieved in the papers without the addition of hemicelluloses (3.14 cm³/ g). It was observed that as the content of hemicelluloses increased, lower bulk were found in the results. In the dose of 5%, it was shown a

reduction of 48.8% on papers with the addition of Hemicelluloses A and 59.9% on papers with the addition of Hemicelluloses B.

Pulps rich in Hemicelluloses tend to produce high density paper and reduced volume, which is not interesting for tissue products. Moreover, printing and writing papers need traction and can benefit from pulps with high hemicellulose content [9, 19, 20].

CONCLUSIONS

Corn cobs are good sources of hemicelluloses, which is an alternative for the use of these carbohydrate residues in the manufacture of papers. The pulps with higher hemicelluloses content of hemicelluloses form paper with lower bulk, higher resistance to drainage and greater tensile and tear strengths. The two fractions of hemicelluloses found, when applied separately, resulted in paper with different physical and mechanical properties.

REFERENCES

1. Fengel, D.; Weneger, G., 1989. Wood chemistry, ultrastructure, reactions. Berlin: Walter de Gruyter.

2. Salmén, L.; Olsson, A-M., 1998. "Interaction between hemicelluloses, lignin and cellulose: structure – property relations". In: INTERNATIONAL SYMPOSIUM ON WOOD AND PULPING CHEMISTRY. Proceedings… Montreal: CPPA.

3. Silva, S. S.; Carvalho, R. R.; Fonseca J. L.;Garcia, R. B., 1998. Extração e Caracterização de Xilanas de Sabugos de Milho. Polímeros: Ciência e Tecnologia. Abril/Junho.

4. Yllner, S.; Enström, B., 1956. Studies on the adsorption of xylan on cellulose fibres during the sulphate cook. Part 1, Svensk Papperstidn, v. 5, p. 229-232.

5. Yllner, S.; Enström, B., 1957. Studies of the adsorption of xylan on cellulose fibres during the sulphate cook. Part. 2, Svensk Papperstidning, v. 60, n. 6, p. 449.

6. Aurell, R., 1965. Increasing kraft pulp yield by redeposition of hemicelluloses. Tappi 48 (2), 80-84.

7. Hansson, J.-Å.; Hartler, N., 1969. Sorption of hemicelluloses on Cellulose Fibres Part 1. Sorption of Xylans. Svensk Papperstidn, v. 72, p. 521–530.

8. Henriksson, Å.; Gatenholm, P., 2001. Controlled assembly of glucuronoxylans onto cellulose fibres. Holzforschung, Berlin, v. 55, n. 5, p. 494-502.

9. Schönberg, C.; Oksanem, T.; Suurnäkki, A.; Kettunem, H.; Buchert, J., 2001. The importance of xylan for the strength properties of spruce kraft fibres. Holzforschung, Berlin, v. 55, n. 6, p. 639-644.

10. Linder, A.; Bergman, R.; Bodin, A.; Gatenholm, P., 2003. Mechanism of assembly of xylan onto cellulose surfaces. Langmuir, v. 19, n. 12, p. 5072-5077.

11. Danielsson, S.; Lindström, M. E., 2005. Influence of birch xylan adsorption during kraft cooking on softwood pulp strength. Nordic Pulp & Paper Research Journal, Stockholm, v. 20, n. 4, p. 436-441.

12. Danielsson, S., 2007. Xylan reactions in kraft cooking. Ph.D thesis, Department of Fibre and Polymer Technology, KTH, Stockholm.

13. Köhnke, T.; gatenholm, P., 2007. The effect of controlled glucouronoxylan adsorption on drying-induced strength loss of bleached softwood pulp. Nordic Pulp & Paper Research Journal, Stockholm, v. 22, n. 4, p. 508-515.

14. Köhnke, T.; Pujolras, C.; Roubroeks, J. P.; Gatenholm., 2008. The effect of barley husk arabinoxylan adsorption on the properties of cellulose fibres. Cellulose, v. 15, n. 4, p. 537-546, ago.

15. Muguet, M. C. S., Colodette, J. L., and Pedrazzi, C., 2010. "Xylans deposition onto eucalyptus pulp fibers during oxygen delignification. Part 1: The influence of NaOH charge, reaction time and temperature," In: XXI Encontro Nacional da TECNICELPA / VI CIADICYP. Lisboa, Portugal.

16. Silva, J. C., 2011. Aplicação de enzimas, extração e adição de hemiceluloses combinadas com ondas ultrassônicas para desenvolvimento de propriedades de papéis reciclados. Master thesis - Universidade Federal de Viçosa, Brazil.

17. Milanez, A. F.; Barth, P. P. O.; Pinho, N. C.; Vesz, J. B. V., 1982. Influência das hemiceluloses nas propriedades óticas e físico-mecânicas da polpa. In: XV CONGRESSO E EXPOSIÇÃO ANUAL DE CELULOSE E PAPEL ABTCP, São Paulo. Anais… São Paulo: ABTCP, p. 155-170.

18. Molin, U.; Teder, A., 2002. Importance of cellulose/hemicellulose ratio for pulp strength. Nordic Pulp & Paper Research Journal, Stockholm, v. 17, n. 1, p. 14-19.

19. Anjos, O.; Santos. A.; Simões. R., 2005. "Efeito do teor de hemiceluloses na qualidade do papel produzido com fibra de Eucalipto". In: V CONGRESSO FLORESTAL NACIONAL, 2005, Portugal. Actas das comunicações. Viseu: SPCF.

20. Molina, E. M. A.; Mogollón, G.; Colodette, J. L., 2008. "Efecto de las xilanas en la refinabilidad y propiedades físico-mecánicas de pulpa kraft de eucalyptus spp.". In: CONGRESO IBEROAMERICANO de INVESTIGACIÓN en CELULOSA y PAPEL, 2008, Guadalajara. Anais... CIADICYP.

21. Manfredi , M., Oliveira, R. C., 2010. "Aplicação de tratamento ultrassônico da polpa e adição de xilanas na indústria de fibras secundária," In XXI Encontro Nacional da TECNICELPA / VI CIADICYP, Lisboa, Portugal.

22. Foelkel, C. E. B., 2007. As fibras dos eucaliptos e as qualidades requeridas na celulose Kraft para a fabricação de papel. Eucalyptus Online Book & Newsletter.

23. Leopold, B.; McIntosh, D. C., 1961. Chemical compositon and physical properties of wood fibres. III: Tensile strength of individual fibres from alkali extracted loblolly pine holocelulose. Tappi Journal v. 44, p. 235-240.

24. Petterson, S. E.; Rydholm, S. A., 1961. Hemicelluloses and paper properties of birch pulps. Svensk Paperstidning, v. 64, p. 4-17.

25. Spiegelberg, H. L., 1966. The effect of hemicelluloses on the mechanical properties of individual pulp fibres, Tappi Journal, v. 49, n.9, p. 388.

26. Kettunem, J.; Laine, J. E., Yrjälä, I.; Virkola, N.-E., 1982. Aspects of strength development in fibres produced by different pulping methods. Paperi Ja Puu, Helsinki, v. 64, n. 4, p. 205-211.

27. Osterberg, M.; Laine, J.; Stenius, P.; Kumpulaine, A.; Claesson, P. M., 2001. Forces between Xylan-Coated Surfaces: Effect of Polymer Charge Density and Background Electrolyte. Journal of Colloid and Interface Science, v. 242, p. 59–66.

28. Wang, X., 2006. Improving the papermaking properties of kraft pulp by controlling hornification and internal fibrillation. Doctoral Thesis, Helsinki University of Technology. Helsinki, Finland.

29. SILVEIRA, R.F.M., 2010. Atividades biológicas de xilana de sabugo de milho. Master thesis – Universidade Federal do Rio Grande do Norte, Natal.

30. Wallis A., Wearne R., Wright P., 1996. Chemical Analysis of Polysaccharides in Plantation Eucalyptus wood and Pulps. Appita Journal 49:258-262.

31. TAPPI Standard Procedures. 2001. TAPPI Press, Atlanta, USA.

32. Goldschmid, O., 1971. Lignins: occurrence, formation, structure and reations", Sarkanen; K. V.; Ludwig, C. H., eds.; John Wiley & Sons: New York.

33. Scott, R. W., 1979. Colometric determination of hexuronic acids in plant materials. Analytical Chemistry, n. 7, p. 936-941.

34. Solár R., Kacik F., Melcer I., 1987. Simple method for determination of O-acetyl groups in wood and related materials. Nordic Pulp and Paper Research Journal 4:139-141.

35. Anglés, M., Reguant, J., Martínez, J., Farriol, X., Montané, D., & Salvadó, J., 1997. Influence of the ash fraction on the mass balance during the summative analysis of high-ash content lignocellulosics. Bioresource Technology, 59, 185–193.

36. Van Dongen F.E.M., Van Eylen D., Kabel M.A., 2011. Characterization of substituents in xylans from corn cobs and stover. Carbohydrate Polymers 86:722-731.

37. Lili W., Yijun J., Chunhu L., Xiutao L., Lingqian M., Wei W., Xindong M., 2011. "Microwave-assisted hydrolysis of corn cob for xylose production in formic acid". In: International Conference Materials for Renewable Energy & Environment (ICMREE), p. 332-335.

38. Garrote, G., Cruz, J.M., Moure, A., om ngue , H., Parajó, J.C., 2004. Antioxidant activity of byproducts from the hydrolytic processing of selected lignocellulosic materials. Trends in Food Science & Technology 15, 191-200.

39. Batalha, L. A. R.; Colodette, J. L.; Gomide, J. L.; Barbosa, L. C. A.; Maltha, C. R. A.; Gomes, F. J. B., 2012. Dissolving pulp production from bamboo. BioResources 7(1), 640-651.

40. Salomão, K. G., 2001. Características e branqueabilidade de polpas kraft/ polissulfeto de eucalyptus e de pinus. Master thesis – Universidade Federal de Viçosa, Brazil.

Chapter 2

Biofilm from xylan-rich hemicelluloses

Abstract

Hemicellulose is a widely abundant polysaccharide in nature. Xylan-rich hemicelluloses were isolated of corn cob. Part of this material was acetylated and films from hemicelluloses non and modified were prepared. Reinforced agents as NFC, PAE resin and plasticizers were used in the films preparation. Non reinforced films were more brittle than others. HPLC, NMR and FTIR-ATR were used to characterize the material. Hydrophilicity of the films were evaluated by the contact angle with water and the mechanical properties were evaluated through tensile tests. Hemicellulose isolation can be considered efficient. The acetylation using pyridine and acetic anhydride allowed a substitution degree of 1.90. Reinforced films showed higher mechanical properties. The acetylation process resulted in highervalues of tensile index and strain for all formulation, if compared to unmodified hemicelluloses. All the films presented air passage resistence higher than 3 hours (10 cm^3).

Keywords: corn cob; mechanical properties; NFC; PAE resin; plasticizers.

INTRODUCTION

Hemicelluloses are polysaccharides widely abundant in nature, representing about 20–35% of lignocellulosic biomass. They are estimated to account for one-third of all renewable organic carbon available on earth (PRADE, 1995; SJOSTROM, 1981, SALAM, 2011). Unlike cellulose or starch, hemicelluloses have not yet been used in broad industrial applications similar to cellulose or starch (SUN et al., 2004; SALAM, 2011).

The content of xylan in corncob could go upto 40 g/100 g, the highest among of all the agricultural products (YANG et al., 2004). Hemicelluloses comprise about ∼20–35% of most plant materials, depending on the particular plant species, for example, wheat straw 32%, barley straw 32%, oat straw 27%, rye straw 31%, rice straw 25%, sunflower husk 23%, sugarcane rind 22%, and corn cobs 37% (SAHA, 2003).

The properties of hemicelluloses can be modified by, for example, partial hydrolysis, oxidation, reduction, etherification or esterification of hydroxyl groups, and cross linking. Acetylation of hemicellulose hydroxyl groups to increase hydrophobicity is an approach to increase water resistance and thus the product applications of hemicellulose (SUN et al., 2003). The resulting derivatives offer potential applications for the production of biodegradable plastics, resins and films. Several reports have also been made on the film forming properties of xylan and its blends (BUCHANAN et al., 2003;

GABRIELII et al., 2000; GOKSU et al., 2007; KAYSERILIOGLU et al., 2003; SHAIKH et al., 2009). However, some xylan-derived products have already found some commercial applications for ethanol production, xylitol, and xylooligosaccharides (DEUTSCHMANN and DEKKER, 2012; EGÜÉS, 2014).

Generally, biodegradable films are prepared by the casting method where the filmogenic suspension is deposited on a suitable surface and dried later. The film formation involves inter- and intramolecular bonds, thereby forming a semi-rigid three-dimensional network that retains and immobilizes the solvent. Whatever the production process, the transformation of the filmogenic solution in films or coverings is the result of intermolecular interactions, which allows structural strength (CARVALHO, 1997; MEIRA, 2012).

According to Lavorgna et al. (2010), a variety of strategies have been explored to improve the mechanical and barrier properties of the packaging films based on biopolymers, such as chitosan, including the addition of plasticizers (SRINIVASA et al. 2007), the preparation of blends using other biodegradable polymers (CORRELO et al. 2005), also the preparation of nanocomposites (RAY and BOUSMINA, 2005).

This study aimed to produce biofilm from hemicelluloses extracted from corn cob. Acetylation process was used to increase the hydrofilicity and the mechanical properties of the films. Besides, reinforced agents as NFC, PAE resin and plasticizers were used to help the enhancing of tensile resistance and strain, resulting in more flexible and resistant films.

METHODOLOGY

Hemicelluloses isolation

Hemicelluloses were obtained according to Silva et al. (2015), with adaptations. The procedure was repeated several times until the desired amounts of hemicelluloses were obtained.

Initially, corn cobs were exposed to sunlight for 48 hours to dry. They were then crushed in a mill and classified through a series of sieves. The fraction retained between 40 mesh and 60 mesh screens were used in the following steps.

The crushed material was subjected to aqueous extraction at a ratio of 30 g of powdered corn cobs to 1,000 ml of distilled water with constant stirring for 12 hours. Then,

the mixture was centrifuged and the solid phase was dried in climatic room at 23 °C and 50 % humidity for 24 hours.

After drying, the material obtained was subjected to the delignification process at 1:10 ratio(w/v) using hydrogen peroxide 2% (w/v) at pH 11 (adjusted with NaOH) and 70°C for 2 h. The delignified raw material was washed with distilled water with three times the volume of suspention.

Solubilization of hemicelluloses was performed by alkaline treatment, when the material was then subjected to 10% NaOH (w/w) at 25°C for 24 h, in low agitation, with 10% NaOH of corn cob powder at room temperature. A ratio of 1:10 (powder: NaOH) was used. Then, the solution was neutralized by adding glacial acetic acid to reach pH=7.0. The hemicelluloses were precipitated by the addition of ethanol in the proportion of three volumes of ethanol to 1 volume of the solution. The obtained product was centrifuged for 10 minutes, at 4000 rpm, resulting in a consistency of 20%.

Yield determination

The following formula was used to calculate yield of hemicelluloses isolation:

$$Y(\%) = \frac{m1}{m0} * 100$$

in which:

Y: yield

m1: final mass

m0: initial mass

NFC preparation

NFCs were prepared from bleached elemental chlorine free kraft wood fibers produced from Oak and provided as a never dried pulp with solid content of approximately 20 % (w/w). Typically, 1.2 % fiber suspension in water was processed in a high-pressure microfluidizer (Microfluidizer M- 110 T, Microfluidics Corp). The samples were passed twenty times through an intensifier pump that increased the pressure, followed by an interaction chamber which defibrillated the fibers by shear forces and impacts against the channel walls and colliding streams. The resulting NFC suspension was collected and stored at 4 °C in a cold room until needed.

Acetylation

The esterification of arabinoxylan was carried out using experimental conditions, as described by Stepan et al. (2011). Dry powder of hemicelluloses AX samples (1.00 g) were dispersed in formamide (25 mL). Pyridine (40 mL) was added, followed by acetic acid anhydride (6.6 mL). After stirring at room temperature for 3 h, another portion of acetic anhydride (6.6 mL) was added, followed by the same amount after other 3 h. After 30 h, the viscous dark solution was poured (under vigorous stirring) into 1.3 L of 2% ice-cold hydrochloric acid. The white fluffy precipitate was filtered on a buchner funnel with filter paper and washed with excess (0.5 L) deionized water, then with 0.5 L methanol and finally with 0.5 L diethyl-ether. The samples were then dried in fume hood overnight.

Quantitative chemical characterization

The carbohydrate composition of raw materials was established by High Performance Anion Exchange Chromatography with Pulse Amperometric Detection (HPAEC-PAD) after pre-treatment (30°C, 1 h) with aqueous 72% H_2SO_4 followed by hydrolysis with 3% H_2SO_4 in an autoclave (100°C, 3 h). HPAEC-PAD was carried out in a Dionex ICS-3000 system equipped with a CarboPac PA1 (250 x 4mm) analytical column. The monosaccharides were separated isocratically with 0.001 M NaOH (45 min, flowrate 1 mL/min) [30]. The solid residue after hydrolysis was considered as Klason lignin according to T222 cm-11 standard procedure [31]. Ashes were determined by calcination according to TAPPI standard T211 om-12 [31]. Acid soluble lignin was determined by measuring the UV-absorbance of the filtrate at 205 nm [32]. Total uronic acids in raw materials hydrolysates were measured by the colorimetric method involving 3,5-dimethylphenol [33]. The content of acetyl groups was also determined [34]. All results were calculated from two replicate determinations.

Pentosan quantification

The determination of pentosan content was made in according to TAPPI223 cm-10. Initially, 1 g of the sample was put in a boiling flask with 100 ml of sulfuric acid at (12% w/v). The flask was connected to the simple distillation apparatus, so it was added 300 mL of sufuric acid into separatory funnel. During the boiling time, pentosans were recovered by steam distillation. In the next step, the hydrolysate was heated and the distillate was collected in a 500 mL erlenmeyer flask immersed in an ice bath. For each 30

ml of hydrolysate obtained in the distillation, it was added 30 mL acid until reaching 300 mL of hydrolysate. The results were calculated from two replicate determinations.

It was added 50 mL of destilated water and 250 g of crushed ice to 300 mL of hydrolysate. Then, 20 mL of potassium bromate-bromide (0,2N) was added. After 5 minutes, 10 mL of the solution of potassium iodide (10 %) were mixed quickly. The solution was titrated with $Na_2S_2O_3$ (0,1 N) using corn starch as indicator.

Calculation of the pentosans content in the test specimen:

$$Pentosans(\%) = \left(\frac{7.5 * N * (V2 - V1)}{w}\right) - 1$$

Where:

N = normality of $Na_2S_2O_3$ solution

V2 = volume of $Na_2S_2O_3$ solution consumed in the blank test (mL)

V1 = volume of $Na_2S_2O_3$ solution consumed in the titration (mL)

w = od sample weight (g)

Nuclear magnetic resonance analysis

Nuclear magnetic resonance analysis (NMR) measurements were carried out on the isolated hemicelluloses, acetylated and non-acetylated (native). The native and acetylated hemicelluloses (~10mg) were dissolved in 0.4 mL DMSO-d6 and $CDCl_3$-d6, respectively. One dimensional 1 H NMR spectra was acquired with an MERCURY-300/Varian spectrometer at 300.069 MHz (32 k data points, 30 excitation pulse duration of 2.2 ls, spectral width of 6 kHz, acquisition time of 3.3 s and relaxation delay of 10 ms) in 5 mm probes with direct detection, using TMS as internal standard (d = 0.00).

Degree of substitution (DS)

The degree of substitution (DS) of modified arabinoxylan was determined through the Equation below. The data obtained by 1H-NMR spectra.

$$DS = \frac{Im}{(3 * Ix) + (2 * Ia)}$$

In which

DS: degree of substitution

Im: area of methyl protons of ester chains at 1.9–2.0 ppm

Ix: area of anomeric proton of xylan at 4.5 ppm

Ia: area of anomeric proton of d-Arabinofuranosyl anomeric at 5.0 ppm

Fourier transform infrared spectroscopy - Attenuated total reflection (FTIR-ATR)

A Varian 660-IR spectrometer equipped with a liquid nitrogen-cooled mercury cadmium telluride detector and an attenuated total reflectance (ATR) probe was used in this work. The sample was put on the ATR probe to collect FTIR spectrum. During the experiment, 60 scans were coadded to achieve an acceptable signal-to-noise ratio, with wave number ranging from $4000\,cm^{-1}$ to $500\,cm^{-1}$. All the spectra were recorded at a resolution of $4\,cm^{-1}$.

Acetyl groups

The acetyl groups were liberated by acidolysis of 300 mg hemicelluloses, added 20 mL of oxalic acid solution (1.2 mol/L), at high temperature (120°C) during 80 minutes (SÓLAR et al., 1987). Then, 200 mL of destilated water was added, the pH was adjusted to 3±0.1 (10% NaOH), and the volume was completed to 200 mL. The acetic acid was then quantified by HPLC equipment.

Casting films

The films were prepared by dissolving 1 g of arabinoxylan (AX) and acetylated arabinoxylan (AXac) in water and chloroform (30 mL), respectively. The other components (NFC, PAE resin and plasticizers) were dosed based on the dry hemicelluloses weight (w/w). Samples solubilizated in deionized water were dried at 45 °C, overnight. The samples solubilizated in chloroform were covered with a glass cover with only a small opening to prevent a too fast solvent evaporation that would result in an uneven surface or formation of bubbles in the films, which were allowed to dry in a fume hood.

Ten samples of each formulatio were preparedn. Table 1 summarizes the composition of the films.

Table 1. Formulation of different films.

Film	Kind of arabinoxylan (1g)	Solvent (30mL)	Nanocellulose (5%)	Resin (5%)	Plasticizer (5%)
F1	AX	water	-	-	-
F2	AX	water	NFC	-	-

F3	AX	water	-	PAE	-
F4	AX	water	-	-	Potassium biphthalate
F5	AX	water	-	-	Polyethylene glycol
F6	AX	water	-	-	Glycerol
F7	AX	water	NFC	-	Potassium biphthalate
F8	AX	water	NFC	-	Polyethylene glycol
F9	AX	water	NFC	-	Glycerol
F10	AX	water	-	PAE	Potassium biphthalate
F11	AX	water	-	PAE	Polyethylene glycol
F12	AX	water	-	PAE	Glycerol
F13	AXac	chloroform	-	-	-
F14	AXac	chloroform	NFC	-	-
F15	AXac	chloroform	-	PAE	-
F16	AXac	chloroform	-	-	Potassium biphthalate
F17	AXac	chloroform	-	-	Polyethylene glycol
F18	AXac	chloroform	-	-	Glycerol
F19	AXac	chloroform	NFC	-	Potassium biphthalate
F20	AXac	chloroform	NFC	-	Polyethylene glycol
F21	AXac	chloroform	NFC	-	Glycerol
F22	AXac	chloroform	-	PAE	Potassium biphthalate
F23	AXac	chloroform	-	PAE	Polyethylene glycol
F24	AXac	chloroform	-	PAE	Glycerol

Contact angle measurement

The hydrophobic/hydrophilic character of the films was measured by static contact angle. An optical microscope was adaptated and the Image Pro Plus software, version 3.0.1, was used to measure the angle of the drop under the film. A 5 µL drop of deionized water was placed on the surface of the films, and the contact angle was read after 30 s of contact. Three measurements were carried out for each sample and the average values were calculated.

Determination of mechanical properties by tensile testing

The mechanical properties of the films were evaluated in tensile mode on an Instron 4204, using a computerized system for acquisition, analysis and output of datas, with 100 mm of initial distance between clamps, test speed of 25 mm / min and load cell capacity of 1000 N. Five specimens were tested for each sample and the preparation of these proof bodies were made in a paper cutter. The films were tested in ambient conditions with relative humidity of 50 ± 2% and temperature of 23 ± 1 °C (TAPPI 402 SP- 98).

RESULTS AND DISCUSSION

As shown in Table 2, the process used to isolate hemicelluloses can be considered efficient i.e. from raw material, with the total concentration of xylose and arabinose (monomers observed in this study) of 33.4%; it was obtained xylose and arabinose concentration of 53 %, from a process with yield of 60 %. Therefore, the xylose- and arabinose final yield was 31.8 %, which means 25.24 % of xylan and 2.75% of arabinan i.e. 27.99 % of arabinoxylan.

Table 2. Carbohydrates analysis of raw material (RM) and isolated hemicelluloses (IH)

	Glc[a]	**Xyl[a]**	**Ara[a]**	**Gal[a]**	**Man[a]**	**AG**	**AX[b]**	**X/A[c]**
RM	47.1	28.0	5.4	2.2	0.2	2.9	29.39	0.19
IH	5.7	47.8	5.2	0.9	-	12.1	46.64	9.19

[a]Abbreviations. Ara: arabinose; xyl: xylose; man: mannose; gal: galactose; glc: glucose; AG: acetyl groups;
[b]AX: 0,88*(% xyl + % ara);
[c]X/A: xylose to arabinose ratio

To assure that the values obtained by carbohydrate analysis were correct, the pentosan analysis was performed. This procedure is justified because part and/or all material could have been converted into other compounds during the hydrolysis process, such as furfural. The result obtained to pentosans in the isolated hemicelluloses material was of 52 %, which validates the carbohydrate analysis.

Initially, it was possible to realize the difference in the coloring between the native and the modified arabinoxylan, wherein the latter changed from dark yellow to light yellow. The production of arabinoxylan acetates was evaluated through FTIR-ATR and NMR.

FTIR-ATR spectrum of arabinoxylan and acetylated arabinoxylan were shown in Figure 1 A and B, respectively. The typical signal pattern for hemicellulosic moiety, and had a specific band maximum in the 1200–1000 cm^{-1} region (SUN et al., 2004). At 1037 cm^{-1}, was possible to see stretching and bending vibrations of C–O, C–C, C–OH, and C–O–C. According to Sun et al. (2004), bands between 1175 and 1000 cm^{-1} are typical of xylans. It was possible to see two low-intensity shoulders at 1037 cm^{-1} peak (at 1175 and 990 cm^{-1}), which have been reported to be attached only at positions of the xylopyranosyl constituents (SUN and TOMKINSON, 2002). The intensity changes of these two bands indicate the contribution of arabinosyl substituent. Therefore, it was used for the identification of arabinoxylan structures. That is, this band gives variation in spectral shape depending on the branches at the O-2 and O-3 positions (SUN et al., 2004).

The FT-IR was carried out, mainly, to assure that the acetylation process really had happened. The bands found at 3323 and 2981–2885 cm^{-1} indicate the OH stretching and CH bond deformation of CH2 CH3 groups, respectively (EGÜÉS et al., 2014). The prominent band around 3323 cm^{-1} (Figure 1.A) represents the hydroxyl stretching vibrations of the hemicelluloses and water involved in hydrogen bonding (SUN et al. 2004). The decrease of the band at 3323 cm^{-1} (Figure 1.B) indicates that hydroxyl groups and adsorbed water were almost completely substituted during acetylation process. Other two peaks at 1552 and at 1412 cm^{-1} were observed and correspond to CH and OH bending, respectively (SUN and TOMKINSON, 2002; EGÜÉS et al., 2014). Acetylation could be clearly verified by the presence of three important ester bands at 1735 cm^{-1}, C=O ester, at 1369 cm^{-1}, -C-CH_3, and at 1212 cm^{-1}, -C-O- stretching band (SUN, SUN,ZHAO, et al., 2004). The lack of peaks at 1840–1760 cm^{-1} (Figure 1.B) suggests that the product is free from the unreacted acetic anhydride (SUN, SUN, ZHAO, et al., 2004).

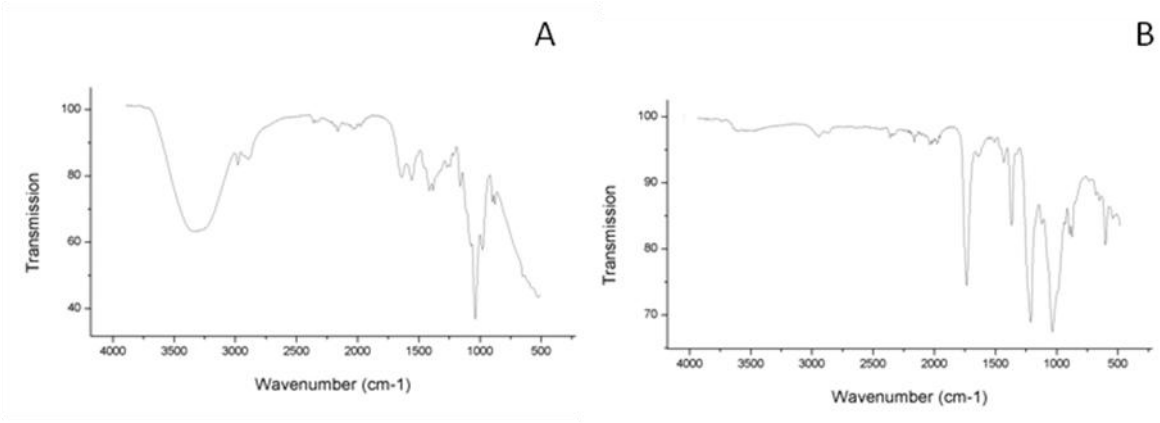

Figure 1. FT-IR spectra. A) unmodified hemicelluloses B) acetylated hemicelluloses

The efficiency of acetylation reaction was also verified by ^{1}H NMR, as shown in the Figure 2. Important peaks appeared in the spectrum at 1.9-2.0, 4.5 and 5.0 ppm, indicating methyl protons of ester chains, anomeric proton of xylan and anomeric proton of d-Arabinofuranosyl, respectively (EGÜÉS et al., 2014; SUN et al., 2004). Also, the acetyl group analysis indicated the presence of 16.1% of acetyl groups after the acetylation process.

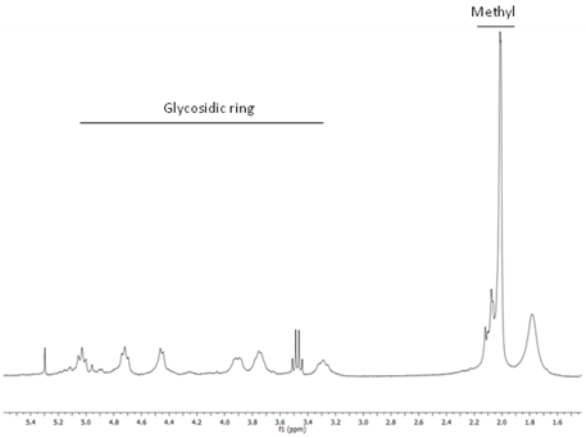

Figure 2. 1H NMR spectrum acetylated hemicelluloses (dissolved in CDCl3-d6).

The value of DS acetytaled arabinoxylan was 1.90. Taking into account that the average number of available OH groups per xylan unit is 2 and per arabinose is 3, the degree of substitution maximum that should be achievedwas also calculated. The degree of Arabinose substitution of xylan is the key factor that positively affects the maximum degree of substitution and the ratio obtained among xylose and arabinose was 9.19 i.e., to each 9 units of xylose there is 1 unit of arabinose, aproximely, as exemplify in the Figure 3.B. So, the maximum degree of substitution of this material is 2.076, obtained through the sum of available OH groups per sugares multiplied by the sugares concentraction. Other authors found different values to DS of different raw material by NMR spectrum e.g. Ren et al. (2007) obtained degree of substitution of acetylated hemicelluloses between 0.49 and 1.53 by variation of the conditions of reaction, such as reaction temperature, reaction time, dosage of catalyst and amount of acetic anhydride. Egüés et al. (2014) achieved a DS of 1.9 to arabinoxylan from corncob.

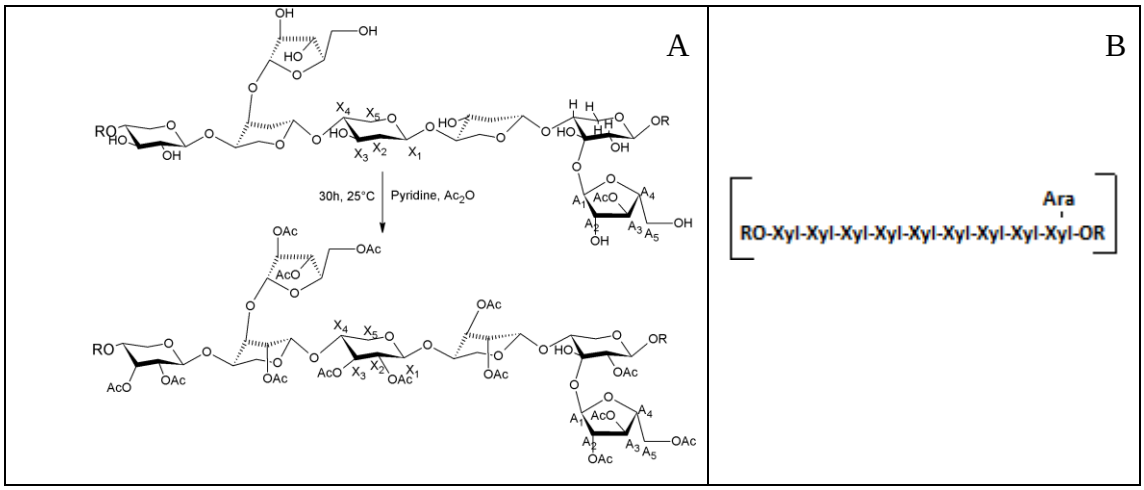

Figure 3. A. Acetylation reaction. B. Arabinoxylan structure

The results obtained through contact angle measurement (Table 3) allowed to divide the formed films in two groups. The first one is composed by films from unmodified hemicelluloses (contact angle, 0° to 30.64°), which presented a hydrophilic feature. These may be due to the larger availability of reactive OH-groups on the surfaces of these films (F1-F12). The film (F1) soak water rapidly (contact angle, 0°) and some specimens were dissolved in contact with water, which classifies this film as superhydrophilic (ARKLES, 2006). The second group, composed by films from modified hemicelluloses (F13-F24), presented a contact angle of 99.01° to 101.70°. This range of values classifies the films as hydrophobic. As the hydrophobicity increases, the contact angle of the droplets with the surface increases. Surfaces with contact angles greater than 90° are designated as hydrophobic (ARKLES, 2006). Hydrophobicity dependson the efficiency of acetylation process, i.e. by the hydroxyl groups substituted by acetyl groups (it indicated by DS). The avarage of the contact angle measurements might indicate a trend, but there were no significant differences between the samples, into the same group, because of the overlap of the standard deviation of the measurements.

Mechanical property data (tensile index, strain and MOE) of acetylated and non-hemicelluloses-based films were shown in Table 3. All treatments made with hemicelluloses resulted in films with higher strength if compared with film composed exclusively by non acetylated hemicelluloses (Formulation F1). Films of this formulation (F1) were more brittle, in the tensile test, showing lower strain capacity and breaking at smaller extension rates than the other samples. This is supported by the strain and tensile index values.

Table 3. Mechanical properties and water contact angle of films

Arabinoxylan					**Acetylated arabinoxylan**				
Film	**Tensile index (N.m/g)**	**Strain (%)**	**MOE (MN.m/Kg)**	**Contact angle (°)**	**Film**	**Tensile index (N.m/g)**	**Strain (%)**	**MOE (MN.m/Kg)**	**Contact angle (°)**
F1	11.98 ± 2.62	0.11 ± 0.06	3.50 ± 0.05	0.00 ± 0.00	F13	33.52 ± 2.28	0.39 ± 0.06	3.87 ± 0.08	100.16 ± 0.15
F2	15.95 ± 0.93	0.68 ± 0.13	3.35 ±0.06	4.34 ± 0.78	F14	40.82 ± 3.87	0.66 ± 0.08	3.21 ± 1.76	99.06 ± 0.66
F3	16.02 ± 4.30	0.43 ± 0.17	4.04 ± 1.33	12.12 ± 0.28	F15	41.45 ± 0.64	0.45 ± 0.08	3.65 ± 0.03	100.42 ± 0.08
F4	16.23 ± 2.96	2.48 ± 0.09	1.67 ± 0.02	26.24 ± 1.82	F16	34.95 ± 0.92	5.28 ± 0.04	0.67 ± 0.06	100.66 ± 0.23
F5	17.10 ± 0.76	2.11 ± 0.09	1.39 ± 0.07	30.18 ± 0.25	F17	35.33 ± 0.85	9.61 ± 0.17	0.39 ± 0.05	101.18 ± 0.11
F6	16.98 ± 0.62	2.53 ± 0.15	2.03 ±0.18	20.34 ± 0.21	F18	38.45 ± 1.33	9.83 ± 0.88	0.45 ± 0.93	99.01 ± 0.34
F7	17.28 ± 1.87	2.75 ± 0.14	1.54 ± 0.03	27.78 ± 0.23	F19	49.56 ± 0.94	9.43 ± 0.14	0.54 ± 0.03	101.40 ± 0.23
F8	18.23 ± 2.44	3.73 ± 0.09	1.39 ± 0.05	30.64 ± 0.34	F20	59.17 ± 2.69	9.65 ± 0.08	0.39 ± 0.03	101.30 ± 0.07
F9	18.02 ± 0.23	2.98 ± 0.23	1.53 ± 0.99	24.76 ± 0.23	F21	58.05 ± 3.98	9.54 ± 0.98	0.42 ± 0.43	99.23 ± 0.09

F10	16.50 ± 3.61	1.59 ± 0.024	1.69 ± 0.62	27.5 ± 0.21	F22	35.21 ± 1.34	4.64 ± 0.21	0.70 ± 0.03	101.44 ± 0.05
F11	17.33 ± 0.48	1.23 ± 0.09	1.34 ± 0.02	30.26 ± 0.18	F23	37.45 ± 0.85	4.98 ± 0.06	0.34 ± 0.04	101.70 ± 0.20
F12	18.21 ± 1.02	2.02 ± 0.054	1.32 ± 0.32	25.01 ± 0.21	F24	39.01 ± 0.99	4.93 ± 1.23	0.54 ± 0.78	99.98 ± 0.32

The addition of reinforced agents as NFC, and other components such as resin and plasticizers resulted in improved mechanical properties of the films. In the group of unmodified hemicelluloses, the addition of PAE resin resulted in a more rigid film, with higher MOE (4.04 MN.m/Kg). The addition of the plasticizers gave to films a ductility feature, as the films presented great elongation requesting less or the same force as those films without the addition of plasticizers. Also considering this group, the combination of hemicelluloses, NFC and polyethylene glycol (formulation F8) resulted in a set of values that indicates that this formulation is the best, allowing uses for examples to packing. The film F8 showed an increase of 52.17 % over the tensile index, 3,290.90 % increase in deformation and reduction of 60.29 % in the MOE compared to F1. An increase of 6.61 % over the tensile index, 76.77 % increase in deformation and the same value to MOE compared to F5, showing that the introduction of NFC in the polymer matrix resulted in a tougher film. Egüés et al. (2014) obtained films from corn cob with 9.02 MPa of stress and higher strain (8.10 %) if compared to this study. Films produced from chitosan,were very brittle. and After addition of polyethylene glycol, Fiori and Gabiraba (2014) reported that the films showed an increase of 38% in stress at break, a 95% increase in deformation and reduction of 28.75% modulus (Young). Films from corn hull arabinoxylan containing glycerol and sorbitol exhibited negative dependency on plasticizer concentration for tensile strength and elastic modulus, although increasing plasticizer concentration increased elongation (ZHANG and WHISTLER, 2004).

The acetylation process resulted in higher values of tensile index and strain for all formulation, if compared to unmodified hemicelluloses. Only the acetylation (F13) provided an increasing of 179.80 % over the tensile index, 254.54 % increase in deformation and a increase of 10.57 % in the MOE, compared to F1. Egüés et al. (2014) also observed an increased tensile strength, elongation at break and Young's modulus after the acetylation process of arabinoxylan. According to these authors, the elongation improved, due to internal plasticization of acetyl groups. At the same time, the strength and modulus were enhanced, owed to the elimination of OH groups and reduced water sensitivity. In the films from acetylated hemicelluloses added of plasticizers, the properties

as tensile strength (evaluated by tensile index) and strain increased although the MOE decreased, which shows the capacity of these additives to decrease film rigidness.

All the films presented an air passage resistence higher than 3 hours (10 cm^3).

CONCLUSIONS

The results obtained in this study showed that the hemicelluloses extraction process was efficient. The isolated hemicelluloses from corn cob allowed the biofilm production with mechanical properties values near to the expected to use like coating and packing films. The acetylation improved the mechanical properties of films even more, besides increasing the hydrophobicity of the films. The reinforced agents used (NFC, PAE resin and plasticizers) allowed the enhancing of the films although the addition of these materials did not significantly influence the wetting by water, evaluated by contact angle analysis. The addition of plasticizers resulted in films with higher tensile strength and strain values, wherein the combination of Polyethylene glycol with NFC resulted in greater films in both groups, from unmodified and acetylated hemicelluloses. All the biofilms presented efficient property of air barrier.

SUGGESTIONS FOR FUTURE WORK

- Use a process of purification and clarification of hemicelluloses obtained and obtantion of biofilms with this material;
- Evaluate the effects of storage in the mechanical properties;
- Perform biodegradability testing of the formed films;
- Optimize the addition of reinforcing agents, obtaining the best dosage of application of each additive;
- Use an acetylation process within the green chemistry concepts.

REFERENCES

Prade, R. A. Xylanases: From biology to biotechnology. Biotechnology and Genetic Engineering Reviews, 13, 101–131. (1995)

Sjöström, E. Wood chemistry, fundamentals and applications. San Diego: Academic Press. (1981)

Salam et al. Carbohydrate Polymers 84. 1221–1229 (2011)

Sun, X. F., Sun, R. C., & Sun, J. X. Oleoylation of sugarcane bagasse hemicelluloses using N-bromosuccinimide as a catalyst. Journal of the Science of Food and Agriculture, 84(8), 800–810 (2004).

Sun, X.F., Sun, R.C., Tomkinson, J., Baird, M.S. Preparation of sugarcane bagasse hemicellulosic succinates using NBS as a catalyst. Carbohydr. Polym. 53 (4), 483–495. (2003)

Buchanan, C. M., Buchanan, N. L., Debenham, J. S., Gatenholm, P., Jacobsson, M., Shelton, M. C., et al. Preparation and characterization of arabinoxylan esters and arabinoxylan ester/cellulose ester polymer blends. Carbohydrate Polymers, 52(4), 345–357 (2003)

Gabrielii, I., Gatenholm, P., Glasser, W. G., Jain, R. K., & Kenne, L. Separation, characterization and hydrogel-formation of hemicellulose from aspen wood. Carbohydrate Polymers, 43(4), 367–374 (2000)

Goksu, E. I., Karamanlioglu, M., Bakir, U., Yilmaz, L., & Yilmazer, U. Production and characterization of films from cotton stalk xylan. Journal of Agricultural and Food Chemistry, 55(26), 10685–10691 (2007)

Kayserilioglu, B. S., Bakir, U., Yilmaz, L., & Akkas, N. Use of xylan, an agricultural by-product, in wheat gluten based biodegradable films: Mechanical, solubility and water vapor transfer rate properties. Bioresource Technology, 87(3), 239 246 (2003).

Shaikh, H. M., Pandare, K. V., Nair, G., & Varma, A. J. Utilization of sugarcane bagasse cellulose for producing cellulose acetates: Novel use of residual hemicellulose as plasticizer. Carbohydrate Polymers, 76(1), 23–29 (2009)

Deutschmann, R., & Dekker, R. F. H. From plant biomass to bio basedchemicals: Latest developments in xylan research. Biotechnology Advances, 30,1627–1640 (2012)

Egüés et al. / Carbohydrate Polymers 102, 12– 20 (2014)

Meira,V. Preparação e caracterização de filmes de amido modificado por reticulação, acetilação e com adição de lipídio e celulose bacteriana. Thesis. Florianópolis (2012)

Carvalho, R.A. Desenvolvimento e caracterização de biofilmes a base de gelatina. Dissertação de Mestrado. Universidade Estadual de Campinas, Faculdade de Engenharia de Alimentos, (1997)

Silva et al. Extraction, Addition and Characterization of Hemicelluloses from Corn Cobs to Development of Paper Properties. Procedia Materials Science. Volume 8C, Pages 793-801 (2015)

Stepan et al. Arabinose Content of Arabinoxylans Contributes to Flexibility of Acetylated Arabinoxylan Films. Journal of Applied Polymer Science (2012)

TAPPI Standard Procedures. TAPPI Press, Atlanta, USA (2001)

Goldschmid, O., Lignins: occurrence, formation, structure and reations", Sarkanen; K. V.; Ludwig, C. H., eds.; John Wiley & Sons: New York. (1971)

Scott, R. W. Colometric determination of hexuronic acids in plant materials. Analytical Chemistry, n. 7, p. 936-941 (1979)

Solár R., Kacik F., Melcer I. Simple method for determination of O-acetyl groups in wood and related materials. Nordic Pulp and Paper Research Journal 4:139-141 (1987)

Sun et al. Fractional extraction and structural characterization of sugarcane bagasse hemicelluloses. Carbohydrate Polymers 56, 195–204 (2004)

Sun, R. C., & Tomkinson, J. Characterization of hemicelluloses obtained by classical and ultrasonically assisted extractions from wheat straw. Carbohydrate Polymers, 50, 263–271 (2002)

Sun, X. F., Sun, R. C., Zhao, L., & Sun, J. X. (2004). Acetylation of sugarcane bagassehemicelluloses under mild reaction conditions by using NBS as a catalyst. Journalof Applied Polymer Science, 92, 53–61.

Ren, J.L., Sun, R.C., Liu, C.F., Coa, Z.N., Luo, W. Acetylation of wheat straw hemicelluloses in ionic liquid using iodine as a catalyst. Carbohydr. Polym. 70 (4), 406–414 (2007)

Arkles, B. Hydrophobicity, Hydrophilicity and Silanes. Issue of Paint & Coatings Industry magazine (2006)

Zhang and Whistler. Mechanical Properties and Water Vapor Permeability of Thin Film from Corn Hull Arabinoxylan. Journal of Applied Polymer Science, Vol. 93, 2896 2902 (2004)

Chapter 3

Effects of Micro- and Nano- Cellulose Structures on the Pulp and Paper Properties

Abstract
Refining is an extremely important operation in the papermaking industry because it promotes changes in the fibrillar structure, which provides a higher grade of paper. However, this operation, when performed in inadequate intensity may result in reduced quality of the paper. Under this view, the nanocelluloses arise, which may partially replace the refining operation, when incorporated into the pulp. Thus, the objectives of this study were obtaining and characterizing cellulose nano- and micro- fibrils, and cellulose nanocrystals. Also, to evaluate the effect of incorporation of cellulose nano- and micro-fibrils and nanocrystals in the unbleached pinus pulp, on the physical and mechanical paper properties, for paper production for packaging purposes. The microfibrillated celluloses, nanofibrillated celluloses and cellulose nanocrystals obtained were characterizaded through analyses that evaluated the thermal degradation, zeta potencial and sizes of cellulose structures, X-ray diffraction and thermal degradation. The nanocelluloses were added in unbleached hardwood kraft pulp, previously refined in different intensities, and the physical and mechanical properties of the paper produced were evaluated. It was possible to realize that properties dependent on higher fiber bonding were enhanced with the incorporation of nanocelluloses. However, the properties dependenton the intrinsic strength of the fiber and its length decrease when added to refined pulps at higher intensities. Thus, it was observed that the treatments suggested in this study influenced significantly the mechanical strength properties of the paper, but it should be considered that the incorporation of nanocelluloses (MFC, NFC and CNC) to make paper should be performed considering some very important parameters, such as the amount to be added and the degree of refining of the initial pulp.

Keywords: nanocelluloses, microfibrillated cellulose, nanofibrillated cellulose, cellulose nanocrystal, nanostructured paper

---

INTRODUCTION

In the last decade, there was a growing interest from industry in the use of nano-sized cellulose, especially for polymer applications in packaging, biomedicine, adhesives, fibers, electronics and automotives (ZIMMERMANN et al., 2010). Nanocelluloses are described as the products or extracts from native cellulose (found in plants, animals, and bacteria) composed of the nanoscaled structure material (LIN and DUFRESNE, 2014). Nanocellulose is considered a sustainable nanomaterial due to its ready availability, biodegradability, and biocompatibility (HAORAN WEI et al, 2014). In papermaking, nanotechnological advances were reported about a decade ago, though it could not be

commercialized at a large scale. Nanofiber, nanofiller, nanocomposites and nanoscale chemicals are being investigated to be used in pulp and paper applications (CHAUHAN and K.CHAKRABARTI, 2012).

Three types of nanocellulosic materials have been investigated in recent decades. The first is microfibrillated cellulose, which is prepared by mechanical processes that involve very high shear forces to defibrillate cellulose fibers; the second – cellulose nanocrystals, which are prepared by the acid hydrolysis of cellulose fibers, followed by mechanical action; and the third – nanocomposites, which may be the combination of the first and second types of nanocellulosic materials, along with polymers or other matrices (CHAUHAN and CHAKRABARTI, 2012).

Recent studies have shown that microfibrillated cellulose (MFC) can be used as strength enhancer (IWAMOTO et al. 2007; ERIKSEN et al. 2008; AHOLA et al. 2008; SUBRAMANIAM 2008; MÖRSEBURG, CHINGA-CARRASCO 2011; ZIMMERMANN et al. 2010; TAIPALE et al. 2010; HII et al, 2012). MFC could be as small as 3-10 nm in thickness with typically a broad range of 20-40 nm, since it consists of aggregates of cellulose microfibrils (CHAUHAN & K.CHAKRABARTI, 2012). Eriksen et al. (2008) found significant tensile index increase at 4% addition of MFC to TMP handsheets, independent of the production method. Mörseburg and Chinga-Carrasco (2009) added MFC to clay loaded layered TMP sheets and found that the strength properties improved. The addition of MFC also increased air resistance (ERIKSEN et al. 2008; SUBRAMANIAM 2008). Taipela et al. (2010) found that the optimal level of MFC addition would maintain or improve strength properties without impeding dewatering. Synergy effects of MFC– filler interactions can counteract the reduction in strength properties from filler addition while improving light scattering (MÖRSEBURG and CHINGA-CARRASCO, 2009).

The benefits of using NFC as reinforcement in paper have been explored only recently, but there are signs of improvement in permeability and tensile index (ERIKSEN et al. (2008); MÖRSEBURG, CHINGA-CARRASCO 2009, TAIPALE et al. 2010), ZHANG et al. 2012, GONZÁLEZ, 2012). Cellulose nanopaper is a network composed of intertwined nanofibrils, with an aspect ratio exceeding 100 and with randomin-the-plane nanofibril orientation (HENRIKSSON et al., 2008). The nanopaper obtained, after NFC, exhibited high tensile properties, high optical transparency, and low thermal expansion properties. (WANG et al., 2013). The improvement in mechanical properties of paper after

the addition of NFC can be compared with the properties of paper made from both unbeaten and slightly beaten pulps (GONZALEZ et al., 2012).

According to Samir et al. (2005) and Silva and D'Almeida (2009), CNC has potential for industrial application. These authors cite two fields of application: The first, for optical applications in security papers, and the second, for the improvement of the mechanical resistance of low-thickness polyelectrolyte films in lithium cells.

The main properties of papers for the manufacture of flexible packaging papers are high tensile strength, burst and tear. These physical and mechanical properties, along with the weight, thickness and moisture, give the papers made the necessary requirements of quality to meet the purposes intended, (ASSOCIAÇÃO BRASILEIRA TÉCNICA DE CELULOSE E PAPEL, 1994). According to the Associação Brasileira Técnica de Celulose e Papel (1994), the papers for the production of rigid packaging must provide the high resistance to ring compression, corrugated compressive strength and stiffness as their main properties, and should provide the highest relationship of "resistance / weight of the structure" the possible. For such, a determining factor is the quality of the produced pulp and the delignification degree. The kraft pulp for the manufacture of paper for rigid packaging generally exhibits Kappa numbers between 70 and 100, providing great contributions to the paper stiffness properties (FRINHANI and DALTOÉ, 2012).

Based on these data, the objectives of this study were obtaining and characterizing cellulose nano- and micro- fibrils, and cellulose nanocrystals and evaluating the effect of the incorporation of cellulose nano- and micro- fibrils and nanocrystals in the unbleached pinus pulp, on the physical and mechanical paper properties, for paper production for packaging purposes.

MATERIAL AND METHODS

MFC preparation

Industrial MFC was used in this study. An unbleached softwood pulp was processed using a combined refining and enzymatic pre-treatment followed by high-pressure homogenization.

NFC preparation

NFCs were prepared from unbleached kraft wood fibers produced from Oak and provided as a never dried pulp with a solids content of approximately 20 % (w/w).

Typically, 1.2 % fiber suspension in water was processed in a high-pressure microfluidizer (Microfluidizer M- 110 T, Microfluidics Corp). Samples were passed twenty times through an intensifier pump that increased the pressure, followed by an interaction chamber which defibrillated the fibers by shear forces and impacts against the channel walls and colliding streams. The resulting NFC suspension was collected and stored at 4 °C in a cold room until needed.

CNC preparation

Initially, 30g of cotton was added in 1.5 L of NaOH solution (4%) at 80 °C, during 2 hours. Then, the liquid was filtred and the cotton was washed until the complete removal of sodium hydroxide, finalizing with use 500 mL of acetone. Hydrolysis was performed at 55 °C with 65% H2SO4 at 1-to-10 (w:v) pulp-to-acid ratio. The reaction was stopped by diluting ten times with deionized water. The suspension of CNC was filtered on a glass fiber circle with a pore size of 1.2 μm to remove the larger particles. Centrifugation of the solution at 4,000 rpm for 25 min separated the solids from the acidic liquid in the suspension. The remaining CNC was washed with deionized water three times (15,000 rpm, 20 m), until further centrifugation was incapable of further precipitation of the solid content from water. Finally, the CNC suspension was placed in a dialysis tubing cellulose membrane (43mm x 27mm, Sigma-Aldrich), dialyzed against flowing deionized water until the pH did not change.

Transmission Electron Microscopy (TEM)

Nanoparticle shape was observed by transmission electron microscopy (Zeiss EM 109) operated at 80 KV. For each sample, 20 μL of a suitably diluted MFC, NFC or CNC suspension was applied to a TEM grid (FCF 300-Cu, Formvar® carbon film on a 300 mesh copper grid). Samples were stained with 2% (w/v) uranyl acetate.

Zeta potencial and sizes of cellulose structures

The zeta potential and size of nanoceluloses were determined by dynamic light scattering technique (Dynamic Light Scattering - DSL) and by measuring the electrophoretic mobility using the equipment Zetasizer, Nano Series from Malvern Instruments. Aliquots (3 ml) of each sample were taken and placed in polystirene latex cuvette at 25 °C, performing the dilution more concentrated samples for reading in the

equipment. The samples used to size determination received one drop of sodium pyrophosphate solution (0.1%).

X-ray diffraction

The X-ray diffraction analyses were made at room temperature, using Diffraction System model X' Pert PRO (PANalytical) diffractometer. A Co-kα radiation (λ = 1,78890 Å) with Ni-filter was used as the radiation source and the generator as set to 40 kV and 30 mA in the 2θ range of 5 to 50°, with speed of 3°/min.

The amount of crystalline cellulose in the total cellulose can be expressed by the x-ray "crystallinity index" (Cl) defined the equation bellow:

$$CI=100*[(I_{002}-I_{am})/I_{002}]$$

where I_{002} means the intensity of the principal Cellulose I peak close to 2θ = 26° and I_{am} is the intensity attributed to amorphous cellulose given close to 2θ = 21° after baseline correction, according to literature (BROWNING, 1967; FENGEL and WEGENER, 1989).

Thermal Degradation Measurements

The dehydration and degradation behavior of nanocelluloses was characterized through thermo-gravimetric analysis (TGA) with a DTG-60H, Shimadzu, in a nitrogen atmosphere. Specimens of 5 – 10 mg were tested at temperature ranging from 90 to 550 °C. The heating rate was 10 $^{o}C.min^{-1}$ and the nitrogen flow rate was 50ml/min. The weight-loss rate was obtained from derivative thermogravimetric (DTG) data. The onset degradation temperature was defined as the intersection of tangents drawn from thermo-gravimetric curve, one before inflection caused by the degradation and another from the cellulose degradation step.

Nanostructured paper production

To paper formation, it was used a unbleached Kraft pulp from Pinus. After the pulp had been refined, in different intensities until obtaining pulp with °SR maximum of 55 ±5, the cellulose micro and nanostructures, MFC, NFC and CNC, were added to the fibrous suspension, at 0.2 % consistency, at the homogenizer, where they were sustained at least for 10 minutes. Then, handsheets were formed according to TAPPI standard T205 [31] and to compression tests were formed handsheets of 120g/m². The cellulose micro and nanostructures tested as strength additive were 0 %, 1%, 2.5% and 5% based on the dry weight of the pulp.

Physical and mechanical tests

The formed handsheets were placed in an environment with a relative humidity of 50 ± 2% and a temperature of 23 ± 1 °C (TAPPI 402 SP- 98) [31].

Experimental tests were performed according to standard procedures and methodologies, according TAPPI [31], as shown in the table below.

Table 1. Analytical Procedures for analysis of pulps

Test	Methodologies
Drainage resistance	TAPPI 200 sp-01
Tensile resistance	TAPPI 494 om-96
Ring crush test	TAPPI 822 om-93
Corrugated medium test	TAPPI 809 om-93
Tear resistance	TAPPI T 414 om-98
Burst resistance	TAPPI 403 om-97
Air passage resistance	TAPPI 460 om-96

RESULTS AND DISCUSSION

Morphology

As observed (Figure 1), the dispersion between MFC, NFC and CNC happened differently. The dispersion difference between micro/nanofibrils and whiskers could be related to the possibility of entanglement due to the higher length (SIQUEIRA et al., 2009, TONOLI, 2012) and fiber flexibility.

The diameter and length, morphological characterization of nanocelluloses, were performed by Transmission electron microscopy (TEM) observations together with the results from Zetasizer instrument, respectively. The TEM images (Figure 1) showed average diameteres of MFC, NFC and CNC of 60 ± 16, 5.7 ± 0.4, 5.0 ± 0.3, respectively. The Zetasizer analisys showed that average length of MFC was 9,495 d.nm, of NFC was 104.15 d.nm, and of CNC was 84 d.nm. These values agree well with dimensions for similar MFC fibers found in the literature (LAVOINE et al., 2012; SIQUEIRA et al. 2009; SIRÓ and PLACKETT, 2010; MOON, 2011). According to Moon (2011), the MFC particles have a high aspect ratio (10–100 nm wide, 0.5–10's mm in length), the NFCs have a high aspect ratio (4–20 nm wide, 500–2000 nm in length) and the CNCs have a high aspect ratio (3–5 nm wide, 50–500 nm in length). However, depending on the raw material source and the treatment applied, the aspect ratio and dimensions of each type of cellulose nano structure will differ.

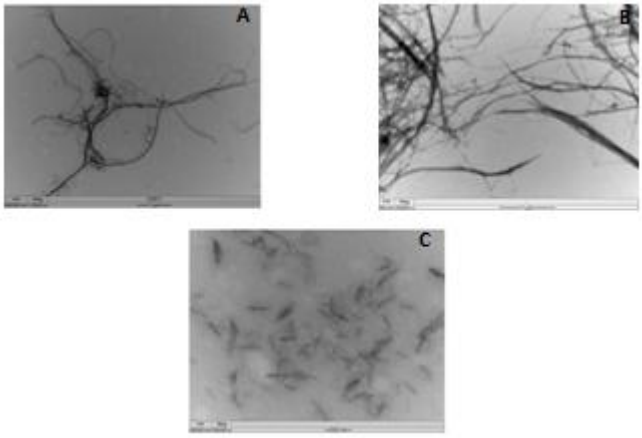

Figure 1. Transmission electron microscope images. A) Microfibillated celluloses – 12,000X mag; B) Nanofibrillated celluloses – 20,000X mag; C) Cellulose nanocrystals – 50,000Xmag.

Zeta potential

The average values of zeta potential found for the nanoceluloses type MFC, NFC and CNC were -19.1, -30.1 and -0.58 mV, respectively. Higher values of zeta-potential indicate higher capacity of dispersion in water, while low values indicate low dispersion stability (TONOLI, 2012). The nanocelluloses obtained by Damasio (2015) showed values to zeta potential of -56,96 and -26,86 mV to CNC and NFC, respectively.

Whiskers prepared with sulphuric acid present negative charge surface, while those prepared with hydrochloric acid are not charged (SAMIR et al., 2005), but the CNC isolated in this study presetend the zeta potential nearly to zero. According to Tonoli (2012), the increase in hydrolysis time from 30 to 60 min increased the sulphur content, but decreased the zeta-potential of the whiskers. Dong et al. (1998) reported the decrease of length and surface charge with higher hydrolysis time in cotton and sulphuric acid. Other explanation to this zeta potential value is in the protonation of the ester groups in function of the pH. Reising et al. (2012) related on their study that at low pH ~2, a ~-30 mV potential was measured, and with increasing pH, the potential became more negative until it reached ~-60 mV and then stayed constant from a pH of ~3 to ~8.5. Additional increases in pH resulted in the potential becoming less negative monotonically to ~-30 mV at pH 12, giving the pH vs. zeta potential curve a “bathtub” shape. The more positive potentials at low pH may be explained by protonation of the sulphate ester groups. However, the cause of the more positive potentials at basic conditions is unclear, but they may be due to sulphate ester hydrolysis under base catalysis or an ionic strength effect due to added ions (REISING et al., 2012).

Cristalinity index (MFC, NFC, CNC)

The diffractions of nanocelluloses are shown in Figure 2. The diffraction patterns of MFC and NFC, which the amorphous and crystalline peaks at 21.80°<2θ<22.08° (110) and 26.43°°<2θ<26.72° (002), respectively, confirmed that only cellulose I was present in these samples (Liu and Hu, 2008). However, on diffraction pattern of CNC, it was possible to realize that crystalline peak was split into two weaker peaks located at 2θ=24.10° (110) and 2θ=26.46° (002), showing typical cellulose II structure (YUE, 2007). The crystal structure of cellulose I in cotton native cellulose may have been converted to that of cellulose II during the isolation process of CNC, with mercerization. Mercerization is the name given to the conversion accomplished by swelling native cellulose fibers in concentrated sodium hydroxide solution (KOLPAK, 1978). Although no dissolution occurs, the swelling allows for the reorganization of the chains, and cellulose II results when the swelling agent is removed. This treatment leads to improvement in the properties of cotton yarns and fabrics, and the effects of the various processing parameters have been very well characterized (KOLPAK, 1978). The crystallinity index of CNC decreased with increased alkali concentration level, indicating that NaOH had a strong effect in the destruction of the crystalline region (YUE, 2007).

The calculated crystallinity index (CI) values of MFC, NFC and CNC were 79.76%, 85.28% and 98.07%, respectively.

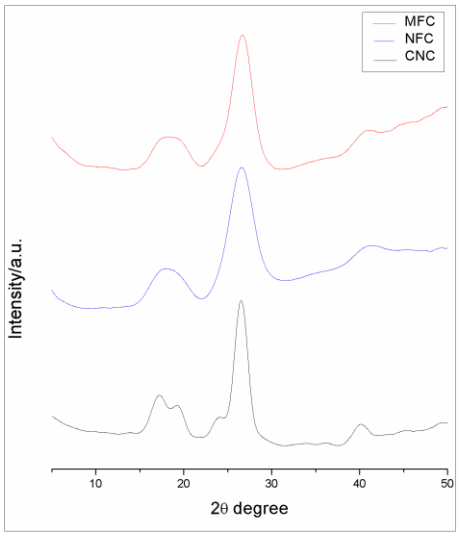

Figure 2. X-ray diffraction of MFC, NFC and CNC

Thermal Degradation Measurements

The thermogravimetric curves TG / DTG of MFC, NFC and CNC were shown in Figure 3. The thermogravimetric curves TG represent the percentage weight loss ,

according to temperature, while the DTG curve corresponds to the first derivative of the TG curves and shows the mass change over time, recorded according to temperature.

Thermal stability is essential for the effective use of nanocelluloses as reinforcing material. The typical processing temperature of thermoplastic materials is above 200 ° C, so the nanocelluloses which are increasingly used as reinforcing agents should be assessed for thermomechanical behavior (ROMAN and WINTER., 2004; NETO et al, 2013).

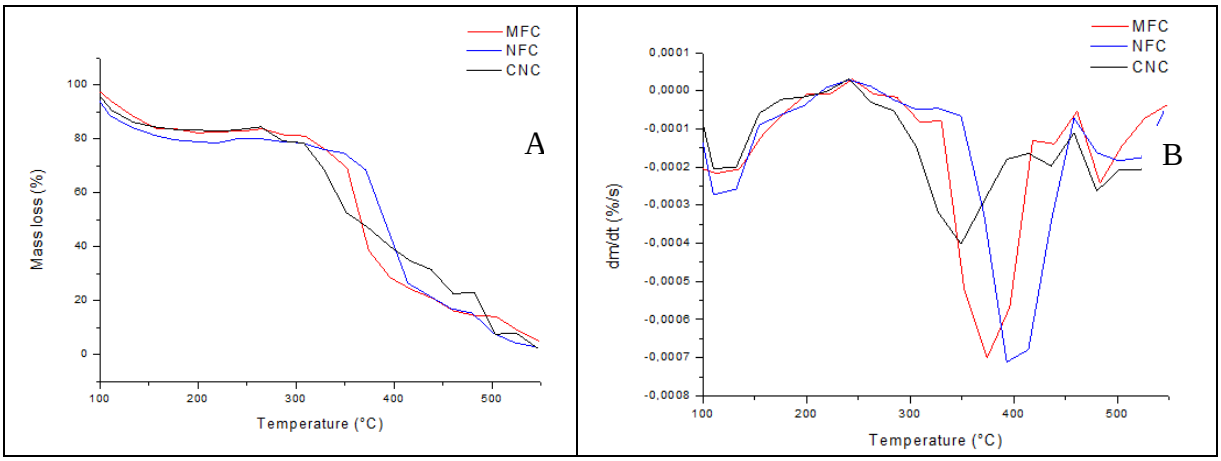

Figure 3. Thermal Degradation analysis. A) Thermogravimetric degradation - TG; B) First derivative of the TG curves - DTG.

Thermogravimetric degradation curves tend to be similar, since MFC, NFC and CNC have a resembling composition. However, the presence of other components should change the maximum degradation temperature, such as the sulfate groups, which accelerate the degradation reactions (ROMAN and WINTER, 2004) in the case of cellulose nanocrystals. In addition, the hemicelluloses and lignin present in the MFC and NFC structure cause changes in the initial degradation temperature, which decreases its value (YANG et al, 2007; MORÁN et al., 2008).

It is widely accepted that the primary thermal decomposition of cellulosic materials occurs between 200 and 400 °C (FISHER et al., 2002). The initial decomposition of the components takes place mostly in the amorphous regions (MOSTSHARI and MOAFI, 2007).

The temperatures from 30 to 130 °C can be characterized as the region where the loss of surface moisture or water non-chemically bound to the nanostructure (DAMASIO, 2015). In this study, this temperature was close to 150 °C, for all nanostructures.

Table 2. Remarkable temperature peaks during the thermal degradation

Nanocellulose	Thermal degradation (° C)			Total mass loss (%)
	Tonset	Tmax	Tendset	
MFC	274	374	419	94.60
NFC	315	391-413	434	96.59
CNC	262	349	372	97.01

CNC is more stable to degradation than MFC and NFC, which can be proved in Figure 3, where it is possible to see that the slope of degradation curve is softer. The level of higher degradation of MFC and NFC is more abrupt. The initial temperature of degradation of MFC was 274 °C;of NFC, 315 °C and of CNC, 262 °C, as shown in Table 2, wherein the temperature of maximum degradation presented a peak at 374 °C, 391-413 °C, 349 °C for MFC, NFC and CNC, respectively.

Physical and mechanical properties of papers

The physical and mechanical properties of pulp and papers clearly improved after the addition of MFC, NFC and CNC, and this improvement rose progressively with the percentage of these nanocellulose structures. The effects of 0, 1, 2.5 and 5% (dry pulp basis) nanocelluloses added to pulp were described below, according to energy consumption during refining.

Drainage resistance

The drainage resistance of pulp was measured in this study through Schopper-Riegler method (ºSR), which measures the amount of water removed from a fiber suspension poured on a fine screen.

Observing only the effects of the refining, it was possible to see the variation from 15 to 49 °SR, requesting 0 to 145 wh (Figure 1), whereas considering only the effect of the addition of nanocelluloses (x=0) resulted in an increase of 66.6, 33.33 and 26.67 % in the Schopper-Riegler degree, for MFC, NFC and CNC, respectively. By combining the effect of refining with the addition of nanocelluloses to a pulp that required 60 Wh energy during refining and presented 17°SR initially, the pulp reinforced with 5% MFC, NFC and CNC showed 36, 36 and 25 °SR, respectively. The addition of nanocelluloses led to lower drainage rate, compared to refining.

Other authors also observed the same tendency to increase drainage resistance with the incorporation of nanocelluloses in the pulp (DAMASIO, 2015; KUMAR el al. (2014); GONZÁLEZ et al., 2012; POTULSKI, 2012; ANKERFORS, 2015). The MFC negatively

affected dewatering, but even though dewatering was reduced, the dry content after pressing was still higher for all dosages of MFC than for the reference point (ANKERFORS, 2015).

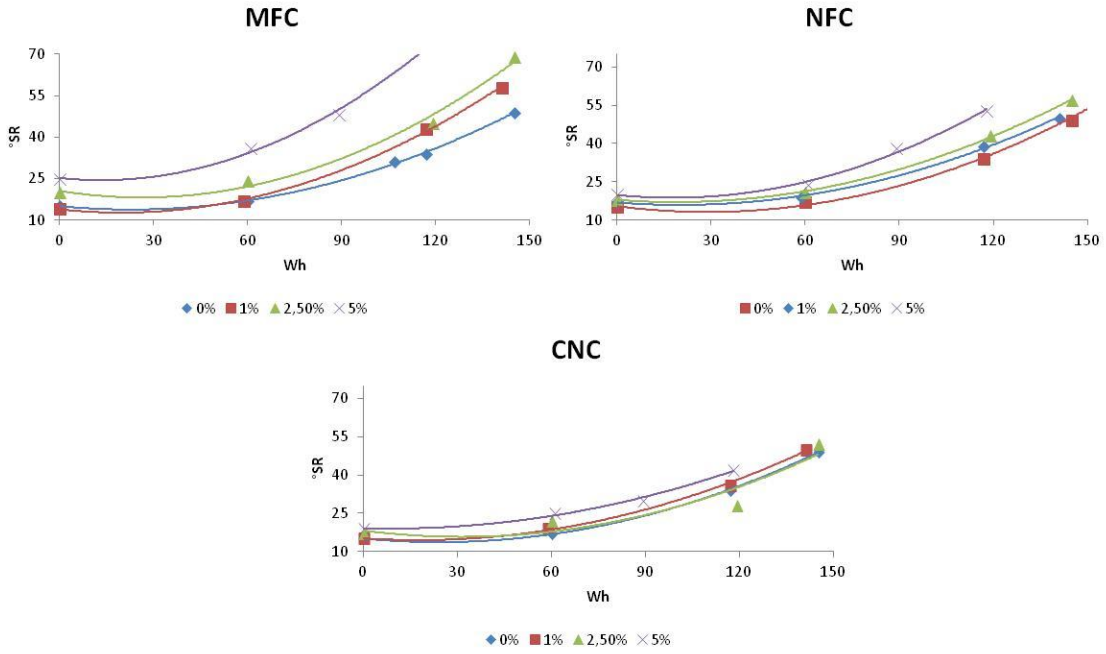

Figure 1- Drainage resistance

Damasio (2015) observed that pulps refined in 2.000, 3.000 and 5.000 revolutions improved 78, 89 and 34 % the °SR with addition of 12% CNF, compared to pulp without CNF dosage, respectively. The pulp reinforced with 9%wt NFC experienced a °SR increase of 200% compared to the non-reiforced suspension (GONZÁLES et al., 2012).

Tensile resistance

The tensile resistance, measured in this study through tensile index, is the tensile force required to produce a rupture in a strip of paper (SILVA, 2011). Tensile strength is influenced by fiber strength, fiber bonding and fiber length.

As shown in Figure 4, the tensile index of reference pulp (0% nanocelluloses) was enhanced 268.44, 300.40 and 381.90 %, requesting 60, 117 and 145 Wh, respectively, compared to the unrefined pulp. The highest results were observed with incorporation of MFC, compared to NFC and CNC at the same proportion. The incorporation of 1, 2.5 and 5% of MFC, NFC and CNC in unrefined pulp (17.68 N.m/g) achieved maximum tensile index of 49.89, 31.89 and 20.89 N.m/g, respectively.

To achieve a tensile index of 65.14 N.m/g, it was consumed 60 Wh for the initial pulp. With the addition of 5% MFC, NFC and CNC, the same tensile index requested as

estimated by regression equation, 16.72, 42.28 and 59.57 Wh, respectively. The saving in consumption energy was 43.28 Wh to MFC, 17.72 Wh for NFC and 0.43 Wh for CNC.

The presence of nanocelluloses in the pulp enhanced the interaction of cellulose fibers by filling the empty spaces between fibers during paper sheet formation, helping to create a better bonding area and leading higher mechanical properties values to properties dependent on this characteristic (fiber bonding), similarly to those obtained after refining, requesting lower energy consumption. The great results obtained through MFC and NFC incorporation can be associated to the presence of micro and nano-fibrils, which result in bigger interlacement with fibers. Although the CNC presents great surface area (DAMASIO, 2015), its rigid structure results in lower bond fiber-CNC-fiber.

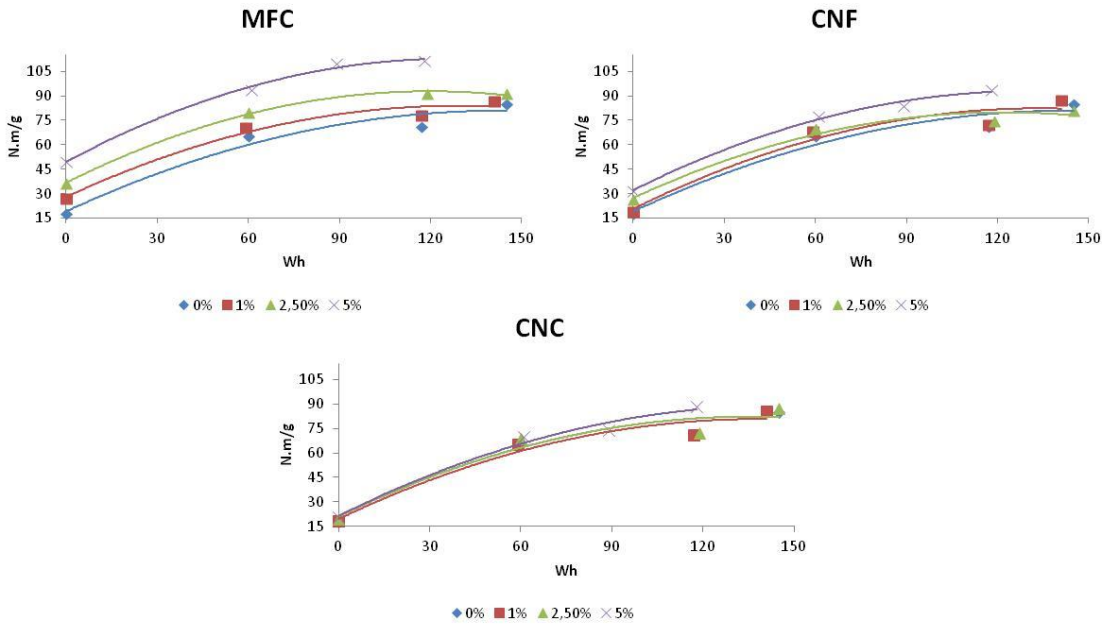

Figure 4- Tensile resistance

Reported by Potulski (2012), the incorporation of MFC considerably improved the tensile index of unrefined pulp, but the combination of refining and 6% wt MFC addition resulted in a slight decrease in the tensile resistance. Gonzáles et al. (2012) reported that the tensile index was enhanced by 24.5% with 3% wt NFC, reaching 67% and 100% for pulp reinforced with 6 and 9 wt% NFC, respectively. Results obtained at 9 wt% were superior to those of Eucalyptus pulp beaten at 1250 revolutions, but did not come close to the values observed in pulp beaten at 2500 or 3750 revolutions (GONZÁLES, 2012). The addition of CNC improved the tensile index in 12.5% compared with unrefined pulp. In the same study, the authors showed that the combination of CNC and starch increased the tensile index in 43.5% (SILVA, 2012).

Compression strength

Compressive strength is one of the most important properties of papers that will later be subjected to compression and stacking, including corrugated cardboard sheets for packaging purposes (SILVA, 2011; SILVA et al, 2013). In this study, the compression strength was evaluated in two ways. The first was the Ring Crush Test (RCT) and the second, the Corrugated Medium Test (CMT).

Ring Crush Test - RCT

Ring Crush Test is the strenght required to crush the sample, through vertical displacement of the movable part of a press on the stationary part. RCT is considered the most important test for assessing the quality of a paper for making paperboard (FRINHANI, 2012).

This property, as well as the tear resistance, is dependent not only on fiber wall strength, but also on the number of interfiber bonds. These factors have a synergistic effect and increase stability under compression column (CASTANHO and OLIVEIRA, 2000).

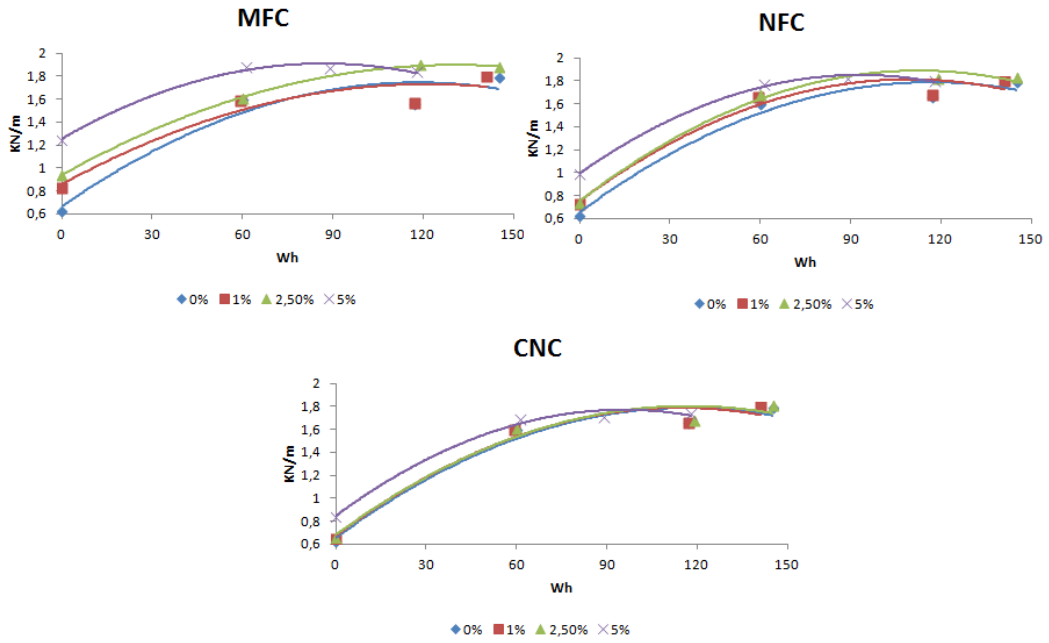

Figure 5- Ring crush test

Note that only with the addition of nanocelluloses enhancements in the RCT were obtained, compared with the initial pulp (x=0), as shown in Figure 5. With the incorporation of 5% of MFC, NFC and CNC, increases of 98.41, 57.14 and 33.33% were observed, compared to unrefined pulp without reinforcement of any kind of

nanocelluloses. The highest increases in RCT were obtained using MFC, which achieved 1.88 KN/m as the maximum RCT value.

However, it was observed that the combination of high intensity refining with the largest dosages of nanocelluloses decreased RCT values. It is postulated that this behavior is due to the weakening cell wall of fibers, consequence of higher refining intensity, with the presence of nanocelluloses that are believed to provide a structure of the weaker cell walls due to the process of achievement.

Corrugated Medium Test - CMT

The compressive strength of corrugated, evaluated in this study by Corrugated Medium Test method, has been determined by the compression of paper samples after being subjected to a corrugator, at high temperatures, for the formation of waves, positioned between two bars with a certain roughness. The compression speed was kept constant until the collapse of the sample. The corrugated compressive resistance value was expressed as a function of the force applied during the testing (SILVA, 2011).

As can be seen in Figure 6, the addition of MFC as much as NFC and CNC, was capable of providing increments comparing with the unreinforced pulp, but these effects were clearly realized at dosage of 5%. This increase is probably related to the increased number of interfibrilar bondings and better formability of the fiber network provided by the introduction of the smaller structures.

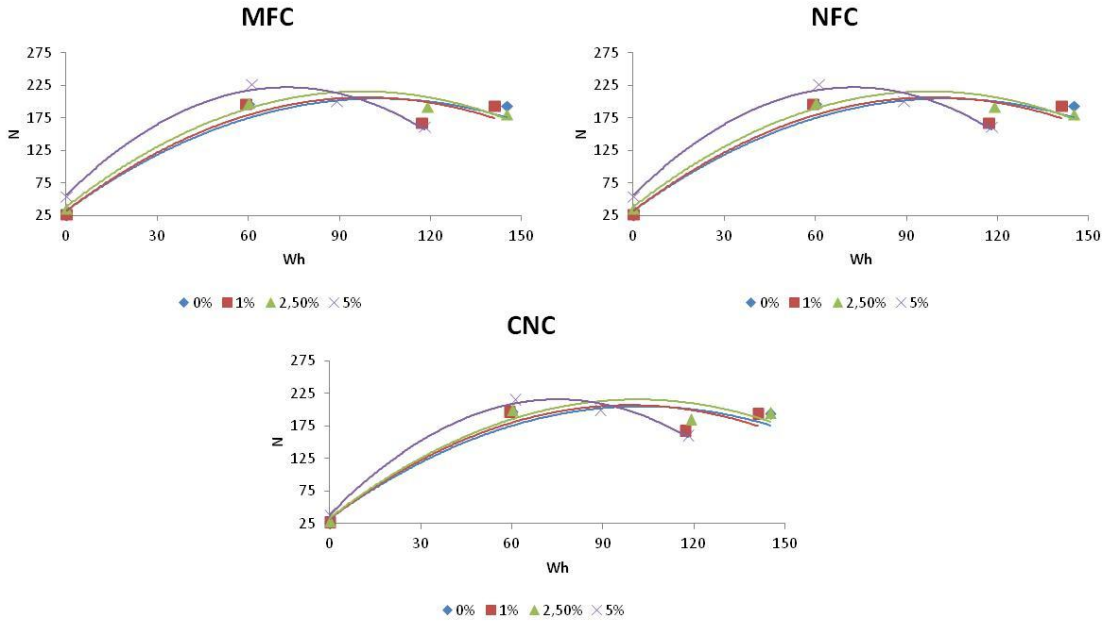

Figure 6- Corrugated medium test

To achieve a CMT of 196.97 N, 60 Wh were consumed during the refining of initial pulp. With the addition of 5% MFC, NFC and CNC, for the same energy consumption, the CMT values obtained were 256.94, 226.94 and 215.94 N, respectively. For this same MFC, NFC and CNC dosage, to obtain a CMT of 196.97 N, it would be necessary to consume 25.82, 44.27 and 50.70 Wh, respectively.

Tear resistance

The tear resistance, evaluated by tear index, measures the mechanical work required to continue a tear, already started, until a predetermined distance (KLOCK, 2000; SILVA, 2011). Some factors influencing the tear index, such as the intrinsic resistance of fiber (determined primarily by the cell wall thickness), fiber length and bond strength interfibers.

As shown in Figure 6, the tear index of reference pulp (0% nanocelluloses) slightly improved until 60Wh, but as the refining intensity increased, the tear index decreased. The addition of 5% MFC, NFC and CNC in unrefined pulp resulted in increases of 111.20, 48.10 and 17.88 %, respectively. Refining combined with dosage of nanocelluloses reduced tear index.

One of the primary purposes of the refining is the reduction in average fiber length. Sincethis dimension is important in the development of the tear strenght, it is expected that pulp refining, together the addition of small structures, can reduce tear index. The same behavior was observed by Damásio (2015), Gonzáles (2012) and Potulski et al (2014). An unrefined pulp increased in 45 and 70 % in relation to initial pulp (DAMASIO, 2015) by adding 6 and 12% CNF. Gonzáles et al. (2012) reported that suspensions reinforced with 9% wt NFC exhibited increases of 80%, similarly to the growth seen in pulp beaten between at 1250 and 2500 revolutions. Potulski et al (2014) related that the addition of MFC in unrefined pulp resulted in increase of 158% in the tear index, but this improvement was less (41%) than the results seen in beaten

suspensions.

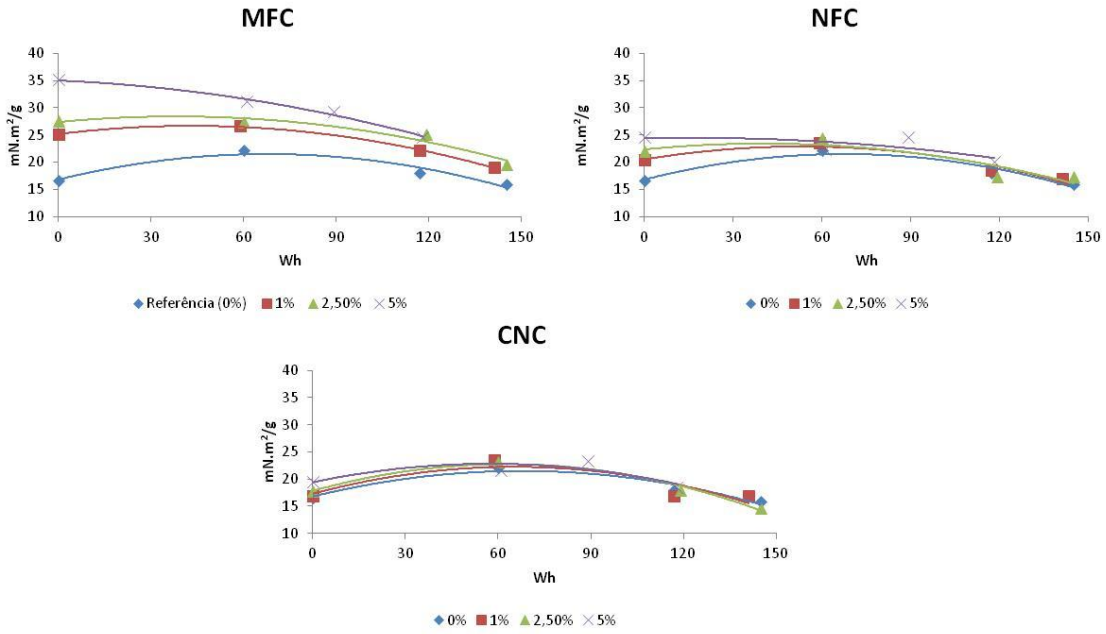

Figure 6- Tear resistance

Therefore, it is believed that, initially, adding nanocellulosic structures in pulps refined in more moderate intensities results in a higher interfiber bonding, consequently increasing properties that depend on this characteristic. However, the combination of increased refining intensities of pulp with higher dosages structures with weaker cell walls, results in the overcoming of effects of increased number of inter-fiber bonds, thereby decreasing the values of the properties.

Burst resistance

Burst resistance is the pressure required to produce the burst of material, while applying increasing pressure transmitted by a circular elastic diaphragm area (SILVA, 2011). Burst resistance, measured in this study by burst index, tells how much pressure paper can tolerate before rupture. It is important for bag paper.

The incorporation of nanocelulosesallows increases, compared to the reference pulp. Regardless of the refining intensity, more significant increases were observed with the use of MFC, as shown in Figure 7. Although the combination of refining with nanocellulose dosage resulted in larger increments, the refining effect (120 Wh) provided greater increment of 437.08% from to the initial pulp, if compared with nanocelluloses dosage in unrefined pulp. The addition of 5% MFC in unrefined pulp resulted a improvement of 223.60 % in the burst index, as shown in Figure 7, while the addition of

5% NFC and CNC both resulted in an increase of 40.45%. It was observed maximum values for the burst index of 6.95, 5.73 and 5.28 KPa.m²/g with the addition of 5% MFC, NFC and CNC, respectively.

The probable explanation for the observed trend for the burst resistance was similar to that for the tensile strength; the two properties are affected by the same factors, particularly the binding ability between the fibers, chief among them. Other factors that may affect these properties are the length of the fibers, the refining process and the formation of leaf structure (FERREIRA, 2008).

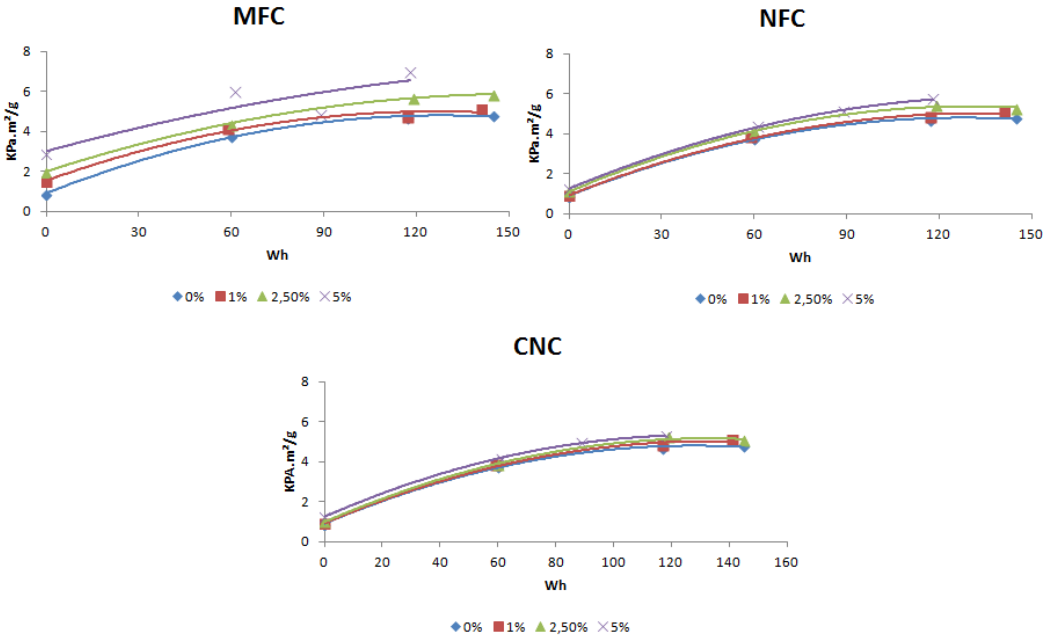

Figure 7- Burst resistance

Potulski et al (2014) observed variation of 1.00 to 6.02 KPa.m²/g by adding MFC in pulp and combining with PFI refining. Gonzáles et al. (2012) reported that the best improvements were observed in pulp with 9 wt% NFC (2.72 times in comparison to non-reinforced pulp). Nevertheless, this improvement was still less than the values obtained for pulp beaten at 2500 revolutions.

Air resistance

The resistance to the passage of air, offered by the paper structure, when a pressure difference exists between two sides of paper, was determined in this study by the Gurley Method. It is measured as the time for a given volume of air to flow through a

specimen under specified conditions. Air resistance is indirect indicator of degree of beating, compaction of fibers and type and amount of fillers (SILVA, 2011).

Observing only the effects of the refining, it was possible to see the variation from 0.48 to 52.49 s/100cm³ in air passage resistance, requesting 0 to 145 wh (Figure 8), whereas considering only the effect of the 5% nanocelluloses addition (x=0) resulted in an increase of 10.42, 93.75 and 31.25 % in air passage resistance, for MFC, NFC and CNC, respectively. By combining the effect of refining with the addition of nanocelluloses to a pulp which required 60 Wh energy during refining, which initially presented 0.83 s/100cm³ , the pulp reinforced with 5% MFC, NFC and CNC showed 5.78, 5.78 and 7.78 s/100cm³, respectively.

The addition of NFC in pulps refined at different intensities increased air passage resistance. The same pattern was observed by Damasio (2015), where the addition of 6 to 12% CNF increased air passage resistance of 71 and 200%, respectively, at all levels of refining. However, Gonzáles et al. (2012) concluded in their study that, while porosity tends to decrease significantly with beating, the use of NFC prevents the loss in the porosity of paper sheets.

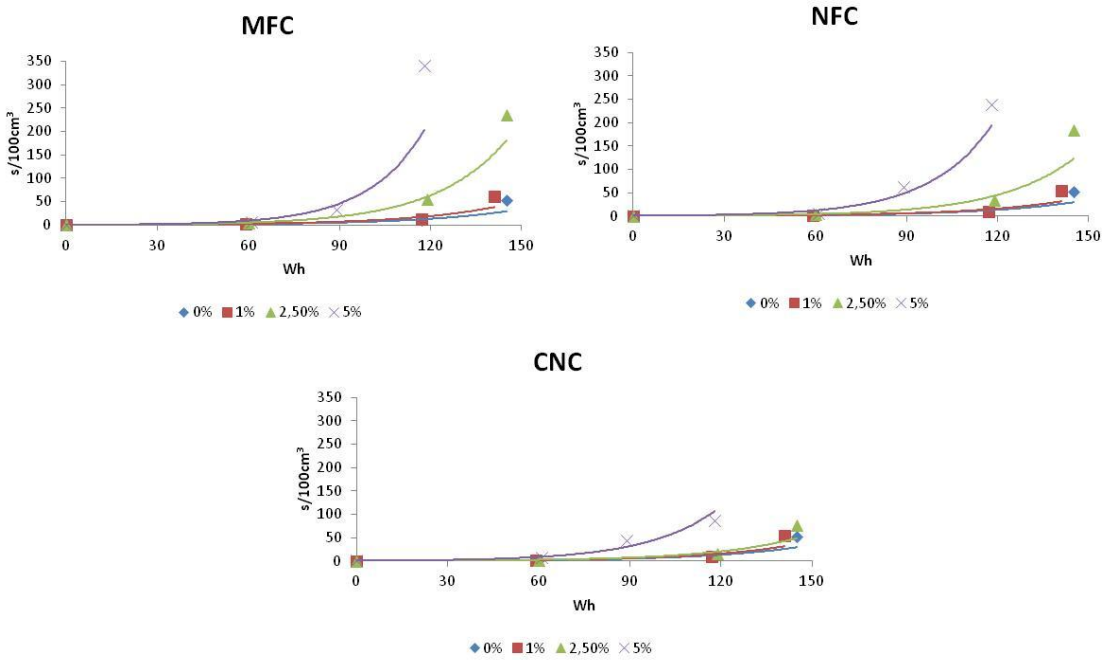

Figure 8- Air resistance

Thus, it was observed that the treatment suggested in this study influenced significantly the mechanical strength properties of the paper, but it should be considered

that the incorporation of nanocelluloses (MFC, NFC and CNC) to make paper must consider some very important parameters, such as the amount to be added and the degree of refining the initial pulp.

CONCLUSION

- The morphological characterization of nanocelluloses produced followed the range of values obtained in the literature.
- The zeta potential of MFC, NFC and CNC were -19.1, -30.1 and -0.58 mV, respectively, and was influenced by the process of obtainment and pH of the analyzed suspension.
- The crystallinity index found for MFC, NFC and CNC were 79.76%, 85.28% and 98.07%, respectively, and directly affected the stability of nanostructures
- All the mechanical properties analyzed were affected by the addition of nanocelluloses, which increased the mechanical properties with increased nanocelluloses dosage.
- The combination of beating and nanocellulose addition must be performed carefully, because the wronguse of one of them can decrease paper mechanical strength.
- The 5% dosage of MFC was the treatment that provided highest paper increments.

Further works

- To evaluate the effect of retaining nanostructures, according to the variation of zeta potential (influenced by pH and conductivity) and hence the impact on the physical and mechanical properties of paper.
- The costs to production of nanocelluloses must be carefully analyzed in order to evaluate the actual advantages of using nanocelluloses as partial substitute for refining in the papermaking industry.

REFERENCES

Zimmermann et al. Properties of nanofibrillated cellulose from different raw materials and its reinforcement potential. Carbohydrate Polymers, v. 79, (2010)

Lin and Dufresne. Nanocellulose in biomedicine: Current status and future prospect. European Polymer Journal, v. 59, p. 302–325, (2014)

Haoran Wei et al. Environmental science and engineering applications of nanocellulose-based nanocomposites. Environmental Science Nano. 1, 302 (2014)

Chauhan and Chakrabarti. Use of nanotechnology for high performance cellulosic and papermaking products. Cellulose chemistry and technology. Cellulose Chem. Technol., 46 (5-6), 389-400 (2012)

Hii et al. The effect of MFC on the pressability and paper properties of TMP and GCC based sheets. 388 Nordic Pulp and Paper Research Journal Vol 27 no.2 (2012)

Iwamoto, S., Nakagaito, A.N., Yano, H. Nano-fibrillated of pulp fibers for the processing of transparent nanocomposites. Appl Phys A, 89, 461-466 (2007)

Eriksen et al. The use of microfibrillated cellulose produced from kraft pulp as strength enhancer in TMP paper. Nord Pulp Pap Res J., 23(3), 299-304. (2008)

Ahola, S., Österberg, M., Laine, J. Cellulose nanofibrils – adsorption with poly(amideamine) epichlorohydrin studied by QCMD and application as a paper strength additive. Cellulose, 14, 303- 314 (2008)

Subramaniam, R., Engineering fine paper by utilising the structural elements of the raw materials. Doctoral dissertation. Helsinki university of Technology. TKK, Espoo, Finland. (2008)

Mörseburg, K., Chinga-Carrasco, G., Assessing the combined benefits of clay and nanofibrillated cellulose in layered TMP-based sheets. Cellulose, 16, 795-806 (2009)

Chinga-Carrasco, G., Cellulose fibres, nanofibrils and microfibrils: The morphological sequence of MFC components from a plant physiology and fibre technology point of view. Nanoscale research letters 6, 417 (2011)

Taipele, T., Österberg, M., Nykänen, A., Ruokolainen, J., Laine, J., Effect of microfibrillated cellulose and fines on the drainage of kraft pulp suspension and paper strength. Cellulose, 17, 1005-1020 (2010)

Zhang, et al. Effect of cellulose nanofiber dimensions on sheet forming through filtration. Cellulose 19, 561-574 (2012)

González et al. nanofibrillated cellulose as paper additive in Eucalyptus pulps. BioResources, 7(4) 5167-5180 (2012)

Silva, J. C. Aplicação de enzimas, extração e adição de hemiceluloses combinadas com ondas ultrassônicas para desenvolvimento de propriedades de papéis reciclados. 184 p. Dissertation, M.Sc. - Viçosa/ Brazil (2011).

Silva et al, combinação dos tratamentos enzimáticos, mecânicos e ultrassônicos para o melhoramento das propriedades de polpas secundárias, Cerne, Lavras, v. 19, n. 4, p. 653-660, out./dez. (2013)

Azizi Samir MAS, Alloin F, DufresneA., Review of recent research into cellulosic whiskers, their properties and their application in nanocomposite field. Biomacromolecules 6(2):612–626 (2005)

Silva and D'Almeida. Nanocristais de celulose. O PAPEL vol. 70, num. 07, pp. 34 - 52 JUL (2009)

Associação Brasileira Técnica De Celulose E Papel. Técnicas de Fabricação de Papéis e Cartões para Embalagem. São Paulo: Klabin fabricadora de papel e celulose S/A, n. 21, p. 64, (1994)

Frinhani and Daltoé. Comparação das propriedades físico-mecânicas de polpas celulósicas Kappa 45 e Kappa 100 destinada à fabricação de papéis para embalagens rígidas. Unoesc & Ciência – ACET, Joaçaba, v. 3, n. 1, p. 65-74, jan./jun. (2012)

Browning, B. L. Methods of Wood Chemistry. New York: Interscience Publishers, v. 2, p. 385-823 (1967)

Fengel, D.; Wegener, G. Wood: chemistry, ultrastructure, reactions. New York: Gruyter, 613 p. (1989)

Siqueira, G.; Bras, J.; Dufresne, A. Cellulose whiskers versus microfibrils: Influence of the nature of the nanoparticle and its surface functionalization on the thermal and mechanical properties of nanocomposites. Biomacromolecules, v. 10, p. 425–432, (2009)

Tonoli et al. Cellulose micro/nanofibres from Eucalyptus kraft pulp: Preparation and properties. Carbohydrate Polymers, v. 89, p. 80– 88, (2012)

Lavoine et al. Microfibrillated cellulose coatings as new release systems foractive packaging. Carbohydrate Polymers 103, 528– 537 (2014)

Moon, R. J., Martini, A., Nairn, J., Simonsen, J., & Youngblood, J. Cellulose nano-materials review: Structure, properties and nanocomposites. Chemical SocietyReviews, 40, 3941–3994 (2011)

Siqueira et al. Cellulosic bionanocomposites: A reviewof preparation, properties and applications. Polymers, 2(4), 728–765 (2010)

Siró and Plackett. Microfibrillated cellulose and new nanocomposite materials: A review. Cellulose, 17(3), 459–494 (2010)

Damasio, R. Caracterização E Aplicações De Celuloses Nanofibrilada (Cnf) E Nanocristalina (Cnc). Dissertation, M.Sc. Viçosa/Brazil. (2015)

Reising et al.. Effect of particle alignment on mechanical properties of neat cellulose nanocrystal films. J Sci Technol For Prod Process; 2:32–41 (2012)

Liu and Hu. X-ray diffraction study of bamboo fibers treated with NaOH. Fiber Polym 9:735-739 (2008)

Yue. A comparative study of cellulose i and ii fibers and nanocrystals. Thesis, M.Sc., Louisiana/ USA. (2007)

Kolpak et al. Mercerization of cellulose: 1. Determination of the structure of mercerized cotton, Polymer 19, 123–131 (1978)

Roman, M., Winter, W.T. Effect of sulfate groups from sulfuric acid hydrolysis on the thermal degradation behavior of bacterial cellulose. Biomacromolecules v. 5, p. 1671–1677, (2004).

Neto et al. Extraction and characterization of cellulose nanocrystals from agro-industrial residue – Soy hulls. Industrial Crops and Products, v. 42, p. 480– 488, (2013).

Yang, H.; Yan, R.; Chen, H.; Lee, D. H.; Zheng, C. Characteristics of hemicellulose, cellulose and lignin pyrolysis. Fuel, v. 86, p. 1781-1788, (2007).

Morán et al. Extraction of cellulose and preparation of nanocellulose from sisal fibres. Cellulose, v. 15, p. 149–159, (2008).

Kumar, A.; Singh, S. P,; Singh, A. K. Preparation and characterization of cellulose nanofibers from bleached pulp using a mechanical treatment method. Tappi Journal, v. 13, n. 5, p. 25-31, (2014).

Ankerfors, M. Microfibrillated cellulose: Energy-efficient preparation techniques and applications in paper. Thesis. Stockholm / Sweden, (2015).

Silva, J. C., Aplicação de enzimas, extração e adição de hemiceluloses combinadas com ondas ultrassônicas para desenvolvimento de propriedades de papéis reciclados. Master thesis - Universidade Federal de Viçosa, Brazil (2011)

Potulski., Efeito da incorporação de microfibrilas de celulose sobre as propriedades do papel.Dissertation, M. Sc.. Universidade Federal do Paraná, Curitiba (2012)

Silva et al. Utilização de complexos de polieletrólitos de fontes Renováveis como alternativa para melhorar as propriedades de resistência do papel. XIX Congresso Brasileiro de Engenharia Química. Búzios. (2012)

Castanho, C. G. ; Oliveira, R. C. . Estudos de Aproveitamento de Rejeito Fibroso Industrial da Polpação Kraft de Eucalipto na Produção de Papéis Reciclados. In: 33º Congresso da ABTCP-TAPPI, São Paulo-SP (2000)

Chapter 4

Nanofibrillated cellulose and Xylan -Rich Hemicelluloses-Based Aerogel

Abstract

Low-density aerogels based on nanofibrillated cellulose (NFC), from bleached elemental chlorine free kraft wood fibers produced from oak, and Xylan-rich hemicelluloses (Xylan), were developed by water freeze drying, previously immersed in liquid nitrogen. Typically, 1.2 % fiber suspension in water was processed passing twenty times by a high-pressure microfluidizer. The xylan- rich hemicelluloses (Xylan) were obtained from corn cob, through alkaline extraction carried out by using sodium hydroxide solution, followed by precipitation using ethanol. Polyamide epichlorohydrin (PAE) resin and is widely used as a wet strength additive in the paper industry, was adopted to crosslink the aerogels. After had mixed manual and vigorously the NFC suspension and Xylan in different ratios (100% NFC, 70:30% - NFC:Xylan, 50:50% - NFC:Xylan, 30:70% - NFC:Xylan and 100% Xylan), the samples were submerged in liquid nitrogen and sequentially frozen samples were dried in Freeze dryer. The crosslinking of aerogels was achieved by curing the freeze-dried samples containing the crosslinker in a vacuum oven at 120 °C for 3 h. The produced aerogels showed that ratio NFC:xylan influence the shape, resistance, surface area, absorbent capacity and water retention values, features evaluated in this study.

Keywords: aerogels, nanofibrillated cellulose, xylan-rich hemicelluloses.

INTRODUCTION

Aerogels are part of an important class of lightweight materials, with high porosity, low solid content and good dimensional stability and strength. Aerogels may have a number of applications because of their specific textural properties, such as low density, large connected pore volumes, high surface area, narrow pore size distribution, etc [1]. In addition, their low heat conductivity and large inner surface area [2] make the aerogels interesting to use in different ways, such as gas or liquid permeation and adsorption, thermal and acoustic isolation, optical applications, carriers for catalysis or drug release [3].

Although aerogels can be prepared from an extensive range of materials, cellulose is a particular promising candidate for addressing novel application [4]. Cellulose is the most abundant and renewable biopolymer on earth and its utilization for assorted applications has seen a renaissance in research development [5-7], representing around 10^{12} tons of the total annual biomass production [8]. Cellulose, a linear, partially crystalline 1,4-β-glucan, is environmentally friendly, biocompatible, and inexhaustible source of raw material and

one of the major components of annual plants (~33%), wood (~50%), and cotton (~90%)[9,10]. Nanofibrillated Cellulose (NFC) refers to cellulose fibers that have been fibrillated to achieve agglomerates of cellulose microfibril units; NFCs have nanoscale (less than 100 nm) diameter and typical length of several micrometers [11]. Aerogels based on nanofibrillated cellulose (NFC) may offer environmental advantages, since NFC is obtained from renewable resources and no harmful solvents are required during processing. NFC aqueous dispersion is prepared by the disintegration of pulped wood fiber cell walls. In the plant cell wall, cellulose is the reinforcing constituent of high strength and modulus, due to its extended chain structure [12].

In addition to cellulose, hemicellulose is the quantitatively most important group of naturally occurring polymers in plants. Despite its great potential, there have so far been few application possibilities for hemicellulose. Unlike cellulose, hemicellulose is dependent on the irregularly composed group of polysaccharides, which is the result of their plant origin. For instance, xylan-based hydrogel has already shown potential for biocompatibility because of its reported non-cytotoxic effect [13]. After the extractive process described by Oliveira et al. [14], corn cob xylan seems to be an off-white fine powder with limited flowability. Xylan powder consists of a mixture of aggregated and non-aggregated particles with irregular morphology, a spherical shape, and rough surface [14].

Aerogels are obtained by carefully drying wet gels. Drying methods such as freeze drying or supercritical drying have been applied to maintain the openness of the structure. These methods preserve intramolecular hydrogen bonding and the entangled long partly amorphous nanofibers [15]. Freeze drying, which is the method used in this work, uses a dispersion, an aqueous gel, or a frozen solution. The solvent is removed by sublimation under high vacuum; by using this technique, the spaces vacated by the solvent crystals become pores. The morphology of the crystals depends on the freezing conditions or the specific cooling protocol used (cooling rate and pressure, mainly) which thus impacts the structure of the final porous aerogel [16].

In view of the facts mentioned above, this study aimed to develop a material, with high surface area and low density, based on xylan-type hemicelluloses and nanofibrillated cellulose, and assess its features.

EXPERIMENTAL

Xylan-rich hemicelluloses isolation

Hemicelluloses were obtained according to Silva et al. (2013), with adaptations. The procedure was repeated several times until the obtain desired amounts of hemicelluloses.

Initially, corn cobs were exposed to dry for 48 hours. They were then crushed in a mill and classified through a series of sieves. The fraction retained between screens of 40 mesh and 60 mesh were used in the following steps.

The crushed material was subjected to aqueous extraction at a ratio of 30 g of powdered corn cobs to 1,000 ml of distilled water with constant stirring for 12 hours. Then the mixture was centrifuged and the solid phase was dried in climatic room at 23 °C and 50 % humidity for 24 hours.

After drying, the material obtained above was subjected to the delignification process at H = 1:10(w/v) using hydrogen peroxide 2% (w/v) at pH 11 (adjusted with NaOH) and 70°C for 2 h. The delignified raw material was washed with distilled water with three times the volume of suspention.

Solubilization of hemicelluloses was performed by alkaline treatment, when the material was then subjected to 10% NaOH (w/w) at 25°C for 24 h, at low agitation, with 10% NaOH of corn cob powder at room temperature. A ratio of 1:10 (powder: NaOH) was used. Then, the solution was neutralized by adding glacial acetic acid to reach pH=7.0. The hemicelluloses were precipitated by the addition of ethanol at the proportion of three volumes of ethanol to 1 volume of the solution. The obtained product was centrifuged for 10 minutes, at 4000 rpm, resulting in a consistency of 20%.

NFCs preparation

NFCs were prepared from bleached elemental chlorine free kraft wood fibers produced from oak and provided as a never dried pulp with a solid content of approximately 20 % (w/w). Typically, 1.2 % fiber suspension in water was processed in a high-pressure microfluidizer (Microfluidizer M- 110 T, Microfluidics Corp.). The samples were passed twenty times through an intensifier pump that increased the pressure, followed by an interaction chamber which defibrillated the fibers by shear forces and impacts against the channel walls and colliding streams. The resulting NFC suspension was collected and stored at 4 °C in a cold room until needed.

Preparation of the aerogels (100:0 – 0:100)

The NFC suspensions obtained were concentrated into dispersion with 4 % solids content upon centrifugation at 12,000 rpm for 1.5 h twice (Beckman Coulter Optima L-90K Ultracentrifuge with a 70 Ti rotating head). It was prepared a mixture of NFC:hemicelluloses ratios ranging from 100:0 to 0:100.

Weighted amount (2.5% of the solid weight of CNFs) of crosslinker (epichlorohydrin resin) was added to the suspension under mechanical stirring. These gels were cast in molds. The samples were submerged in liquid nitrogen for 5 minutes. Finally, the frozen samples were dried in a Freezone 2.5 (BabConco) Freeze dryer, at a sublimation temperature of -52 °C and a pressure of 0.160 mbar, for 44 hours. The crosslinking of aerogels was achieved by curing the freeze-dried samples containing the crosslinker in a vacuum oven at 120 °C for 3 h. The aerogels were finally stored in a desiccator with silica gel until use.

Density

The density of the aerogels was determined after sample degassing for at least 24 h. The density (ρ) of each sample was determined according to the equation below.

$$\rho = \frac{w}{V}$$

Where:

ρ = the density

w= weight

V= volume

Volume and Shrinkage determination

The aerogel shape is determined according to the mold used. The mold selected had cylindrical internal shape, with dimensions of 7 x 7 x 37 mm. Thus, the aerogels produced had a cylindrical shape too. The volume was determined by the equation below.

$$V = \pi.r^2.h$$

Where:

V = volume

π = Pi, approximately 3.142

r = radius of the circular end of the cylinder

h = height of the cylinder

The shrinkage was determined based on the volume of the mold, according to the equation below.

$$S(\%) = \frac{100-(V.100)}{V_{mold}}$$

Where:

S = shrinkage

V = volume of aerogel

V_{mold} = volume of used mold

Scanning electron microscopy images (SEM)

The specimens were fixed on a metal stub using carbon tape and coated with a double-layer coating consisting of graphite and gold–palladium using Agar HR sputter coaters. A Hitachi S- 4800 scanning electron microscope operated at 1 kV was used to capture secondary electron images of aerogel cross-sections.

Surface area

The specific surface areas were determined by N_2 adsorption/ desorption measurements at the temperature of liquid nitrogen (Gemini, Micromeritics, USA). Both adsorption and desorption isotherms were measured and the surface area was determined from the adsorption results using the Brunauer–Emmet–Teller (BET) method. Before measurement, the samples were dried at a temperature of 105 °C, during 4 h.

Absorbent capacity (AC)

The absorbent capacity was determined by the ratio between the dried and wet mass of the same aerogel, according to the equation below. After the determination of the dried mass, the samples were immersed in water, for 2 h.

$$AC = \frac{m1-m2}{m2}$$

Where:

m1 = mass of the wet aerogel

m2 = mass of the dry aerogel

Water Retention Value (WRV)

The ratio of the mass of water retained after centrifugation under specified conditions by a wet aerogel sample to the oven-dry mass of the same aerogel sample was determinated. The measurement of water retention value (WRV) was based on the ISO standard method 23714:2012. The calculation of WRV followed the expression below, in duplicate.

$$WRV\ (\%) = \frac{m1-m2}{m2} * 100$$

Where:

m1 = mass of the centrifuged wet test aerogel

m2 = mass of the dry test aerogel

RESULTS AND DISCUSSION

By using the method introduced in the Experimental section, homogenous aerogels were obtained from pure NFC and xylan-rich hemicelluloses and also from their mixtures, as shown in Figure 1. The NFC aerogels presented white color, while those obtained from pure and/or xylan in their composition presented yellowish color. The xylan materials were brittle; in contrast, the NFC aerogels were more rigid. The brittleness of xylan-based aerogels disappeared or was extensively reduced by the addition of NFC loading, i.e., in composite aerogels. The 100% NFC aerogels obtained are highly flexible and can be compressed without cracking.

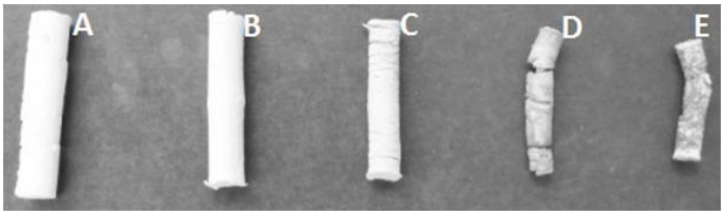

Figure 1. Aerogels in different compositions: A) 100% NFC; B) 70:30 NFC-xylan; C) 50:50 NFC-xylan; D) 30:70 NFC-xylan, E) 100% xylan.

Another feature presented was the reduction the volume of aerogels with the addition of xylan, as shown in Figure 2A. The shrinkage of aerogels (Figura 2B) was based on the internal volume of the used mold (1.42 cm^3). The aerogels did not shrink noticeably at

100% NFC aerogels and 70:30 NFC-xylan, with values of 2.70 and 5.41 %, respectively. However, aerogels with higher amounts of xylan shrank upon drying. The highest shrinkage observed was of 71.04% in 100% xylan aerogels. The same behavior was found by J. Arboleda et al [16], whose investigation showed a shrinkage of 27%. These authors considered this shrinkage especially helpful because it facilitated the removal of the aerogel sample from the mold.

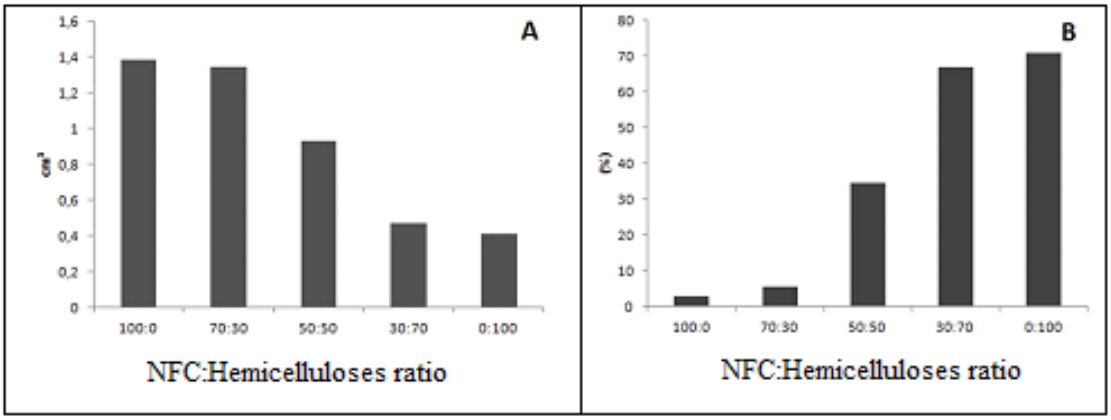

Figure 2. A) Volume of aerogels in different compositions; B) Shrinkage of aerogels in different compositions.

The average density of each aerogel varied hugely according to their composition, which were of 0.07, 0.09, 0.11, 0.12 and 0.61 g.cm-3 to 100% NFC, 70:30, 50:50, 30:70, 100% xylan, respectively. These values are directly related to the solid content of the precursor aqueous gel before freezing. Also, it is well known that through hydrogen bonding, water molecules can be absorbed to xylan chains. These water molecules induce self-assembling of the backbone of xylan in a three-fold, left-handed conformation. Such helix forming phenomenon is well described in several other polysaccharides like β-(1→3)-linked D-xylans, and β-(1→3)-linked D-glucans. In the case of xylan-based hydrogels, the presence of bonded water molecules may contribute to the crosslinking which ‘‘indirectly’’ increases the density of network junction points in the case of non-acetylated xylan based hydrogels [19].

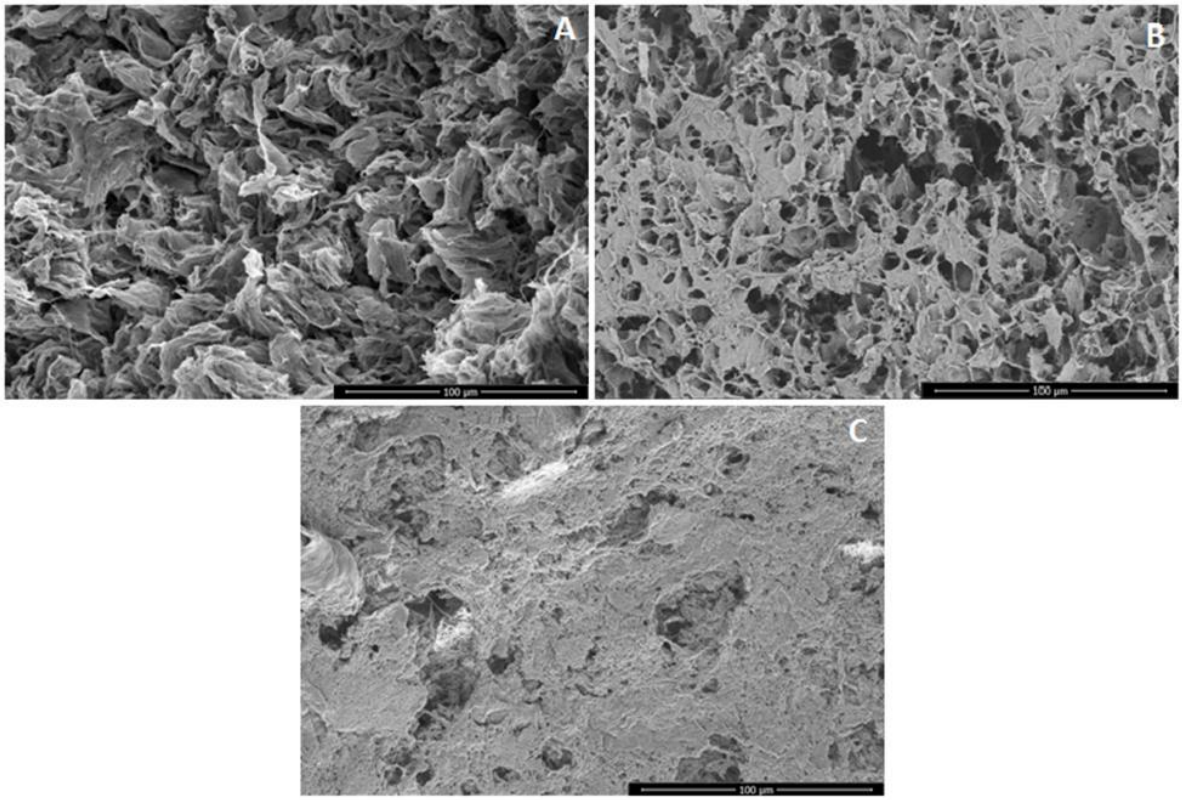

Figure 3. SEM images of aerogels cross section. Mag.: 500x, Scale bars: 100 µm. (A) 0:100; (B) 50:50; (C) 100:0

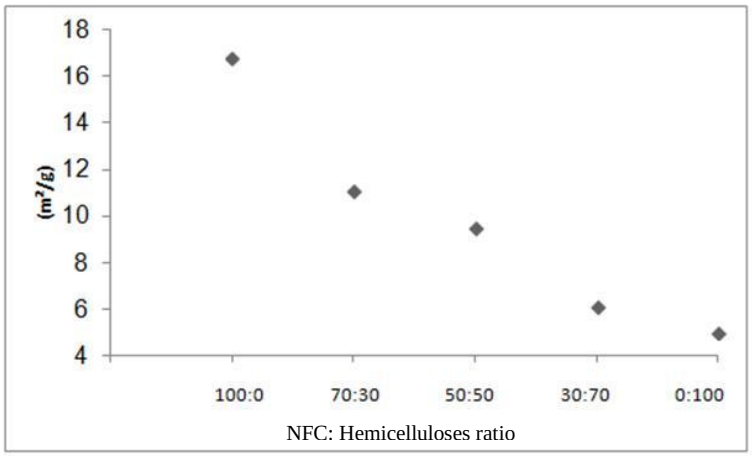

Figure 4. Surface area ($m^2.g^{-1}$) of aerogels in different compositions.

All formulations using xylan were affected in their internal structure, wherein the higher the xylan content, the smaller the internal porosity of aerogels, and the pores seem to be shallower, as shown in Figure 3. As a result, the surface area decreased significantly (Figura 4). The production of materials with surface area as higher as possible is desirable, since it may help to realize the property advantages associated with nanostructured composites. There is a huge range of surface area reported. These values are dependent on variables such as solid content in the wet gel, the material used, use or not of solvent

exchange, the method used in aerogel synthesis, etc. Cross-linked phenolic biopolymers are indeed characterized by long polymer chains leading to steric hindrance, hence preventing the formation of very narrow pores related to high surface areas [20]. In contrast, organic aerogels based on smaller synthetic molecules, such as resorcinol, may present surface areas as high as 800 $m^2.g^{-1}$ [21]. Also, there are reports of NFC aerogels with surface areas of 20 and 70 m².g-1 produced by vacuum drying or fast freezing [22]. Jin et al. [23] and Cai et al. [24] also reported higher surface area of regenerated cellulose aerogels prepared by tert-butanol freeze-drying compared to water freeze-drying (70–120 vs. 160–190 $m^2.g^{-1}$ and 142 vs. 332 $m^2.g^{-1}$, respectively).

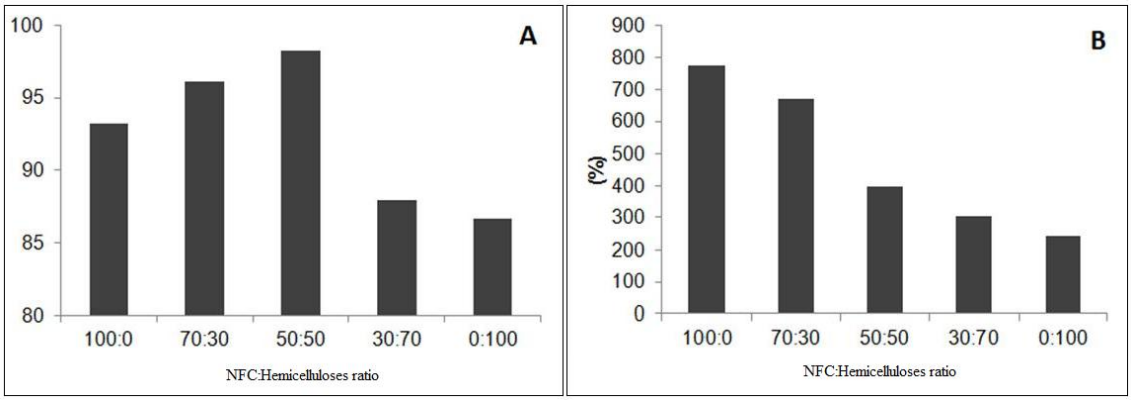

Figure 5. Water sorption. A) Absorbent capacity; B) Water Retention Value (WRV).

The superabsorbent properties were shown in Figure 5. The results of absorbent capacity showed that 1 g of the 100% NFC, 70:30 NFC-Xylan, 50:50 NFC-Xylan, 30:70 NFC-Xylan and 100% Xylan aerogels can absorb 93.25, 96.09, 98.24, 87.98, 86.67 g respectively, as shown in Figure 5A. Initially, the absorption capacity increased, but in composition with an amount of xylan higher than 50%, these values decreased. These results jointly with the water retention values (Figure 5.B) did not follow a known behavior. Typically, in cellulose pulp, the water retention value (WRV) correlated with the total xylan content or with the total charges of fibers [25]. However, this phenomenon is presumably a result of pore structure difference due to the shrinkage occurred by aerogels during drying. The superabsorbent properties of cellulose aerogel depend not only on the hydrophilic nature of cellulose but also largely on the storability of those nano- and micro-sized pores inside. It is normal that over crosslinking will lead to shrinkage of the pores, while insufficient crosslinking may give raise to pore collapse due to the disassociation of interconnected NFC/MFC in water [26].

CONCLUSIONS

It was demonstrated that it is possible to obtain Nanofibrillated cellulose and Xylan - Rich Hemicelluloses-based aerogels from oak and corn cob, respectively, with low density, prepared using water freeze drying, previously immersed in liquid nitrogen. Aerogels with higher amount of xylan presented brittle structure and shallower pores while their resistence can be improved by utilizing NFC. The developed aerogels showed high water absorbent capacity while maintaining their integrity, being dependent on xylan content and surface area. The aerogels showed a hierarchical porous architecture with shrinkage that increased accordingto lower NFC/Xylan ratio.

REFERENCES

1. J. Fricke and T. Tillotson., Thin Solid Films Thin Solid Films, Volume 297, pp 1-332 (1997).
2. Cai J, Kimura S, Wada M, Kuga S, Zhang L. Cellulose aerogels from aqueous alkali hydroxide–urea solution. ChemSusChem (1):149–54 (2008).
3. Olsson RT, Samir M, Salazar-Alvarez G, Belova L, Strom V, Berglund LA, et al. Making flexible magnetic aerogels and stiff magnetic nanopaper using cellulose nanofibrils as templates. Nature Nanotechnology, 5:584 (2010).
4. Silva T. C. F., Habibi Y., Colodette, J. L., Lucia, L. A. Nanofibrillated Cellulose-based aerogels: a new chemical approach for tuning their micro-architectures – Doctoral Thesis, 2:25-41 (2011).
5. He, X., Xiao, Q., Lu, C., Wang, Y., Zhang, X., Zhao, J., et al., Uniax-ially aligned electrospun all-cellulose nanocomposite nanofibers reinforcedwith cellulose nanocrystals: Scaffold for tissue engineering. Biomacromolecules, (2014).
6. Pan, S., & Ragauskas, A. J., Preparation of superabsorbent cellulosic hydrogels.Carbohydrate Polymers, 87, 1410–1418 (2012).
7. Pirani, S., & Hashaikeh, R., Nanocrystalline cellulose extraction process andutilization of the byproduct for biofuels production. Carbohydrate Polymers, 93,357–363 (2013).
8. Heinze, T. and Liebert, T., in Polymer Science: A Comprehensive Reference, eds. McGrath, J. E., Hickner, M. A. and Höfer, R., Elsevier, (10)5:83- 152 (2012).
9. Perez, S. and Samain, D., in Advances in Carbohydrate Chemistry and Biochemistry, ed. Derek, H., Academic Press, 64, pp. 25-116 (2010).
10. Hon, D. N. S., in Chemical Modification of Lignocellulosic Materials, ed. Hon, D. N. S., Marcel Dekker Inc, New York, ch. 1 (1996).
11. Karim Missoum, Mohamed Naceur Belgacem and Julien Bras, Nanofibrillated Cellulose Surface Modification: A Review, Materials, 6: 1745-1766 (2013).
12. Nishino T, Takano K, Nakamae K. Elastic-modulus of the crystalline regions of cellulose polymorphs. Journal of Polymer Science Part B: Polymer Physics, 33:1647–51 (1995).
13. S. Tanodekaew, S. Channasanon and P. Uppanan, J. Appl. Polym. Sci.100, 1914–1918 (2006).
14. Oliveira, E. E., Silva, A. E., Nagashima Jr, T., Gomes, M. C. S., Aguiar, L. M., Marcelino, H. R., Araujo, I. B., Bayer, M. P., Ricardo, N. M. P. S., Oliveira, A. G. &

Egito, E. S. T., Xylan from corn cobs, a promising polymer for drug delivery: Production and characterization. Bioresource Technology, 101, (14):5402- 5406 (2010).
15. Marjo Pääkkö,a Jaana Vapaavuori,a Riitta Silvennoinen,a Harri Kosonen,a Mikael Ankerfors,b Tom Lindström,b Lars A. Berglundc and Olli Ikkala*, Long and entangled native cellulose I nanofibers allow flexible aerogels and hierarchically porous templates for functionalities, Soft Matter, (4):2492-2499 (2008).
16. Julio C. Arboleda, Mark Hughes, Lucian A. Lucia, Janne Laine, Kalle Ekman, Orlando J. Rojas, Soy protein–nanocellulose composite aerogels, Cellulose, 20:2417–2426 (2013).
17. J.C. Silva, R. C. Oliveira, A. S. Neto, V. C. Pimentel, A. A. Santos, Extraction, addition and characterization of hemicelluloses from corncobs to development of properties of papers. Simposio Internacional sobre Materiales Lignocelulósicos. Puerto Iguazu, Argentina (2013).
18. Simone S. Silva, Rosiane R. Carvalho, José Luis C. Fonseca e Rosangela B. Garcia, Extração e Caracterização de Xilanas de Sabugos de Milho, Polímeros: Ciência e Tecnologia - Abr/Jun: 25-33 (1998).
19. Teresa Cristina Fonseca Silva, Youssef Habibi, Jorge Luiz Colodette and Lucian A. Lucia, The influence of the chemical and structural features of xylan on the physical properties of its derived hydrogels, Soft Matter (2010).
20. L. I. Grishechko, G. Amaral-Labat, A. Szczurek, V. Fierro, B. N. Kuznetsov, A. Pizzi and A. Celzard, Ind. Crops Prod., 41, 347 (2013).
21. H. Tamon, H. Ishizaka, M. Mikami and M. Okazaki, Carbon, 35, 791 (1997).
22. Paakko M, Vapaavuori J, Silvennoinen R, Kosonen H, Ankerfors M, Lindstrom T, Berglund LA, Ikkala O Long and entangled native cellulose I nanofibers allow flexible aerogels and hierarchically porous templates for functionalities. Soft Matter 4:2492–2499, (2008).
23. Jin H, Nishiyama Y, Wada M, Kuga S. Nanofibrillar cellulose aerogels. Colloids and Surfaces, 240:63–7 (2004).
24. Cai J, Kimura S, Wada M, Kuga S, Zhang L. Cellulose aerogels from aqueous alkali hydroxide–urea solution. ChemSusChem, 1:149–54 (2008).
25. Schönberg, C.; Oksanen, T.; Suurnäkki, A.; Kettunen, H.; Buchert, J.; The importance of Xylan for the Strenght Properties of spruce Kraft Pulp Fibres. Holzforschung, 55: (6), 639-644 (2005).
26. Wei Zhang,ab Yaan Zhang,b Canhui Lu*a and Yulin Deng, Aerogels from crosslinked cellulose nano/micro-fibrils and their fast shape recovery property in water, Journal of Materials Chemistry, 22, 11642 (2012).

Chapter 5

Adsorption of heavy metal ions from aqueous solutions by NFC reinforced with xylan-rich hemicelluloses -based aerogel

Abstract

In this study, was evaluated the capacity of removal of heavy metal from the aqueous solutions by a bioadsorbent. Aerogels prepared from NFC and reinforced with xylan-rich hemicelluloses were used to the adsorption of Zn^{2+}, Pb^{2+} and Cd^{2+} ions. Influences of the aerogel composition, pH value, adsorption time and the initial concentration of metal ion have been studied. The composition that presented the better adsorption capacity was 50:50 NFC/hemicelluloses, due to the combination of bonding groups available and great surface area. Among the analyzed values, the results showed that the highest adsorption pH value is 7, for all the ions studied. The adsorption capacity to ions Zn^{2+}, Pb^{2+} and Cd^{2+} reaches stability when the adsorption time is 60 min. The adsorption to ions Zn^{2+}, Pb^{2+} and Cd^{2+} increases with increased initial concentration of the metal ions. Also, the adsorption study was carried out in multi-component system and the Pb^{2+} was the metal with higher adsorption on aerogel. The reuse processes of assessed aerogels have proven ineffective.

Keywords: sorption; cation removal; bioadsorbent; corn cobb.

INTRODUCTION

One of higher challenges to humanity is accessibility of clean water. At the current growth rates, the population will be consuming 90% of the available fresh water by 2025 (CARSON and MITCHELL, 1993; AYOUB et al, 2013). Moreover, the increasing level of toxic ionic species that are charged into the environment as industrial wastes represents a serious threat to human health, living resources, and ecological systems (AYOUB et al, 2013).

Heavy metals are considered harmful to the environment and belong to one of the most toxic groups of water pollutants (UTRILLA et al, 2003). Conventional water treatment technologies for heavy metals, such as chemical precipitation and coagulation (CHEN et al., 2009; EL SAMRANI et al., 2008), ion exchange (MISRA et al., 2011), membrane separation (MIN et al., 2012) and electrochemistry (AHMED BASHA et al., 2008), are widely known (LIU et al, 2013). Bioadsorption is arising as a potential alternative to conventional technologies for the adsorption of metal ions from aqueous

solutions as a highly-efficient, cost effective method (SEMERJIAN, 2010; WANG et al., 2010, LIU et al, 2013).

In recent years, a great deal of attention has been diverted toward the production of bioadsorbents from renewable resources, such as starch (DONG et al, 2010), cellulose (O'CONNELL, 2008), lignin (WU et al, 2008), chitin/chitosan (KANNAMBA, 2010), and agricultural wastes (KADIRVELU et al, 2003). These bioadsorbents have many advantages over conventional adsorbents, such as hydrophilic, low costs, biodegradability, high efficiency, minimization of chemical or biological sludge, and good reusability (PENG et al, 2002).

However, the application of untreated plant wastes as adsorbents can also bring several problems such as low adsorption capacity, high chemical oxygen demand (COD) and biological chemical demand (BOD) as well as total organic carbon (TOC) due to the release of soluble organic compounds contained in plant materials (GABALLAH et al., 1997; NAKAJIMA and SAKAGUCHI, 1990, WAN NGAH and HANAFIAH, 2007). In order to utilize biopolymers to remove impurities from water, it is important to strongly bond ionic species to the adsorbent surface (AYOUB et al, 2013).

Aerogels are emerging as a product with appropriated features to this end, such as low density, large connected pore volumes, high surface area, narrow pore size distribution, etc (FRICKE and TILLOTSON, 1997).

Thus, this study aimed to preparea bioadsorbent, an aerogel, from cellulose nanofibrillated (NFC) reinforced with xylan-type hemicelluloses for heavy metal ion removal and recovery. So, the present investigation details the synthesis and characterization of aerogels from different NFC/hemicellulose ratio. Factors affecting the aerogels adsorption capacity, such as pH, ion initial concentration, contact time and competition among ion were evaluated. Methodologies to allow the desorption and reusability of aerogels and heavy metal recovery were also assessed.

EXPERIMENTAL

Hemicelluloses isolation

Hemicelluloses were obtained following the methodology described in literature (SILVA, et al, 2015), with adaptations. The procedure was repeated several times until the desired amounts of hemicelluloses were obtained.

Initially, corn cobs were exposed to sunlight for 48 hours to dry. They were then crushed in a mill and classified through a series of sieves. The fraction retained between 40 mesh and 60 mesh screens were used in the following steps.

The crushed material was subjected to aqueous extraction at a ratio of 30 g of powdered corn cobs to 1,000 ml of distilled water with constant stirring for 12 hours. Then, the mixture was centrifuged and the solid phase was dried in climatic room at 23 ° C and 50 % humidity for 24 hours.

After drying, the material obtained abovewas subjected to the delignification process at H = 1:10(w/v) using hydrogen peroxide 2% (w/v) at pH 11 (adjusted with NaOH) and 70◦C for 2 h. The delignified raw material was washed with distilled water with three times the volume of suspention.

The solubilization of the hemicelluloses was performed by alkaline treatment, when the material was then subjected to 10% NaOH (w/w) at 25◦C for 24 h, under low agitation, with 10% NaOH of corn cob powder, at room temperature. A ratio of 1:10 (powder: NaOH) was used. Then, the solution was neutralized by adding glacial acetic acid to reach pH=7.0. The hemicelluloses were precipitated by the addition of ethanol at the proportion of three volumes of ethanol to 1 volume of the solution. The obtained product was centrifuged for 10 minutes, at 4000 rpm.

NFCs preparation

The NFCs were prepared from bleached elemental chlorine free kraft wood fibers produced from Oak (Betula pendula) and provided as a never dried pulp with a solid content of approximately 20 % (w/w). Typically, 1.2 % fiber suspension in water was processed in a high-pressure microfluidizer (Microfluidizer M- 110 T, Microfluidics Corp). The samples were passed twenty times through an intensifier pump that increased the pressure, followed by an interaction chamber that defibrillated the fibers by shear forces and impacts against the channel walls and colliding streams. The resulting NFC suspension was collected and stored at 4 °C in a cold room until needed.

Preparation of the aerogels (100:0 – 0:100)

The NFC suspensions obtained were concentrated into dispersion with 4 % solid content upon centrifugation at 12,000 rpm for 1.5 h twice (Beckman Coulter Optima L-90K Ultracentrifuge with a 70 Ti rotating head). A mixture of NFC:hemicellulose ratio was prepared ranging from 100:0 to 0:100.

The weighted amount (2.5% of the solid weight of CNFs) of crosslinker (epichlorohydrin resin) was added to the suspension under mechanical stirring. These gels were cast in molds (10 x 10 x 40 mm dimension). The samples were submerged in liquid nitrogen for 5 minutes. Finally, the frozen samples were dried in a Freezone 2.5 (BabConco) Freeze dryer, at a sublimation temperature of -52 °C and a pressure of 0.160 mbar, for 44 hours. The aerogels were finally stored in a desiccator with silica gel until the time for use.

Preparation of heavy metal solutions

The preparation of ions solutions (50−800 mg/L) was carried out by dissolving $Pb(NO_3)_2$, $CdCl_2 \cdot 2.5H_2O$, and $Zn(NO_3)_2 \cdot 6H_2O$, separately, in deionized water. Then, pH adjustment to 5, 7 and 9 was made using NaOH and HNO_3. Deionized water was used in all experimental works.

Adsorption Experiments

Each kind of aerogel (5mg) was put in 25 mL of metal solution (50 mg/L) at 100 rpm during 90 min, at different pH values. At the end of the experiment, the aerogel was removed and the solution was filtered. The metal ion concentration in the filtrate was determined by titration with standard ethylenediaminetetraacetic acid (EDTA) solution (0.01 mol/L) using Erichrome Black T as the indicator (GURGEL et al, 2008; KARNITZ et al, 2007; PENG et al, 2012). The amount of metal ion adsorbed on the aerogel at adsorption equilibrium, qe (mg/g), was calculated according to Equation 1. Also, it was calculated the metal ion adsorption (%) based on the initial concentration, according to Equation 2.

$$qe = \frac{(C0 - Ce) * V}{W} \quad (1) \qquad Adsoption(\%) = \frac{(C0 - Ce) * 100}{C0} \quad (2)$$

Where Co and Ce are the initial and equilibrium metal ion concentrations (mg/L), V is the volume of the metal ion solution used in the adsorption experiment (L), and W is the weight of the aerogel (g), respectively.

Adsorption Kinetics

5 mg of aerogel were put into 25 mL of metal ion solution (100 mg/L), and the mixture was agitated (100 rpm) at optimum pH values obtained from section "Adsorption Experiments" for 10−120 min. The amount of metal ion adsorbed on the aerogel was calculated according to Equations 1 and 2.

Adsorption Isotherms

The effect of the initial metal ion concentration on adsorption capacity was determined ranging the initial concentration of metal ion at an optimum pH value and equilibrium time obtained from section "Adsorption Kinetics". 5 mg of aerogel was put into 25 mL of metal ion solution (50-800 mg/L), and the mixture was agitated (100 rpm). The suspension was filtred and the amount of metal ion adsorbed on the aerogel was calculated according to Equations 1 and 2.

Multi elementary system

5 mg of aerogel was emerged into 25 mL of metal ion solution (proximally 1g/L, 33% from each analized metal). The process was carried out at 7 pH, lasted 90 minutes, 100 rpm. The characterization of adsorption of heavy metals ions in multi elementary system was performed by scanning electron microscopy (SEM) coupled to EDS (Energy Dispersive X-ray Spectroscopy), which enables the determination of the qualitative and semi-quantitative composition of samples from the emission of characteristic X-rays. The samples were previously coated with gold.

Surface area

The specific surface areas were determined by N_2 adsorption/ desorption measurements at the temperature of liquid nitrogen (Gemini, Micromeritics, USA). Both adsorption and desorption isotherms were measured and the surface area was determined from the adsorption results using the Brunauer–Emmet–Teller (BET) method. Before measurement, the samples were dried at a temperature of 105 °C, during 4 h.

Desorption and Reusability of aerogels and metals

Two strategies of desorption and reusability of aerogels were adopted. The first one was based on Peng (2012). In this method, 5 mg of aerogel was put to 50 mL of metal ion solution (100 mg/L), and the mixture was agitated continuously at 7 pH value, during 90

minutes. The aerogel was then withdrawn from the solution with the aid of a tweezer and immersed in deionized water 3 times. Thereafter, the aerogel was dipped into HNO_3 solution (0.5 M) for 2 h under stirring to remove the adsorbed metal ions from the aerogel and then treated with 0.01 M NaOH for 8 h to completely convert COOH groups to COO− groups. The amount of adsorbed and desorbed metal ions was calculated according to eq 1. The second method was based on Xu He (2014). The desorption of aerogel was conducted using 0.1 M NaOH solution as the desorbing agent. The desorption lasted for 4 h under constant magnetic stirring (100 rpm), followed by repeatedly rinsing with deionized water to neutral pH.

RESULTS AND DISCUSSION

Effect of the pH value

Hydronium ion concentration (pH effect) is one of the most important parameters controlling uptake of heavy metals from wastewater and aqueous solutions. The degree of ionization of a species is affected by the pH, e.g., a weak acid or a weak basis (AL-ANBER, n). The acidity of a solution has two effects on metal sorption. Firstly, proton in acid solution can protonate binding sites of the chelating molecules. Secondly, hydroxide in basic solution may complex and precipitate many metals. Therefore, the pH of a solution is the first parameter to be optimized (NGEONTAE et al, 2007).

The initial planning was evaluating the effect of three pH values: 5, 7 and 9, but at pH higher than 7.2,the precipitation of metals occurred, so only the pHs 5 and 7 were assessed. The effect of pH on heavy metal removal efficiencies of aerogels was showed in the Figure 1.

The amount of metal ion adsorbed on the aerogel at adsorption equilibrium of Zn^{2+}, Pb^{2+} and Cd^{2+} remarkably increased from 61.94, 54.01 and 24.52 mg/g at pH 5 to 96.31, 73.48 and 35.71 mg/g at pH 7, respectively, in the composition that provided the higher adsorption (50:50), as shown in Figure 1. So the pH 7 was used in the remaining of this work.

At low pH, COO^- groups are converted into COOH, which reduces their ability of binding to positively charged ions. When pH increases, the COOH groups become deprotonated with the result of negatively charged ligands (COO^-), which easily attracts the positively charged metal ions (PEHLIVAN, 2007; PENG, 2012). Thus, metal ion binding to aerogel is an ion exchange mechanism, which involves an electrostatic interaction between

metallic cations and negatively charged ligands. In addition, a more expanded polymeric network will also favor the diffusion and adsorption of metal ions in the interior of the hydrogel (PENG, 2012), due to the repulsion between negatively charged COO^- groups at higher pH.

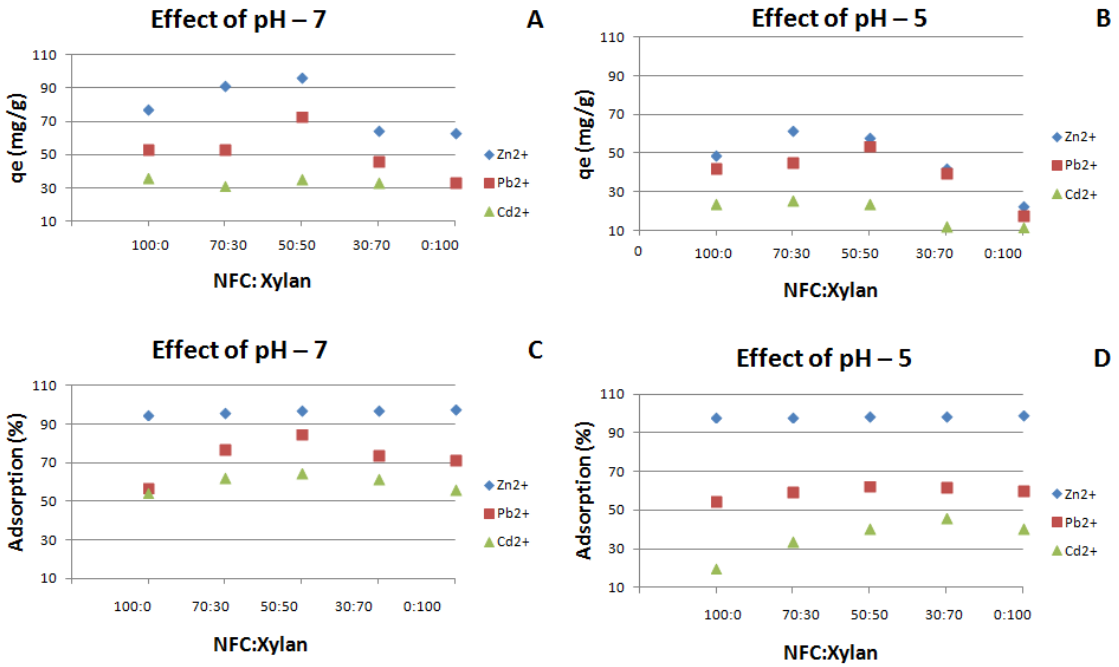

Figure 1. Effect of pH on the metal ion adsorption of aerogels with different NFC/xylan ratio.

Many studies have demonstrated the importance of the carboxyl groups in the sorption of metal ions to biomass materials (MERDY et al., 2002; BAKIR et al., 2009; HUBBE et al., 2011). The capacity of sorption of metal ions to the biomass materials is mainly due to the concentration of the carboxyl groups. The interaction of metal ions with the carboxyl groups takes mainly place by ion exchange. The sorption of metal ions is also pH dependent and an increase in the sorption capacity has been found when the pH of the aqueous solution was increased (OFOMAJA et al., 2010; SEMERJIAN, 2010; REDDY et al., 2011; RAFATULLAH et al., 2012; SU, 2012). Therefore, it was believed that increased proportion of xylan in relation to the NFC would increase the adsorption capacity of the aerogels, but this happened only until 50:50 ratio. Beyond of the presence of functional groups on the surface of the adsorbent material, the adsorption capacity of a material is greatly dependent on the surface area and pore size distribution (NIEDERSBERG, 2012; DURAL, 2011).

The addition of the hemicelluloses rich in xylan resulted in the shrinkage of aerogel. As reported by Silva et al (2015), the aerogels did not shrink noticeably in 100%

NFC aerogels and 70:30 NFC-xylan, with values of 2.70 and 5.41 %, respectively. However, aerogels with higher amounts of xylan shrank upon drying. The highest shrinkage observed was of 71.04% in 100% xylan aerogels. As a result of this shrinkage, it was possible to see the decreasing in the surface area, as shown in the Figure 2 and 3. As the hemicellulose concentration increases, surface area decreases, with values of 16.80; 11.10; 9.53; 6.12 and 5.02 m^2/g, from smaller to higher concentrations, respectively. The pore structure limits the size of molecules that can be adsorbed and the available surface area limits the amount of material that can be adsorbed.

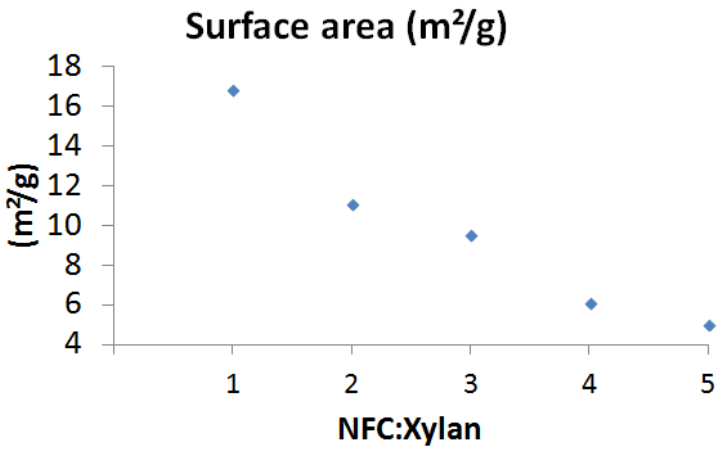

Figure 2. Aerogels surface area in function of NFC/Xylan ratio.

As shown in Figure 3, the internal structure of aerogels is completely dependent of their composition. In Figure 3.A is possible to view a structure more compact and dense of the aerogel formed only xylan-rich hemicelluloses, with granular aspect. The pores of this kind of aerogels are more shallow and rare. Already the aerogel formed exclusively by NFC (Figure 3.C) showed higher porous volume and a smoother internal structure . The aerogel formed by 50% NFC and 50% hemicelluloses (Figure 3.B) presents intermediate features of the two already aerogels cited, as relative internal roughness and porous with high area. The Figure 3.D showed how the loaded aerogels can conserve the internal dimensions same after of immersion in aqueous solution and immediately put in liquid nitrogen and submited to freezedryer. This fact is important considering the reuse of the aerogels for the same aim.

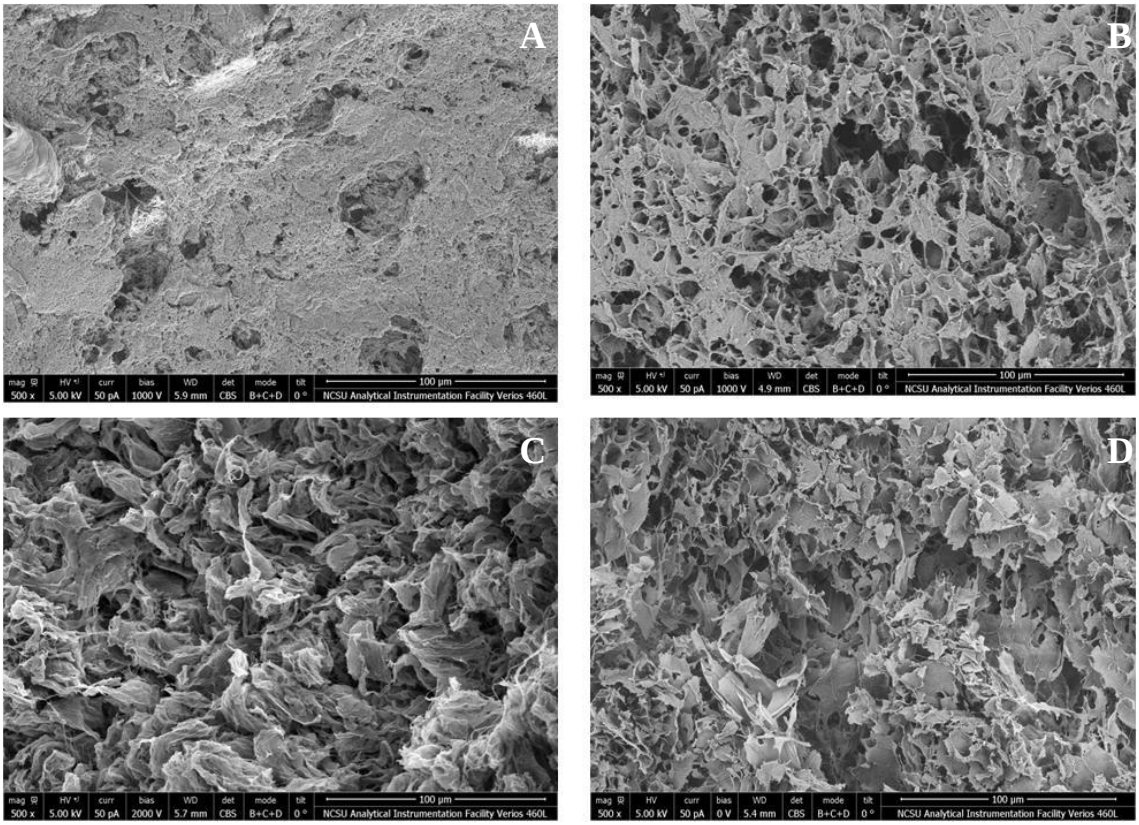

Figure 3. Scanning electron microscopy images – 500x magnitude. A) Aerogel 0:100. B) Aerogel 50:50. C) Aerogel 100:0. D) Loaded aerogel 50:50.

To establish the effect of the hemicelluloses addition in the adsorption, the relative adsorption equilibrium was standardized through the ratio between the adsorption equilibrium and the surface area, as shown in the Figure 4.

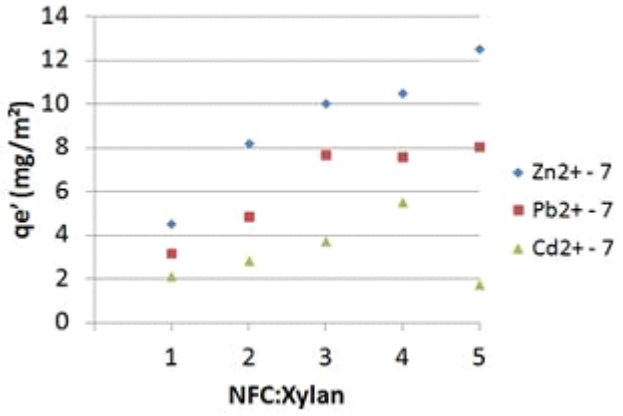

Figure 4. Capacity adsorption/ aerogel surface area, in function of NFC/ xylan ratio.

For the same surface area, at this moment, it was possible to realize the importance of the hemicelluloses content in the adsorption. For Zn^{2+}, the adsorption departed from 4

mg/m² reaching more than 12 mg/m². This increase was also seen for Pb^{2+} and Cd^{2+}, with variation from 3.22 to 8.08 and from 2.14 to 1.77mg/cm², respectively.

Increased adsorption capacities with the increase of hemicelluloses is ascribed to more carboxyl groups being incorporated into the aerogel as the hemicelluloses amount increases (PENG, 2012), whereas the lower adsorption capacities at 30:70 and 0:100 ratio ares likely due to shorter grafting chains and a denser network (Figure 1), which reduces the accessibility of ligands to the active sites of the materials (CHEN and TAN, 2006; YAZDANI et al, 2000; PENG, 2012) and, therefore, lowers the metal ion adsorption capacity. These results indicate that the porous structure is a crucial factor in determining the adsorption capacity of the bioadsorbent.

Effect of the contact time

The effect of the contact time on the adsorption was shown in Figure 5. From Figure 5, it can be seen that the adsorption of the ions Zn^{2+}, Pb^{2+} and Cd^{2+} increases with the extension of adsorption time at short time scale. However, the increasing rate became slower when the adsorption time was higher than 60 min. The short time period for adsorption equilibrium suggests an excellent affinity of the polymeric network for metal ions in aqueous solutions.

Peng (2012) found similar results in their study suggest that the following three stages could be proposed to model the adsorption process. The first stage involved the rapid expansion of the polymeric network and the formation of the macroporous structure because of the highly hydrophilic network and strong electrostatic repulsion. Simultaneously, metal ions began to transport to the external surface of the hydrogel. This stage actually offered considerable macropores for the diffusion of metal ions in the next adsorption stage. The second stage was the diffusion of metal ions into the internal pores of hydrogel through the macropores and then proceeded where they finally adsorbed (the third stage). In the second stage, electrostatic screening resulted in the pores and polymeric network shrinkage. In the last stage, the strong steric hindrance resulted from the internal network shrinkage and made ligands hard to be accessible to metal ions. Therefore, a macroporous structure will favor the diffusion of metal ions and enhance the adsorption capacity of the adsorbent (PENG, 2012).

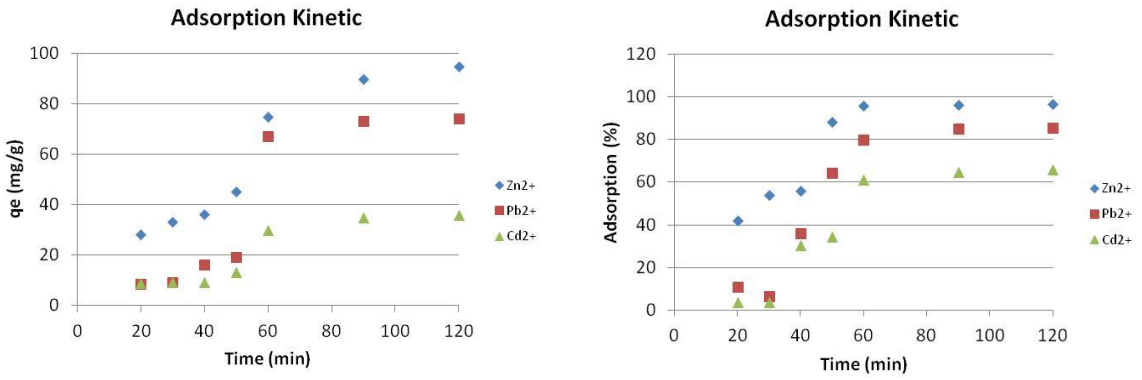

Figure 5. Adsorption kinetics of metal ions onto aerogels composed of 50% of NFC and 50% of xylan, at pH 7.

Effect of metal ion initial concentration

The effect of metal ion initial concentration on the adsorption was shown in Figure 6. It is observed that the adsorption of Zn^{2+}, Pb^{2+} and Cd^{2+} increases with the rise of the initial concentration of the ions, resulting from the fact that the concentration gradient between the liquid and solid increases the driving force and then improves the mass transfer rate greatly.

The adsorption of the adsorbents to Zn^{2+} was the highest, Pb^{2+} came the second, and Cd^{2+} was the lowest. To the ions Zn^{2+} and Pb^{2+}, at low initial concentrations (less than 400 mg/L), adsorption capacities of metal ions increased almost proportionally with the increment in the initial concentrations of metal ions, suggesting that the adsorption process is highly concentration dependent. At higher initial concentrations (more than 400 mg/L), the increase in uptake slowed. In this case, the number of available ligands in the adsorbent actually became the limiting factor that controlled the amount of uptake (PENG, 2012). However, for Cd^{2+}, the continuous increase of the adsorption values, suggests that the adsorption capacity did not achieve the maximum limit. This value can be increasing the initial concentration of the ions or in higher contact time, which is due to the difference of the chemical affinities between the bonding groups, especially the carboxyl, and different metal ions (WANG, 2012).

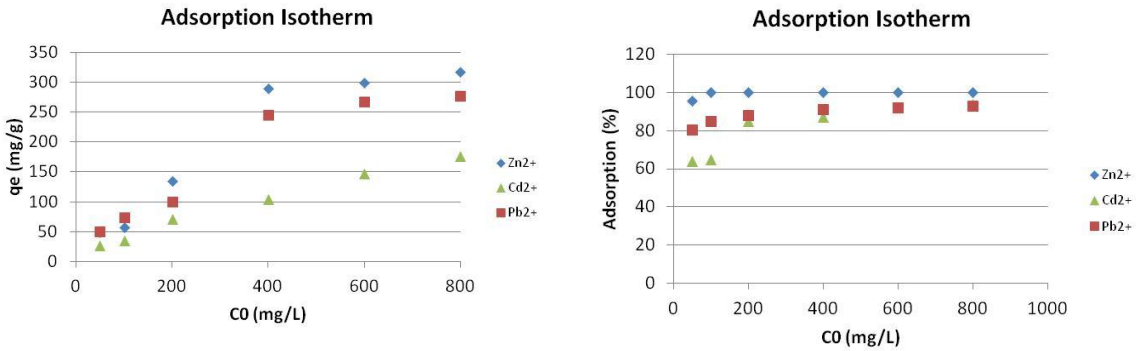

Figure 6. Adsorption isotherms of metal ions onto aerogels composed by 50% of NFC and 50% of xylan, at pH 7.

Adsorption in multi-elementary system

In multi-elementary system, it was observed that addition of three different metals in the solution reduced metal adsorption due to competition from active sites of aerogel. This same trend was observed by Silva (2006), who concluded that the increase of ion concentration, that competes with active sites of the biosorbent, results in the decreasing of maximum capacity of metal removal.

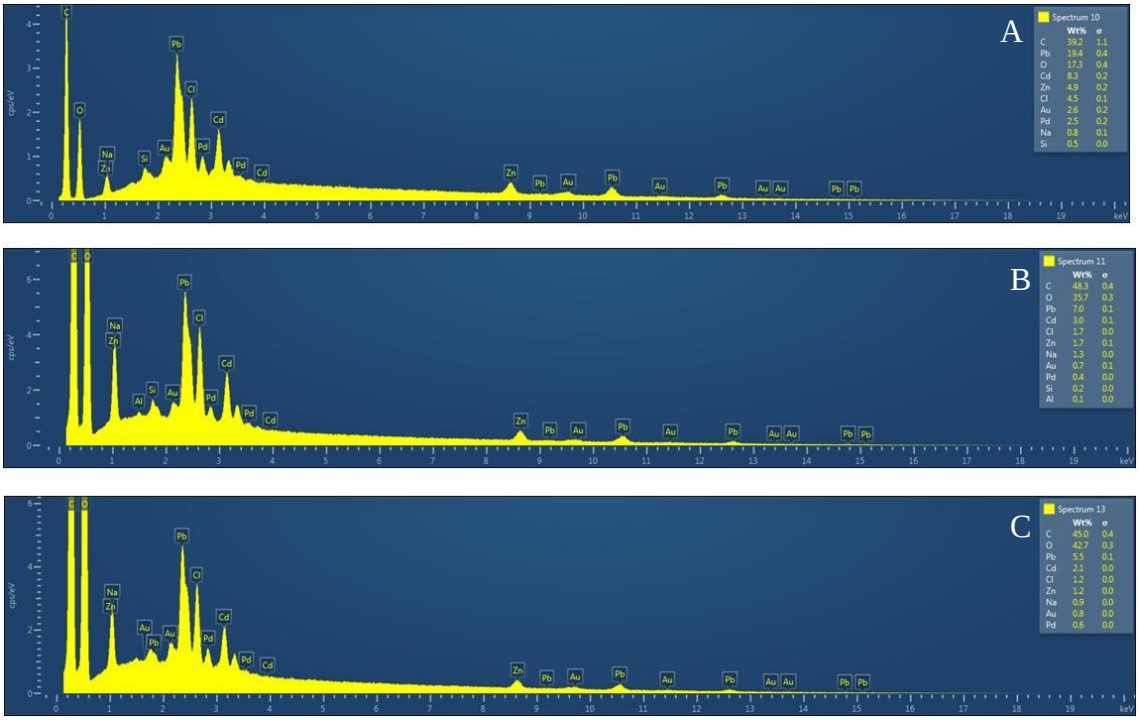

Figure 7. Elemental analysis obtained by EDS analysis of aerogel.

In the evaluated system, the affinity of aerogel was higher for Pb^{2+}, followed by Cd^{2+} and Zn^{2+}, respectively, according to the comparison of the chemical composition.

This result is confirmed by elemental analysis obtained by EDS analysis (Figure 7). In addition, it was possible to realize that the higher concentration happened from the surface to the central region of the aerogel. Through the EDS maps (Figure 8), was possible to indicate the localization of each element and verify that the ions positioned themselves too close together, forming a cluster.

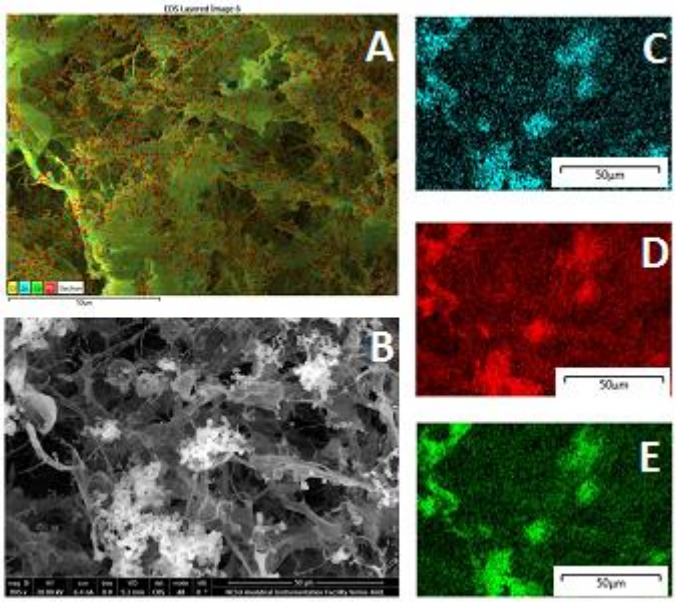

Figure 8. Maps of elements obtained by EDS analysis of aerogel. A) EDS map of Pb, Zn and Cd. B) Scanning electron microscopy image. C) EDS map of Pb. D) EDS map of Zn. E) EDS map of Cd.

Desorption and Reusability of aerogels and metals

In opposition to the results obtained by Peng et al (2012) and Xu He et al (2014), all attempts to desorpt the aerogels were not successful, using either the HNO_3 or the NaOH.

CONCLUSIONS

- The aerogels are capable of adsorptingheavy metals in simple or multi elementary system. In the simple system, the highest adsorption happened with Zn^{2+}.
- The composition affects significantly the adsorption capacity of the metal ion. The ratio most appropriate to remove metal ion was 50% NFC and 50% Hemicelluloses.
- The porous structure is a crucial factor in determining the adsorption capacity of the aerogels.
- As the pH of metal ion solutions increased, the adsorption capacities of Pb^{2+}, Cd^{2+}, and

Zn^{2+} increased.

- An adsorption equilibrium time of about 60 min was obtained.
- The maximum adsorption capacities of Pb^{2+}, Cd^{2+}, and Zn^{2+} were 87, 67, and 98 %, respectively.
- As the inicial concentration of metal ion solutions increased, the adsorption capacities of Pb^{2+}, Cd^{2+}, and Zn^{2+} increased until a determined value. From 400mg/L of initial concentration, the adsorption capacity becomes stable.
- In a multi-elementary system, the aerogels presented affinity of Pb^{2+}>Cd^{2+}>Zn^{2+}, according to the comparison
- The methodologies of desorption and reuse applied were not appropriate and are not suitable for the materials studied.

REFERENCES

Silva et al., Combinação Dos Tratamentos Enzimáticos, Mecânicos E Ultrassônicos Para O Melhoramento Das Propriedades De Polpas Secundárias, Cerne, Lavras, v. 19, n. 4, p. 653-660, out./dez. (2013)

Carson, R., Mitchell, R.C. The value of clean water, Water Resources Research, 29(7), 2445-2454.(1993)

Ayoub et al. Novel Hemicellulose−Chitosan Biosorbent for Water Desalination and Heavy Metal Removal. ACS Sustainable Chem. Eng. 1, 1102−1109 (2013)

Utrilla et al. B ioadsorption of Pb(II), Cd(II), and Cr(VI) on activated carbon from aqueous solutions. Carbon 41 323–330 (2003)

Chen Q, Luo Z, Hills C, Xue G, Tyrer M. Precipitation of heavy metals from wastewater using simulated flue gas: sequent additions of fly ash, lime and carbon dioxide. Water Res 2009;43:2605–14 (2009)

El Samrani AG, Lartiges BS, Villiéras F. Chemical coagulation of combined sewer overflow: heavy metal removal and treatment optimization. Water Res 42: 951–60 (2008)

Misra RK, Jain SK, Khatri PK. Iminodiacetic acid functionalized cation exchange resin for adsorptive removal of Cr(VI), Cd(II), Ni(II) and Pb(II) from their aqueous solutions. J Hazard Mater 185:1508–12 (2011)

Min M, Shen L, Hong G, Zhu M, Zhang Y, Wang X, et al. Micro-nano structure poly(ether sulfones)/poly(ethyleneimine) nanofibrous affinity membranes for adsorption of anionic dyes and heavy metal ions in aqueous solution. Chem Eng J 197: 88-100 (2012)

Ahmed Basha C, Bhadrinarayana NS, Anantharaman N, Meera Sheriffa Begum KM. Heavy metal removal from copper smelting effluent using electrochemical cylindrical flow reactor. J Hazard Mater 152:71–8 (2008)

Liu et al. Adsorption of Pb2+, Cd2+, Cu2+ and Cr3+ onto titanate nanotubes: Competition and effect of inorganic íons. Science of the Total Environment 456–457 171–180 (2013)

Semerjian L. Equilibrium and kinetics of cadmium adsorption from aqueous solutions using untreated Pinus halepensis sawdust. J Hazard Mater 173:236–42 (2010)

Wang L, Yang L, Li Y, Zhang Y, Ma X, Ye Z. Study on adsorption mechanism of Pb(II) and Cu(II) in aqueous solution using PS-EDTA resin. Chem Eng J 163:364–72 9 (2010)

Peng et al. Highly Effective Adsorption of Heavy Metal Ions from Aqueous Solutions by Macroporous Xylan-Rich Hemicelluloses-Based Hydrogel. J. Agric. Food Chem. 60, 3909−3916 (2012)

Dong, A. Q.; Xie, J.; Wang, W. M.; Yu, L. P.; Liu, Q.; Yin, Y. P. A novel method for amino starch preparation and its adsorption for Cu(II) and Cr(VI). J. Hazard. Mater. 181, 448−454 (2010)

O'Connell et al. Heavy metal adsorbents prepared from the modification of cellulose: A review. Bioresour. Technol. 99, 6709−6724 (2008)

Wu, Y.; Zhang, S. Z.; Guo, X. Y.; Huang, H. L. Adsorption of chromium(III) on lignin. Bioresour. Technol. 99, 7709−7715 (2008)

Kannamba, B.; Reddy, K. L.; AppaRao, B. V. Removal of Cu(II) from aqueous solutions using chemically modified chitosan. J. Hazard. Mater. 175, 939−948 (2010)

Kadirvelu, K.; Kavipriya, M.; Karthika, C.; Radhika, M.; Vennilamani, N.; Pattabhi, S. Utilization of various agricultural wastes for activated carbon preparation and application for the removal of dyes and metal ions from aqueous solutions. Bioresour. Technol. 87, 129−132 (2003)

Gaballah, I., Goy, D., Allain, E., Kilbertus, G., Thauront, J., Recovery of copper through decontamination of synthetic solutions using modified barks. Met. Metall. Trans. B 28, 13–23 (1997)

Nakajima, A., Sakaguchi, T., Recovery and removal of uranium by using plant wastes. Biomass 21, 55–63. (1990)

Wan Ngah and Hanafiah. Removal of heavy metal ions from wastewater by chemically modified plant wastes as adsorbents: A review. Bioresource Technology 99, 3935–3948 (2008)

J. Fricke and T. Tillotson., Thin Solid Films Thin Solid Films, Volume 297, pp 1-332 (1997)

Gurgel, L. V. A.; Karnitz Júnior, O.; Gil, R. P. F; Gil, L. F. Adsorption of Cu(II), Cd(II), and Pb(II) from aqueous single metal solutions by cellulose and mercerized cellulose chemically modified with succinic anhydride. Bioresour. Technol. 99, 3077−30839 (2008)

Karnitz, O.; Gurgel, L. V. A.; de Melo, J. C. P.; Botaro, V. R.; Melo, T. M. S.; Gil, R. P. F; Gil, L. F. Adsorption of heavy metal ion from aqueous single metal solution by chemically modified sugarcane bagasse. Bioresour. Technol. 98, 1291−1297 (2007)

Al-Anber. Thermodynamics Approach in the Adsorption of Heavy Metals. www.intechopen.com

Ngeontae, et al. Chemically modified silica gel with aminothioamidoanthraquinone for solid phase extraction and preconcentration of Pb(II), Cu(II), Ni(II), Co(II) and Cd(II). Talanta 71, 1075–1082 (2007)

Pehlivan, E.; Altun, T. Ion-exchange of Pb2+, Cu2+, Zn2+, Cd2+, and Ni2+ ions from aqueous solution by Lewatit CNP 80. J. Hazard. Mater. 140, 299−30 (2007)

Merdy, P., Guillon, E., Aplincourt, M., Dumonceau, J., Vezin, H. Copper Sorption on a Straw Lignin: Experiments and EPR Characterization. Journal of Colloid and Interface Science, 245(1): 24-31 (2002)

Bakir, A., McLoughlin, P., Tofail, S. A. M., Fitzgerald, E. Competitive Sorption of Antimony with Zinc, Nickel, and Aluminum in a Seaweed Based Fixed-bed Sorption Column. CLEAN – Soil, Air, Water, 37(9): 712-719. (2009)

Hubbe, M. A., Hasan, S. H., Ducoste, J. J. Cellulosic substrates for removal of pollutants from aqueous systems: A review. 1. Metals. BioResources 6(2): 2161- 2287. (2011).

Ofomaja, A. E., Unuabonah, E. I., Oladoja, N. A. Competitive modeling for the biosorptive removal of copper and lead ions from aqueous solution by Mansonia wood sawdust. Bioresource Technology, 101(11): 3844-3852. (2010)

Semerjian, L. Equilibrium and kinetics of cadmium adsorption from aqueous solutions using untreated Pinus halepensis sawdust. Journal of Hazardous Materials, 173(1-3): 236-242 (2010)

Reddy, D. H. K., Ramana, D. K. V., Seshaiah, K., Reddy, A. V. R. Biosorption of Ni(II) from aqueous phase by Moringa oleifera bark, a low cost biosorbent. Desalination, 268(1-3): 150-157 (2011)

Rafatullah, M., Sulaiman, O., Hashim, R., Ahmad, A. Removal of cadmium (II) from aqueous solutions by adsorption using meranti wood. Wood Science and Technology, 46(1): 221-241. (2012).

Su, P. Sorption of Metal Ions to Wood, Pulp and Bark Materials. Thesis. Åbo, Finland (2012)

Niedersberg, C. Ensaios de adsorção com carvão ativado produzido a partir da casca do tungue (Aleurites Fordii), resíduo do processo de produção de óleo. Dissertation. (2012)

Dural, M. U. et al. Methylene blue adsorption on activated carbon prepared from Posidonia oceanica (L.) dead leaves: Kinetics and equilibrium studies. Chemical Engineering Journal. v. 168. p. 77-85. (2011)

Silva, J. Nanofibrillated cellulose and Xylan -Rich Hemicelluloses-Based Aerogel. 7th International Colloquium on Eucalyptus Pulp. Vitória/ Brazil 2015

Chen, Y.; Tan, H. Crosslinked carboxymethyl chitosan-gpoly (acrylic acid) copolymer as a novel superadsorbent polymer. Carbohydr. Res. 341, 887−896 (2006)

Yazdani et al. Hydrogels based on modified chitosan, 1-Synthesis and swelling behavior of poly(acrylic acid) grafted chitosan. Macromol. Chem. Phys. 201, 923−930 (2000)

Overall Conclusions

Currently, the industries have been adapting and rearranging, seeking to increase its product portfolio, and some of them, act within the biorefinery concepts. Therefore, in this thesis, it was tried to use raw materials from forest and agricultural sources to improve product characteristics already used as paper, replace products based on petrolio by products of plant origin, such as biofilms, and to propose new products, such as aerogels.

So, in the first chapter of this thesis, it was possible to conclude that corn cobs are good sources of hemicelluloses, and when added in the pulp turn possible the formation of handsheets with lower bulk, higher drainage and greater tensile and tear strengths.

In the second chapter, the results showed that the isolated hemicelluloses, acetylated and non-acetylated, from corn cob allowed the biofilm production with mechanical properties values near to the expected to use like coating and packing films.

In the third chapter, nanocelluloses (MFC, NFC and CNC) were produced and used as reinforced agent on paper. The results obtained showed that the addition of the nanocelluloses on unbleached kraft pulp from Pinus provided an increase in all the mechanical properties analysed.

In the chapter four was described how is possible to obtain Nanofibrillated cellulose and Xylan -Rich Hemicelluloses-based aerogels from oak and corn cob, respectively. The aerogels formed higher amount of xylan presented brittle structure and shallower porous while their resistence can be improved by utilizing NFC. The developed aerogels shown a high absorbent capacity water while maintaining their integrity, being dependent of xylan content and surface area. The aerogels showed a hierarchical porous architecture with shrinkage increasing in function of lower NFC/Xylan ratio.

The last chapter, chapter five, reported a novel NFC reinforced with hemicelluloses-based aerogels as a bioadsorbent were developed for adsorption of heavy metal ions from aqueous solutions. Variables such as pH, initial concentration, contact time in single or multi- elementary system were evaluated and showed the effect of each one in the adsorption.

Thus, the compounds and composites (hemicelluloses and nanocellulose) evaluated in this study proved to have great market potentialto be used in the biorefinery conceptions aiming at higher results of products and process, if coupled to the green chemistry processes.